New Materials and Scaffold Fabrication Method for Nerve Tissue Engineering

A Dissertation
Presented to
The Academic Faculty

by

Christiane B. Gumera

In Partial Fulfillment
of the Requirements for the Degree
Ph.D. in the
School of Biomedical Engineering

Georgia Institute of Technology
May 2009

New Materials and Scaffold Fabrication Method for Nerve Tissue Engineering

Approved by:

Dr. Yadong Wang, Advisor
School of Bioengineering
University of Pittsburgh

Dr. Barbara Boyan
School of Biomedical Engineering
Georgia Institute of Technology

Dr. Gang Bao
School of Biomedical Engineering
Georgia Institute of Technology

Dr. Elliot Chaikof
School of Medicine
Emory University

Dr. Ravi Bellamkonda
School of Biomedical Engineering
Georgia Institute of Technology

Dr. J. Carson Meredith
School of Chemical and Biomolecular Engineering
Georgia Institute of Technology

Date Approved: February 20, 2009

ACKNOWLEDGEMENTS

I wish to thank the following people for their personal and professional support. I would like to thank my advisor, who gave me helpful guidance, criticism, and encouragement throughout my research. I thank my committee members for their time, thoughtful feedback, and discussions. I would like to acknowledge past and current lab members: Dr. Jin Gao, Dr. Zhengwei You, Blaine Zern, Peter Crapo, Justin Papreck, Dr. Keewon Lee, Dr. Daewon Park, Hunghao Chu, and Dr. Yumi Kim. I especially thank Dr. Jin Gao for his patience and time in teaching me how to isolate the tissue explants that were used in the studies. I greatly appreciate the time and effort the following undergraduate researchers contributed into this project: Michael Dorman, for remembering organic chemistry; Miyu Toyoshima and Karun Somani, for their efforts in processing hundreds of photographs; and Andy Zhu, for his help in making scaffolds. I would like to thank our collaborators: Marcus Foston and Matthew DiPrima, both from Dr. Haskell Beckham's lab, for GPC and DSC analyses; Dr. Shelley Pence of the University of Georgia, for discussions regarding acetylcholine receptors; and especially Dr. Paul Kvam for his technical guidance in statistical analysis. I would like to thank the following funding sources: NSF Graduate Research Fellowship, NIH Grant 1R21 EB008565-01A1, and GT-UGA Seed Grant.

Thank you to my family for their understanding, patience, and encouragement that gave me the energy, enthusiasm, and endurance to see this endeavor through. I thank my husband and best friend, Richard Cross, for being my rock through graduate school. I thank my sisters, Janice and Hazel, for giving me strength to pursue my goals. I thank

my parents, Evangeline and Elly Gumera, and my grandmothers, Florencia Jones and Adalberta Bacolor, for teaching me early on the great value of education.

TABLE OF CONTENTS

LIST OF TABLES

LIST OF FIGURES

SUMMARY

Major technical challenges remain before enabling complete functional recovery after a severe nerve injury. Creating a growth permissive environment and directing the extension and myelination of surviving neurons encompass the current goals of nerve regeneration strategies. A potential solution to address these challenges is to promote neurite sprouting and guide the regenerating nerve using biomaterials. We hypothesize that neurite sprouting and extension can be enhanced by using biomaterials as a platform to present biochemical and physical cues. We present a series of biodegradable polymers with varying concentrations of acetylcholine-like motifs and a scaffold fabrication method for producing porous scaffolds containing longitudinally oriented channels.

Acetylcholine is a neurotransmitter involved in neuronal processes, which regulates neurite branching, induces neurite outgrowth, and promotes the formation of synapses. Because of its various roles in neuronal activities, acetylcholine-based materials may also be useful in nerve repair. Acetylcholine-like motifs were incorporated within a polymer by the polycondensation of diglycidyl sebacate, aminoethyl acetate, and leucine ethyl ester, in a manner that permitted control over acetylcholine motif concentration. Diglycidyl sebacate was synthesized by oxidation of diallyl sebacate, while the amine-containing compounds, aminoethyl acetate and leucine ethyl ester, were liberated with sodium carbonate-sodium bicarbonate buffers. Standard analytical techniques were used to quantify acetylcholine motif concentrations, as well as to characterize molecular weights and glass transition temperatures of the polymers. The modular design of synthesizing the polymers can be used to test the effects of presenting

different neurotransmitter motifs, a combination of two or more neurotransmitter motifs, or polymer backbones on neurite sprouting in future studies.

Interactions between the polymers of different acetylcholine motif concentrations and neurons were characterized using rat dorsal root ganglia explants (DRG). We screened the potential application of these materials in nerve tissue engineering using the following criteria: 1) neurite sprouting, 2) neurite length, and 3) distribution of the neurite lengths. The ability of DRG to sprout neurites was influenced by the concentration of acetylcholine motifs of the polymer. All polymers permitted neurite extension and maintained the neuronal phenotype. Addition of acetylcholine receptor antagonists to DRG cultured on the polymers significantly decreased neurite sprouting, suggesting acetylcholine receptors mediate sprouting on the polymers. Future studies may examine how neurons on acetylcholine-based polymers exhibit changes in downstream signaling events and cell excitability that are associated with receptor activation.

In preparation for testing the acetylcholine-based polymers *in vivo*, porous scaffolds with longitudinally oriented channels were fabricated using fiber templating and salt leaching. Scaffolds were made of poly(glycerol sebacate) because of this polymer's comparable mechanical properties to the peripheral nerve and its biocompatibility in nerve regeneration applications. Micro computed tomography, scanning electron microscopy, and cryo-sectioning revealed the presence of longitudinally oriented channels going along the length of the scaffold. Channel volume and average pore size of the scaffolds were controlled by the number of fibers and salt fusion time. Future studies may involve testing the effect of acetylcholine-motifs by coating polymers onto

such scaffolds or assessing the effect of the scaffold's dimensional properties on nerve regeneration.

Chapter 1. INTRODUCTION

1.1 Statement of Problem

Resolving challenges in nerve regeneration will significantly improve the quality of life for millions of individuals and considerably reduce socioeconomic costs associated with such injuries. Nerve injuries are caused by violence, motor vehicle accidents, or sports injury, leading to compression, extension, laceration, or penetration of the nerve. Peripheral nerve damage can lead to sensory loss and neuropathic pain, while spinal cord injury is the most debilitating type of nerve injury. The gold standard for treating large peripheral nerve gaps (> 3 cm) is by using a sensory nerve isolated from another site as an autograft, a treatment that has several drawbacks. Autograft use is associated with morbidity at the donor site, potential mismatch in the dimensions of the nerve being replaced, and does not preclude neuropathic pain after nerve regeneration[1].

In contrast to the ability to treat peripheral nerve injury, there is no current treatment capable of completely restoring functions after spinal cord injury. Spinal cord injury can have very disruptive physical and economic effects on the affected individuals. In the U.S. alone, it is estimated that 11,000 individuals sustain spinal cord injury each year, while more than 250,000 are already affected[2]. Difficulties include respiratory complications, arrhythmias, blood clots, bladder and bowel problems, and reduced reproductive functions[2,3]. Immense costs are associated with current health care and the inability to work after sustaining such nerve injuries. Patient care is estimated to cost more than $4 billion annually in the U.S., a figure that does not include an additional $2.6 billion dollars that is attributed to loss of productivity due to injury[4].

1.2 Addressing Challenges in Nerve Repair Using Biomaterials

The major technical challenges for regenerating the nerve include creating a growth permissive environment and directing the extension and myelination of surviving and regenerating neurons. Until such challenges are addressed, there will continue to be limited treatments that restore complete function following severe nerve injury[5]. Axons in the central nervous system have a poor regenerative response compared to peripheral nerves and the fundamental reasons for this difference are unresolved. The ability to regenerate even a small fraction of the damaged spinal cord in animal models has led to disproportionate returns on neurological function[6]. In treating peripheral nerve injury, the isolation of a nerve autograft leads to permanent sacrifice of the functional nerve. A disparity in autograft dimensions with the injured nerve is an additional limitation which may be addressed by developing alternative approaches that will replace autograft use. A potential solution to address these challenges is to promote neurite sprouting and guide the regenerating nerve using biomaterials[7]. Biomaterials may provide a physical construct to reconnect the severed nerve by serving as a guidance channel, be seeded with the relevant cells to encourage growth as a scaffold, encapsulate growth factors as a delivery vehicle, modulate cells' electrical excitability, or function as a combination of these.

1.3 Hypothesis and Objectives

Our <u>central hypothesis</u> is that neurite sprouting and extension can be enhanced by using biomaterials as a platform to present biochemical and physical

cues. The objective is to control the presentation of biochemical and physical cues in order to test the hypothesis.

Neurotransmitters play an important role in neural cell activities, and the direct integration of neurotransmitter motifs may be an alternative to impart bioactivity to synthetic polymers. Neurotransmitters influence neurite branching in embryonic and adult neurons[8,9], growth-cone turning[10], and may be involved in synapse formation[11,12]. Integration of dopamine into a biodegradable polymer has been shown to influence cell differentiation and neurite sprouting[13]. We hypothesize that biodegradable materials containing neurotransmitter-like motifs promote neurite extension.

In addition to biochemical cues, physical cues presented through topographical features can provide guidance to a variety of cells, including mesenchymal cells, oligodendrocytes, neurons, and macrophages[14]. The growth cone is thought to be involved in causing navigational responses, as axonal extension proceeds through this sensing process. The substrate's adhesiveness[15] and shape[16,17] affects growth cone motility, while pattern dimensions also influence the alignment and length of neurons[18-20]. There is increasing research aimed at identifying effective approaches for directing neurite growth. The effects of contact guidance on directing neurite orientation has been investigated through the use of aligned channels[21-26], fibers [27-31], and in surface patterning techniques[18,32-35]. Because topographical cues play a role in guiding neurite sprouting, we sought to create a micro-porous scaffold containing longitudinal channels with controllable characteristics.

The following specific aims are designed to accomplish the objective and test the central hypothesis:

1. Synthesis of new polymers based on a modular design that enables control of the polymer backbone and the concentration of the acetylcholine-like motif.
2. *In vitro* assessment of neurite sprouting on polymers that contain varying amounts of acetylcholine-like motif.
3. Fabrication of porous scaffolds containing longitudinal channels with controllable properties using salt leaching and fiber templating.

1.4 Nervous System Biology and Responses to Injury

1.4.1 Components and Organization of the Peripheral and Central Nervous System

By understanding the organization and the biology of the nervous system, specific strategies may be developed to overcome the particular challenges associated with peripheral and central nerve repair. The peripheral nervous system (PNS) includes cranial, spinal, and sensory nerves emanating from the brain, from the spinal cord, and to the extremities, respectively. The brain and spinal cord comprise the central nervous system (CNS). The main functional cell of both the CNS and PNS is the neuron. A neuron forms specific contacts (synapses) with other neurons via processes called axons and dendrites to create networks. Neurons secrete chemical messengers, called neurotransmitters, at chemical synapses to propagate electrical signals to be received by the post-synaptic neuron at its dendrites. They also interact with support cells that provide trophic factors: Schwann cells in the PNS or astrocytes and oligodendrocytes in the CNS. Schwann cells and oligodendrocytes coat most neurons with myelin protein that aids in the conduction of electrical signals. Astrocytes promote the myelinating

activity of oligodendrocytes, modulate neurotransmitter uptake and release, and maintain synaptic plasticity[36]. These cells have a significant effect on the regenerative process (See 'PNS and CNS Responses to Injury'). Microglia are another set of cells present in the CNS. Sharing many properties with macrophages, they scavenge cell debris and secrete molecules that affect the immune and inflammatory response in the CNS.

In the peripheral nerve, the myelin sheath envelops one or several axons, which is then surrounded by the endoneurium. The perineurium wraps together several axons and their endoneurium to form bundles (fascicles). A sheath of connective tissue called the epineurium surrounds several fascicles to form the nerve. In the spinal cord, myelinated nerve bundles are found in the spinal tracts (white matter), which carry information to and from the brain. Unmyelinated neurons are located in the gray matter, where synapses are formed between interneurons, sensory (afferent) neurons, and motor (efferent) neurons.

1.4.2 PNS and CNS Responses to Injury

Traumatic injury, as well as degenerative diseases, can considerably alter the architecture and function of peripheral and central nerves. Though neurons and glia function similarly to propagate electrochemical signals in the PNS and CNS, these cells possess dramatically different regenerative responses after injury that depends on their environment. Though CNS neurons were previously believed to be incapable of regeneration, it was shown that neuronal sprouting occurred from an injured spinal cord into a peripheral nerve graft, therefore indicating the role of environment in CNS regeneration[37]. Increasing evidence supports the observation that the regenerative ability

of the nerve is highly influenced by permissive and non-permissive cues in the environment. The different abilities of the CNS and PNS to promote growth may be attributed to the following: 1) in the PNS, the role of Schwann cells in providing trophic factors[38]; 2) in the CNS, the presence of myelin and myelin-associated inhibitors [39]; 3) the suppression of apoptic pathways and activation of anti-apoptotic proteins[40]; and 4) the effect of the glial scar in spinal cord injury[41]. Key events and the role of cellular components are summarized below.

A myriad of neural cell-types, as well as cells of the inflammatory system, are involved in responses after PNS injury. Upon transection, the distal portion of the nerve begins to degenerate due to protease activity and separation from the cell body or soma[7] (**Figure 1.1a**). The proximal portion may also undergo apoptosis, depending on the neuron's age, type, and distance of axotomy from the proximal end[42]. Several hours after injury, growth-related molecules are upregulated, inducing axons and growth cones to sprout from the nodes of Ranvier and the soma. During this time, Schwann cells play a key role in regeneration by increasing their proliferation to form Bands of Bünger and by secreting neurotrophic and chemotactic factors that influence growing axons, adjacent Schwann cells, and macrophages. Schwann cells are also able to expedite the elimination of myelin, which inhibits axonal regrowth, by degrading their own myelin, phagocytosing extracellular myelin, and presenting myelin to macrophages. Two to three days after injury, macrophages infiltrate the site to clear it of cell debris and myelin, which may require up to 2 weeks post-injury for completion.

While small nerve gaps can be repaired by the human body, the regeneration of large nerve gaps (greater than 3 mm) is more difficult. Greater control over the direction

of axon sprouting toward the distal nerve is desired, since inappropriate reconnections lead to neuropathic pain. The direction and rate of axonal re-growth is affected by the presence of substrate or soluble cues that may be growth-permissive or repulsive. Effective spatio-temporal presentation of these cues may be used to better guide the growth cone. In addition to axonal re-growth, improving the myelination of the sprouted axons is also likely to improve functional recovery. This is a challenge since longer denervation of the remaining Schwann cells further reduces their capacity to support regeneration.

Currently, there is no treatment that enables complete functional recovery after spinal cord injury, likely due to significant cell death and the presence of a growth-inhibitory environment. The spinal cord is incapable of regeneration without intervention. Within thirty minutes of axotomy, the proximal and distal axons degenerate hundreds of microns (**Figure 1.1b**). Axons that are not damaged by the initial injury also degenerate from secondary events. The loss of axonal contact causes oligodendrocytes to undergo apoptosis 4-8 days after injury, which is significant since axons can survive up to 7 days post-injury. Surviving oligodendrocytes revert to quiescence and, unlike their Schwann cell counterpart, contribute little to clearing myelin and axonal debris. Myelin and myelin-associated components are inhibitors of axon growth *in vitro*. Due to the blood-spine barrier and limited access to the injury site, macrophages do not play an appreciable role in myelin clearance. Microglia, which are considered to play a role in CNS immune responses, increase proliferation 4-6 days post-injury but fail to develop into fully phagocytic cells. Therefore, myelin can still be found several years after degeneration of the nerve. In addition to myelin, glial scarring at the lesion is another

growth-inhibitory barrier that prevents regeneration. The main inhibitory component of glial scars is chondroitin sulfate proteoglycans, molecules that are secreted by reactive astrocytes and are characterized by a protein core to which highly sulfated glycosaminoglycans are attached. Chondroitin sulfate proteoglycan synthesis can be strongly increased and may be expressed as soon as 24 hours post-injury. Therefore, the majority of current investigations in CNS nerve regeneration focus on increasing cell survival and creating a growth-permissive environment. In addition, increasing the axonal elongation rate, directing axonal sprouting, and improving the myelination of newly sprouted and surviving axons are also highly relevant goals for achieving functional recovery in CNS repair.

Biomaterial-based treatments may be used to encourage re-growth of the nerve after injury by integrating biochemical cues, providing physical guidance through a substrate, or both. Biomaterials in the past have incorporated extracellular matrix (ECM) molecules that have adhesive and growth promoting properties. They have been used to deliver neurotrophic factors to encourage survival of neurons and supporting cells. The material itself may also have intrinsic properties which are not cell-derived that promote growth, such as the use of conductive materials to modulate the neuron's electrical and chemical activities. The material's surface topology and its dimensions have also been used to guide neurite orientation. In general, the goal of using materials in nerve tissue engineering is to enhance the regenerative process by creating a growth-promoting environment and directing axonal growth to reconnect nerves for functional recovery.

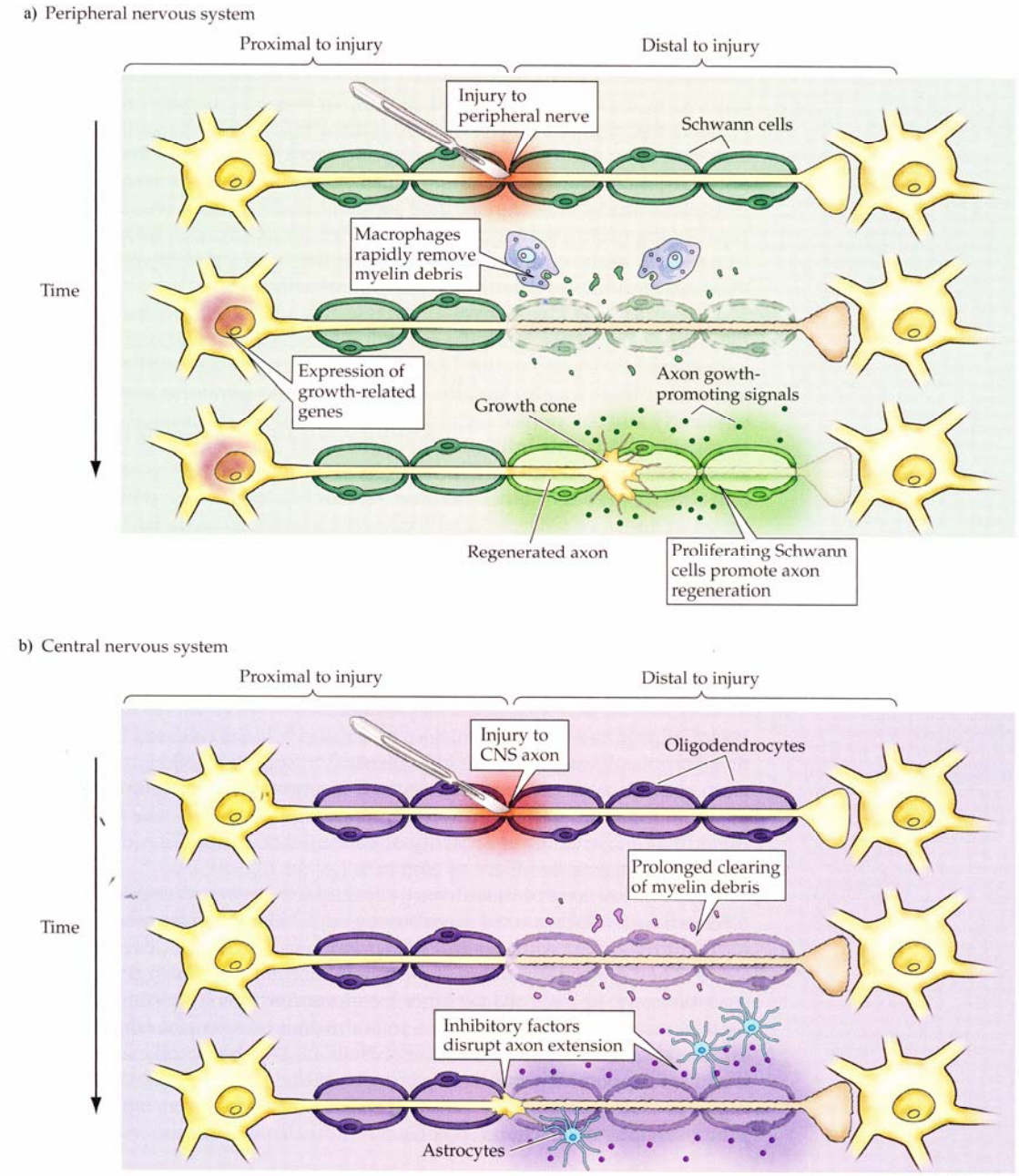

Figure 1.1 Response after injury in the peripheral (a) and central (b) nervous systems[43].

1.5 Biomaterials for Nerve Tissue Engineering

1.5.1 Materials in Cell Therapies

Cells may be delivered to the site of injury to replace lost cells, impart trophic support, or provide neuronal attachment sites through cell adhesion molecules. Those that have been implanted for nerve regeneration include embryonic and adult stem cells, Schwann cells, olfactory ensheathing cells, and genetically modified cells expressing neurotrophic factors. Transplantation of embryonic stem cells has improved locomotor function following spinal cord injury, likely by enhancing myelination and improving axonal conduction[44]. *In vivo* implantation of neural progenitor cells derived from rat embryonic spinal cord has led to neurogenesis of the donor-derived cells and neurite extension of these cells into the host tissue[45]. Ethical concerns associated with using embryonic stem and progenitor cells may make cell therapies using adult cells more feasible, at least in the short term. Transplantation of adult-derived progenitor cells, which can also differentiate into oligodendrocytes *in vivo*, led to increased myelination and improved locomotion after spinal compression[46]. Schwann cells, which are responsible for myelination in the PNS, produce a variety of growth factors, cell-adhesion molecules, and ECM that create a more permissive environment for nerve growth[47,48]. Schwann cells induced greater axonal ingrowth into the lesion[47,49] as well as enhanced the responsiveness to electrical stimulation[50] when implanted after spinal cord injury. Olfactory ensheathing glia cells have also been implanted following nerve injury because they express nerve growth factor (NGF), neurotrophin-4/5, neurotrophin-3, and brain derived neurotrophic factor (BDNF), and can remyelinate demyelinated spinal cord axons[48]. Potential difficulty in isolating these cell types may be alleviated by genetically

modifying non-neural cell types to provide trophic support. For exmple, fibroblasts expressing neurotrophin-3, neurotrophin-4/5, NGF, and BDNF have been delivered to injury sites of chronic and acute models of spinal cord injury[51,52].

Delivery of cells alone to the injury site often results in limited cell retention, likely due to cell death or migration from the site. Biomaterials can be fabricated into scaffolds to locally deliver and promote the retention of the cells and neurotrophic molecules they secrete, as well as provide a physical construct to guide regeneration. Cell-seeded scaffolds may be more effective at guiding growth by localizing the presence of growth-stimulatory molecules. Although growth factor secretion surrounding the site is desirable for creating a growth-permissive environment, random cell spreading may lead to non-directed growth of axons that can cause neuropathic pain. Scaffolds with appropriate biochemical and physical cues may guide axonal extension and target regeneration toward the distal end of the severed nerve. A scaffold may act as an effective barrier to inhibit the infiltration of cells that secrete growth-inhibitory molecules to the injury site. The scaffold properties may also be controlled to improve cell loading, growth factor secretion, and cell differentiation for use of cell-seeded nerve guidance channels.

1.5.1.1 Natural Materials for Cell Therapies

Cellular Grafts. Peripheral nerve grafts, fetal tissue grafts, and autologous vein grafts have been used to support axonal sprouting and extension *in vivo*. CNS neurons can regenerate in a permissive environment, as evidenced by axonal sprouting from a transected spinal cord growing into a peripheral nerve graft[53]. The ability of peripheral

nerve grafts to induce axonal sprouting after spinal cord injury also depends on the age of the recipient: adult rat supraspinal axons did not grow into sciatic nerve grafts while rat neonate neurons did[54,55]. Although CNS axons extended into peripheral nerve grafts, various studies have indicated that animals receiving them were still unable to overcome functional deficits, which include paralysis and minimal hindlimb-forelimb coordination[54]. Axons that entered the nerve grafts did so in a meandering, disorderly manner, unable to grow beyond the distal boundary of the host-graft interface[54]. The inability of axons to cross the boundary indicates that the graft environment may be too growth-permissive to permit axonal exit from it. Alternatively, the duration of axonal sprouting and extension through the peripheral nerve graft may permit scar tissue formation, which acts as a barrier for reconnecting the nerves. While PNS nerve grafts are limited in promoting regeneration in CNS regeneration, there has been some success using fetal tissue grafts to promote neural reconnections across the distal graft-host interface. Fetal spinal cord transplants rescued axotomy-induced retrograde cell death, specifically by preventing death of red nucleus neurons in adult rats[55]. In a study comparing PNS nerve grafts with fetal spinal cord grafts, tissue that regenerated from the latter seamlessly integrated into the spinal cord and extended farther caudally than in the PNS grafts[54]. Limited supply of such grafts and the ethical constraints surrounding their use makes the feasibility of using fetal spinal cord grafts in the clinic questionable. Though they have only been used in PNS regeneration, vein autografts may have applications in CNS repair, as they are more readily available and can be isolated from the patient for use in nerve repair. The vein's ability to promote axonal sprouting and myelination is still not equivalent to that of an autologous peripheral nerve. However,

filling these grafts with collagen and adding Schwann cells to the vein scaffold improved their ability to promote peroneal[56] and sciatic nerve[57] regeneration.

Polysaccharides. Agarose, an alternating co-polymer of 1,4-linked 3,6-anhydro-α-L-galactose and 1,3-linked β-D-galactose, forms a solid below its gel-solution temperature and can be used to encapsulate cells[58,59]. It has been fabricated into nerve guidance scaffolds with uniaxial channels, either through a freeze-drying[60] or a templating method[24]. Scaffolds produced by both methods integrated into the spinal cord lesions, showing Schwann cell infiltration, axonal penetration, and angiogenesis through the channels. Axonal growth can be further enhanced by adding BDNF, either through adsorption by rehydration of the agarose[60], or by loading the channels with bone marrow stromal cells genetically engineered to secrete BDNF[24].

Proteins. Collagen, an ECM protein, can be processed into hydrogels and fabricated into different types of scaffolds. The dimensions of the scaffold and presence of Schwann cells influence collagen's ability to promote growth. Hollow nerve guides of collagen gel were used to investigate the effect of Schwann cell implantation following a thoracic level spinal cord lesion[61]. When fabricated as hollow nerve guides, pure collagen grafts did not support *in vivo* axonal elongation or Schwann cell entry into the matrix. The inclusion of Schwann cells significantly improved the regenerative response, wherein cell-seeded collagen channels promoted axonal sprouting by 14 days and myelination by 28 days after implantation.

Gelatin, the hydrolysis product of collagen, has been investigated in nerve regenerative applications. Hippocampal neural stem cells and Schwann cells have been encapsulated into gelatin foams to improve functional recovery after spinal cord

transection[62]. Neural stem cells or Schwann cells, both transduced with an adenovirus expressing neurotrophin-3, were seeded into gelatin foam. The seeded forms were used to fill the transection site. Animals that received either cell type contained significantly more neurons in the sensorimotor cortex, red nuclei, and Clarke's nuclei than those that did not receive any treatment after spinal cord transection. The higher number of neurons may be attributed to enhanced survival of the neurons, the differentiation of the stem cells into neurons, or trophic support provided by the Schwann cells. With co-transplantation, hindlimb locomotor function was significantly increased while the expression of inhibitory chondroitin sulfate proteoglycans was suppressed.

While collagen and gelatin enables Schwann cell attachment and axonal extension, these ECM proteins must be isolated from animal or human sources. For clinical applications, the risk of pathogen transmission via graft materials must be minimized. Simultaneously, alternative materials that promote regeneration while reducing this risk are desirable.

1.5.1.2 Synthetic Materials for Cell Therapies

Polylactide (PLA) and poly(lactide-co-glycolide) (PLGA) are aliphatic polyesters and polyhydroxyacids have been used to deliver Schwann cells, genetically modified Schwann cells, and neural stem cells for in nerve tissue engineering. Using a porous PLA scaffold, Schwann cells were implanted into a 12 mm sciatic nerve defect in rats. Compared to the isograft control, PLA scaffolds seeded with Schwann cells had nerve fiber density that was significantly lower after four months, with no difference in the mean sciatic functional index[63]. The effect of implanting genetically altered Schwann

cells using PLA has also been investigated. Schwann cells, modified to express a bi-functional neurotrophin with BDNF and neurotrophin-3 activity, were encapsulated in a fibrin solution and implanted into a spinal cord defect using PLA macroporous scaffolds[22]. Myelinated axons extended into the construct 6 weeks after implantation; however, the axons did not extend out of the scaffold containing transduced Schwann cells, nor was there complete functional recovery with this treatment. Neural stem cells within PLGA scaffolds have also been implanted following hemi-section of the spinal cord in rodents. Rats that received scaffolds with stem cells demonstrated significant improvement in open-field locomotion up to 28 days post implantation compared to rats that received cells alone or no treatment at all.[64] However, there was no statistical difference in behavioral outcome between cell-seeded scaffold and scaffold alone.

Poly(hydroxybutyrate) (PHB) is a bacteria-synthesized polymer that degrades into a non-toxic metabolite in mammals[65]. Implanting neonatal Schwann cells using PHB fibers enabled axonal elongation into the rostral and caudal ends following a cervical spinal cord laminectomy[65]. In another study, transplantation of a hollow PHB conduit seeded with Schwann cells into a 10 mm sciatic nerve gap resulted in longer axonal extension into the lesion compared to PHB conduits alone[66]. Schwann cell delivery using PHB scaffolds appears to improve peripheral nerve regeneration as evidenced by the presence and close association of regenerating axons with Schwann cells[66,67]. It is unclear whether Schwann cell-seeded PHB scaffolds would perform better than the gold standard for peripheral nerve regeneration, however, since no autograft controls were included in these experiments.

Poly(acrylonitrile-co-vinylchloride) (PAN/PVC) is a co-polymer with substantial tensile strength that has also been used to investigate the potential therapeutic effects of Schwann cells. The effect of Schwann cells in eliciting axonal growth after spinal cord transection was explored using PAN/PVC nerve guides loaded with Schwann cells in Matrigel[68]. One month after implantation of the nerve guide channels, Schwann cell-seeded constructs exhibited significantly greater myelination and an eight-fold increase in umyelinated axons over Matrigel-only control[68]. PAN/PVC guidance channels seeded with Schwann cells were also used to determine that regenerated CNS axons responded to electrical stimulus and conducted action potentials after spinal cord transection[50]. Although PAN/PVC is not biodegradable, its presence did not preclude axonal extension, myelination, or re-establishment of electrical connections. The PAN/PVC channels minimized connective tissue infiltration but contributed to grey matter necrosis of the spinal cord[69].

Administration of neurotrophins in conjunction with Schwann cell implantation showed promise in eliciting axons to cross the graft-host boundary. The infusion of neurotrophin-3 and BDNF distal to a Schwann cell-filled PAN/PVC channel allowed more axons to re-enter the distal cord after spinal cord laminectomy, with each neurotrophin promoting a different morphology of axonal sprouting[70]. In addition to improving the ability of axons to traverse the lesion, growth factor delivery can also enhance myelination. Adding glial derived neurotrophic factor (GDNF) to a Schwann cell-seeded PAN/PVC channel increased the myelination of axons three-fold, from 11% myelinated axons to 33%[71].

1.5.2 Neurotrophin-containing Materials

The failure of cells to activate regeneration-associated genes and the accompanying lack of neurotrophic support are main contributing factors that hinder nerve repair[72,73]. The application of neurotrophins has been associated with inducing the growth of specific subpopulations of axons, facilitating synaptic transmission, and improving functional recovery[74-77]. The ability of growth factors to impart a positive effect on regeneration has been assessed by directly injecting the molecule of interest to the injury site, or by delivering it via cells or polymer vehicles.

Utilizing biomaterials to deliver growth factors may enable spatio-temporal control over the presentation of bioactive molecules. It is important to locally stimulate regeneration, since non-directed neurite sprouting can cause neuropathic pain. Biomaterials have the potential to achieve local, sustained delivery of neurotrophic factors by encapsulating, facilitating electrostatic interactions, or covalently incorporating them. However, free growth factors are rapidly decomposed by enzymes in the body. A biomaterial delivery matrix can stabilize growth factors, which have a very short half life in the body[78,79]. Using a biomaterial, in effect, may increase the amount of available neurotrophic factor by concentrating it to the desired site of delivery and by preventing its degradation once inside the body. The ability to deliver multiple growth factors in a controlled manner over time is also desired, as a variety of neural and inflammatory cells are involved following nerve injury.

1.5.2.1 Natural Materials for Neurotrophin Delivery

Polysaccharides. Alginate and agarose are polysaccharide-based hydrogels that have been used as delivery vehicles for growth factors and scaffolds for CNS and PNS repair. Alginate encapsulation of growth factors has been used concurrently with autologous nerve transplant in repairing the sciatic nerve. Calcium alginate, an FDA-approved polysaccharide, facilitated continuous release of encapsulated BDNF over 8 weeks *in vitro*[80]. When implanted with autologous fascia tubes to regenerate a 20 mm rat sciatic nerve gap, animals receiving the treatment exhibited greater nerve fiber elongation and significantly less auto-cannibalization, an indicator of neuropathic pain in rats. Agarose is liquid above its gelation temperature and can be used to fill irregular cavities that develop from an injury. A combination of an agarose scaffold with BDNF-loaded lipid micro-tubes has been tested to treat spinal cord injury[81]. Compared to an agarose-only scaffold, the addition of BNDF enhanced axonal extension into the construct. No regenerating fibers, however, re-entered the host tissue[81]. While the addition of growth factors beyond the lesion may promote axon sprouting into the distal region, it is also possible that glial scarring at the boundary or the presence of other inhibitory cues play a role.

The effect of growth factor gradients, presented in soluble form or immobilized within a material, can alter neurite growth. With agarose scaffolds, the effects of NGF amounts and concentration gradients on neurite extension were tested *in vitro*. A compartmentalized diffusion chamber was utilized to create a concentration gradient of soluble NGF within the middle well that contained PC12 cells[82]. The gradient, not the absolute concentration, guided the direction of neurite growth. The potential of an

anisotropic environment to promote regeneration was also assessed in an agarose scaffold containing gradients of laminin and NGF[83]. Following a 20 mm rat sciatic nerve gap, only animals receiving grafts with gradients of both laminin and NGF elicited axonal sprouting into the agarose scaffolds. Though anisotropic grafts led to comparable sciatic nerve re-innervation compared to the autologous nerve, the resulting re-innervation with these treatments were still considerably lower than that provided by the native muscle[83]. Additionally, immunohistochemical staining revealed that nerve grafts and anisotropic scaffolds were deficient in synapses that co-stained for pre- and post-synaptic markers, compared to native nerve[83]. Though regeneration of axons may improve the re-innervation of muscles, re-establishing synaptic connections may also be as critical for complete functional restoration.

Proteins. Proteins that have been used for neurotrophic delivery include gelatin, collagen, fibronectin, silk, and fibrin. The growth factor was incorporated into the protein either through physical adsorption, entrapment, or covalent modification of the material.

Immobilizing growth factors onto scaffolds may prolong the presence of a bioactive molecule at the site of injury. NGF, BDNF, and insulin like growth factor-1 (IGF-1) have each been covalently bound onto gelatin-tricalcium phosphate for repairing a sciatic nerve gap[84]. Electrophysiological studies showed that animals receiving NGF, BDNF, and IGF-1 exhibited a compound muscle action potential, whereas animals treated with gelatin did not. An increase in gastrocnemic muscle weight ratio, a measure of muscle re-innervation, was seen with BDNF treatment, but there was no difference in sciatic functional index between control and growth factor treatments. It is important to

note that in this study, all growth factors were tested individually and each at the same concentration.

It is possible that the potency of eliciting regeneration varies according to growth factor, and that regeneration can be enhanced by using different concentrations of each. Collagen gels were used to study the effects of soluble NGF, GDNF, and CNTF concentrations on DRG neurite growth[85]. This study determined that the optimal concentration for eliciting the longest neurites was different for each growth factor, and demonstrated the potential to further enhance regeneration using a combination of soluble growth factors at varying concentrations.

To enhance regeneration, the release profiles of growth factors may be manipulated by taking advantage of differences in interactions between the growth factor and materials used to deliver them. Variations in handling and preparation of the same material-growth factor combination can be sufficient to affect the release profile. NGF, encapsulated into silk fibroin nerve channels, was released faster into buffer when the scaffolds were prepared by air-drying than those by freeze-drying[86]. In another study utilizing non-covalent interactions, the delivery of neurotrophin-3 adsorbed onto fibronectin mats into a 10mm rat sciatic nerve defect led to increased axonal extension and more myelinated axons compared to fibronectin-only scaffold[87].

Affinity-based binding of the growth factor to the delivery matrices may stabilize the growth factors and control their release. In directed affinity-based loading, interactions that promote binding of the growth factor onto the matrix appear to improve bioactivity. The binding of NGF-β to collagen was enhanced by generating a fusion protein containing the primary sequence of mature NGF-β, the collagen-binding

polypeptide TKKTLRT, and a histidine purification tag[88]. When compared to soluble NGF of equivalent concentration, collagen-bound NGF elicited greater neurite outgrowth and increased survival of PC12 cells, indicating its potential application in nerve repair. A similar approach in the controlled release of growth factors utilized the affinity between heparin and heparin-binding growth factors. An immobilized heparin-binding peptide on a fibrin matrix was used to sequester heparin, which subsequently bound bFGF, NGF-β, BDNF, and neurotrophin-3[89,90]. Delivery of these growth factors to dorsal root ganglia led to significantly longer neurites[89,90]. An *in vivo* study showed increased neural fiber sprouting and integration with neurotrophin-3 and the heparin-based delivery system nine days after acute spinal cord injury; however, there was no improvement in hindlimb motor function at 12 weeks[91,92]. A modification to this fibrin-based delivery system utilized phage-display to identify peptides with NGF affinity[93]. Consensus sequences having significant ability to promote NGF binding were identified and coupled to fibrin via the Factor XIIIa substrate (in italics): *NQEQVSP*NQSPNHTQNRAY, *NQEQVSP*QMRAPTKLPLRY, *NQEQVSP*SVSVKAKKSVNR). While the release profile could be tailored according to the peptide used, an *in vitro* study showed no significant difference in neurite length using the peptide affinity-based delivery system.

1.5.2.2 Synthetic Materials for Neurotrophin Delivery

A variety of growth-factor modified, synthetic polymers have shown potential for applications in nerve tissue engineering. Synthetic materials have delivered physically entrapped neurotrophins, which can be used to create a gradient within scaffolds.

Additionally, polymers have also been used to facilitate genetic modification of cells in order to impart them with an ability to produce growth factors.

Growth factor delivery and topographical guidance using a co-polymer of poly-caprolactone and ethylene phosphate has been investigated in sciatic nerve regeneration. Animals treated with co-polymer that had been electrospun with BDNF exhibited significantly greater number of myelinated axons than fibers without BNDF[28]. Longitudinally aligned fibers containing BDNF promoted significantly more electrophysiological recovery in rats compared to no treatment; however, there was no significant difference with fibers without BDNF. Topological guidance via electrospun poly-caprolactone and ethylene phosphate was sufficient at promoting electrophysiological recovery. Further behavioral testing is needed to assess the effect on functional improvement.

Synthetic polymers have been used to entrap neurotrophic factors within scaffolds or microspheres in order to modulate nerve growth. A PLA tubular scaffold delivered BDNF to treat acute spinal cord transection, enhancing neuronal survival at the rostral interface and more rapid axonal growth into the implant[23]. Axons were found earlier within BDNF-foams, but did not translate into behavioral improvement over scaffolds without BDNF. Another entrapment strategy involves encapsulation of the bioactive molecule to effectively control the rate of growth factor release. Controlled release of NGF has been investigated using PLG, PLGA[25,94], pHEMA-pMMA[94], allowing NGF to be delivered from 220 pg to 8624 pg per cm of scaffold. Properties of the guidance channels, such as the molecular weight of the polymer or porosity of the scaffold, were also tailored to vary the release rate of neurotrophic factors from the scaffold[25]. The

appropriate release kinetics that are effective at creating a growth-permissive and pro-survival environment are still to be determined, as these advanced delivery techniques have not been tested *in vivo*.

Electrical modulation of conducting polymers doped with growth factors may be used to control spatio-temporal presentation of growth factors. NGF and neurotrophin-3 have been incorporated into polypyrroles and their effects tested *in vitro.* NGF that was entrapped during the polymerization of a conducting polymer maintained its bioactivity and induced neurite extension from PC12 cells[95]. Because the polypyrrole-NGF composite did not adequately promote cell attachment, collagen was also incorporated to improve adhesion[95]. Electrical stimulation of polypyrroles containing neurotrophin-3 released more growth factor than unstimulated composites[96,97], likely leading to greater neurite outgrowth seen on stimulated polypyrrole with neurotrophin-3 than on unstimulated composite.

Growth factors have also been immobilized onto synthetic polymers. Immobilized NGF on poly(dimethyl siloxane) maintained its ability to elicit axonal extension from hippocampal neurons *in vitro*[98]. Similar enhancement in polarization and neurite extension in culture was observed when 0.11 ng/mm^2 of immobilized NGF (determined by a FITC-conjugated NGF assay) or 50 ng/ml of soluble NGF was added to the same surface. NGF covalently bound onto pHEMA also retained its bioactivity, demonstrated by the ability of the NGF-pHEMA material to cause PC12 differentiation and subsequent neurite extension[99]. In another study, immobilized gradients of NGF and neurotrophin-3 within pHEMA hydrogels were created in order to assess the effect on neurite guidance. Dorsal root ganglia responded to an immobilized gradient of NGF at

310 ng/ml-mm by orienting neurite growth up the gradient. Furthermore, a lower NGF gradient of 200 ng/ml-mm and neurotrophin-3 gradient of 200 ng/ml-mm[100] elicited guidance, indicating a synergistic effect of the two growth factors on neurite orientation. It is important to clarify that such combination effect is not always observed[85], and may depend on growth factor concentrations as well as the co-localization of neurotrophic receptors[100]. Further investigation is needed to determine which growth factors work in concert to promote regeneration and the mechanisms by which immobilization affects growth responses. The conducting polymer polypyrrole has also been covalently modified with NGF. The combination of electrical and bioactive stimulation significantly enhanced neurite length after 2 days[101]; however, it was not reported whether electrical stimulation prompted increased release of the immobilized NGF.

The methods discussed here have so far utilized materials to deliver bioactive molecules; biomaterials may also be used as carriers of genetic information to impart cells with the ability to produce growth factors. Using PLGA-mediated DNA delivery, cells were induced to produce bioactive NGF that was capable of eliciting neurite extension from dorsal root ganglia. cDNA complexed with Lipofectamine was incorporated into PLGA disks by compression molding, which were then used as substrates for cell-seeding to enhance transduction[102]. The transfection efficiency using PLGA-mediated lipofection reached 48%. PLGA patterned with microchannel widths ranging from 100 to 250 μm have also been used for localized DNA delivery[103]. The channel width affected the transfection efficiency; the 100 μm-wide channels exhibited 16% efficiency whereas the 250 μm-wide channel transduced 52% of the cells. Cells which take up the cDNA can continuously produce the growth factor without depletion.

1.5.3 ECM protein-modified Materials

ECM components are widely used in tissue engineering applications[104] and their particular effects on neural responses have been investigated[105-108]. ECM molecules influence a variety of cellular processes that include cell migration, axonal guidance, synaptogenesis, survival, differentiation and myelination[109,110]. ECM proteins are likely substrates for treating nerve injury because components such as laminin, thrombospondin, vitronectin, and fibronectin have been found to support axonal extension during CNS development[110]. Of these proteins, laminin is the most investigated in nerve tissue engineering applications for its ability to affect neuronal growth, survival, and guidance. When compared against collagens, proteoglycans, and fibronectin, laminin was most effective at promoting neurite outgrowth[111] and also has the ability to elicit outgrowth from a variety of central and peripheral neurons[112,113]. Additionally, particular domains on laminin promote neuronal survival[114] and can induce growth cone turning[115-117]. To impart bioactivity to polymers, most biomimetic approaches have focused on particular domains of laminin, including IKVAV, RNIAEIIKDI[118-120], YIGSR, and RGD[112,121,122]. These epitopes have been integrated into materials to take advantage of the ECM's cell adhesive and growth-promoting properties. The materials may be derived from natural polymers (polysaccharide-based and protein-based) or synthetic polymers.

1.5.3.1 ECM protein-modified Natural Materials

Polysaccharides. Agarose has been covalently modified with laminin and its epitopes to enhance neuronal adhesion, sprouting, and axonal extension. The presence

and density of laminin cues have been found to affect neuronal responses. Immobilization of YIGSR in three-dimensional agarose gels led to enhanced neurite extension *in vitro*[123,124] and significantly greater myelination of spinal cord axons *in vivo* relative to agarose[124]. Neuroblastoma cells attached and sprouted neurites in a dose-dependent manner when seeded onto YIGSR-agarose[125], a trend that was similarly observed in neurite sprouting from dorsal root ganglia cultured on YIGSR-fibrin substrates[126]. The steepness of the gradient also has an effect on neurite extension rate. A bi-phasic response to the gradient steepness was observed while testing the effect of immobilized gradients of laminin in agarose and an optimal laminin gradient that promoted the fastest growth rate *in vitro* was determined[127]. Interestingly, when laminin-gradient scaffolds were implanted following a 20 mm peripheral nerve gap in the rat, the laminin gradient alone did not lead to axonal regeneration, unless an NGF gradient was presented simultaneously[83].

While immobilized gradients may direct axonal growth, creating selectively adhesive regions of agarose has also been used to guide axonal elongation. Agarose was modified with photosensitive S-2-nitrobenzyl-cysteine and exposed to a focused laser beam to selectively incorporate G**RGD**S pentapeptide into 150 to 170 μm-wide channels[128]. The cell-adhesive channels guided neurite outgrowth from dorsal root ganglia. This method may be potentially useful in preventing neuropathic pain by controlling the spatial presentation of cell adhesive regions and guiding axonal reconnection to the targeted organ.

Chitosan scaffolds have been utilized in various tissue engineering applications and are generally considered biocompatible with many tissues[129,130]. Covalently

modified chitosan with YIGSR and IKVAV (each at 780 nmol per gram of chitosan) has enhanced neuronal adhesion, sprouting, and neurite extension *in vitro* when compared with un-modified chitosan[131]. Incorporation of either YIGSR or IKVAV significantly promoted superior cervical ganglion cells extend longer neurites on chitosan, and the immobilization of both peptides induced greater neurite extension than either IKVAV or YIGSR alone[131]. Nerve guidance channels made of YIGSR- or IKVAV-modified chitosan were reported to mediate neuronal sprouting *in vivo* following sciatic nerve injury, but did not significantly improve terminal latency compared to isograft[132,133].

Multiple laminin epitopes may also be used to maximize adhesion and neurite extension. Covalently modified methacrylated dextran with either RGD or YIGSR and IKVAV dissimilarly affected neurite length[134]. Although there was no significant difference in the adhesion of dorsal root ganglion neurons, the average number of neurites was considerably greater on the material with both YIGSR and IKVAV than on RGD-modified dextran[134]. The higher concentration of laminin epitopes might have attributed to the improved sprouting, as the peptide content of the YIGSR and IKVAV-containing scaffold was approximately twice that of the construct modified with RGD. The improved efficacy of incorporating multiple peptides on neurite extension and length has been demonstrated on agarose[123] and on chitosan[131] as well. New materials displaying a combination of peptides may be synthesized using the photo-conjugation technique described in the incorporation of RGDS into hyaluronan[135] and agarose[128]. Alternatively, the entire laminin molecule may be tethered to materials to impart them with its growth promoting properties. For example, methylcellulose covalently modified

with laminin may be useful in nerve repair by enhancing the viability of CNS neurons in cell transplantations[136].

Proteins. Collagen and fibrin modified with ECM derived domains have demonstrated effects on myelination, growth factor secretion, and neurite extension. Combinations of different peptide sequences and their potential interactive effects have been investigated using fibrin-based materials. Both collagen and fibrin are naturally-derived, and are, therefore, readily degraded *in vivo*. Collagen has been used in repairing peripheral nerve gaps[137-139], while fibrin can regulate neural cell activities after nerve injury[140,141].

Collagen has been used to investigate how immobilization of laminin epitopes affects neurite sprouting and sciatic nerve regeneration. Collagen has been modified by cross-linking collagen with YIGSR-conjugated dendrimers[142]. Dorsal root ganglia cultured on YIGSR-modified collagen sprouted greater and longer neurites than on unmodified collagen. Using an RGD-conjugated collagen construct (with 3.5 nM/cm^2 peptide), sciatic nerve regeneration of a 10 mm gap in rats was significantly improved by 30 days compared to a collagen scaffold[143]. The RGD-modified collagen considerably enhanced functional recovery better than collagen or autograft treatments, as indicated by a higher sciatic functional index and statistically improved nerve conduction velocity. The presence of the RGD scaffold is thought to induce the proliferating cells adhered to the construct to secrete trophic factors. Collagen conduits covalently modified with RGD, GHK (found in laminin and collagen), and KRDS (found in human lactoferrin) also affect growth factor production when implanted into 10 mm sciatic nerve gap in

rats[139]. Peptide-modified scaffolds exhibited an upregulation of NGF, neurotrophin-3, NT-4, and GAP-43, when compared to unmodified collagen control.

A fibrin matrix incorporating the peptides IKVAV, RGD, HAV, YIGSR, and RNIAEIIKDI has been used to investigate the optimal peptide density for maximizing neurite growth[126]. A synergistic effect was observed between RGD, YIGSR, IKVAV, and RNIAEIIKDI, and scaffolds containing these peptides contained significantly more axons than un-treated or un-modified fibrin. The synergistic effect was observed with 1.7 mole of peptide (for IKVAV, YIGSR, and RNIAEIIKDI) per mole of fibrinogen, a lower amount of each peptide that is needed for maximizing axonal extension than when the peptide is used independently. Considering the potential interactions between various ECM peptides may give insights into developing materials that effectively promote regeneration and provide greater understanding over the biological pathways involved.

Recently, keratin derived from human hair was shown to have neuroinductive effects[106]. Keratin hydrogel was obtained after oxidizing the cross-links within the protein and isolating the gamma and alpha keratins. More Schwann cells attached onto keratin than fibronectin surfaces *in vitro*. When implanted into a 4 mm defect in mice tibial nerve, the keratin hydrogel promoted better functional improvement over an autograft control. The conduction delay was significantly lower and the amplitude of the motor action potential statistically better over an autograft control. It will be interesting to see this material's efficacy at regenerating longer peripheral nerve gaps or the spinal cord.

1.5.3.2 ECM protein-modified Synthetic Materials

Synthetic materials may incorporate ECM components through either surface or bulk modification. Factors that may determine the manner in which the material is altered include the following: 1) presence and ease of access to appropriate functional groups; 2) intended application of the finished material (i.e. film vs. scaffold); and 3) whether the bulk properties of the material need to be preserved in the material's application. For materials that lack accessible functional groups to allow the conjugation of ECM analogues, surface modification might be the only feasible method to create functional groups that would permit covalent modification with peptides or protein. Surface modification could promote cell interactions with the material surface when maintaining material bulk properties is desirable.

Low cell adhesion to fluoro-polymers and their current use in the clinic make them attractive for surface modification with peptides to encourage selective attachment of neural cells and neurite growth. Including a flanking unit for the epitope may allow the peptide to be presented more closely to its native conformation in laminin[144]. Covalently attaching extended peptides of YIGSR and IKVAV to ePTFE increased neurite length, though it is unclear whether this difference was statistically significant. Fluorinated polypropylene was also modified on the surface with YIGSR and IKVAV, each at 3.6 fmol/cm^2, leading to significantly greater and longer neurites than using either peptide alone[145]. The presence of two adhesive domains and the higher concentration of peptides likely encourage more cells to bind to the material, while the presence of a neurite-growth promoting domain significantly enhances neurite outgrowth. Another

study also confirmed that introduction of CDPG**YIGSR** onto hydroxylated fluorinated ethylenepropylene and PVA surfaces enabled the adhesion of neuroblastoma cells[146].

Surface modification of polypyrroles is important, since directly incorporating bioactive cues in bulk polymers can alter their conductive properties. Polypyrroles that contain a carboxy end have been synthesized to enable the attachment of RGD to the polypyrrole surface[147]. Covalent attachment of ECM analogues to these conducting polymers may improve their applications as neural probes and scaffolds[148] for nerve repair by facilitating cell-material interactions. Another approach to modifying polypyrrole surfaces with laminin-epitopes is through non-covalent interactions. Using a bacteriophage library to identify peptides that are particularly adhesive to polypyrroles, G**RGD**S was grafted on polypyrrole and enabled PC12 cells to adhere to the material[149]. The adhesive peptides stably bound to the polypyrrole in the presence of serum for up to 21 days.

Synthetic polymers that are bulk-modified with ECM epitopes are mostly hydrogels. Poly[N-(2-hydroxypropyl)methacrylamide] (pHPMA) has been modified with RGD for *in vivo* implantation for CNS nerve regeneration, while poly(ethylene oxide) (PEO), pHEMA, and self-assembling peptide nanofibers are currently being investigated *in vitro* for their ability to promote neurite sprouting and extension.

RGD-modified pHPMA scaffolds had a higher density of axons than compared to unmodified pHPMA when implanted into the lesioned optic tract, cerebral cortex[150], or following spinal cord laminectomy[151]. Peptide-conjugated scaffolds also exhibited greater vascularization, and were infiltrated by astrocytes and macrophages. While

vascularization of tissue engineered nerves can facilitate the exchange of nutrients and waste, the presence of astrocytes may inhibit nerve regeneration.

In vitro testing of ECM-modified biomaterials showed that they promote neural adhesion and sprouting, and may influence stem cell differentiation. Immobilized fibronectin on PEO was more effective at eliciting neurite extension from dorsal root ganglia compared to similar concentrations of adsorbed fibronectin on polystyrene[152]. At similar fibronectin concentrations, between 200 ng/cm^2 and 340 ng/cm^2, the immobilized fibronectin elicited neurites to extend twice as long as adsorbed fibronectin. pHEMA has also been modified with both CDPG**YIGSR** and CQAAS**IKVAV** to enhance neuronal adhesion and extension[26]. pHEMA scaffolds containing 92 to 106 μmole/cm^2 of peptide supported attachment and neurite outgrowth from dorsal root ganglia that were comparable to laminin and poly-L-lysine covered surface.

Non-laminin based ECM epitopes have also been used in developing biomimetic materials for nerve regeneration. Covalently linking a tenascin-derived peptide into UltraWeb (an electrospun polyamide matrix) has enhanced neurite outgrowth *in vitro*[153]. Tenascin-C, particularly the alternatively spliced fibronectin type-III repeat D region of this ECM molecule, contains the neurite outgrowth-promoting peptide VFDNFVLK[154]. The peptide significantly enhanced neurite outgrowth on proteoglycans and was more effective than laminin-1, L1 fused to human immunoglobulin, or intact tenascin-C. Compared to its soluble forms, conjugated fibronectin[152] and tenascin-C peptide[153] elicited improved neurite extension from dorsal root ganglia, cerebellar granule, cerebral cortical, hippocampal, and motor neurons. This difference in response may be due to differential activation of signaling pathways that depends on bound substrates.

Another approach to potentially enhance nerve regeneration is by replacing the loss of neurons after injury through biomaterial-induced differentiation of neural progenitor cells. Under regular cell culture conditions, including the use of laminin matrix, most neural progenitor cells will differentiate into glia. Self-assembling nanofibers were modified with IKVAV to facilitate differentiation of neural progenitor stem cells into neurons[155]. Neural progenitor cells that were encapsulated within the gel-like scaffolds migrated within the nanofiber matrix and exhibited neurite outgrowth. IKVAV-modified nanofibers significantly promoted a higher percentage of stem cells to differentiate into neurons than on the laminin and PDL after 7 days. Interestingly, the incorporation of IKVAV into other synthetic polymers has not resulted in enhanced differentiation of progenitor cells. IKVAV-modified phospholipid bilayers, which present the epitope on the surface, did not induce neuronal differentiation over laminin after 8 days[156]. Neuronal differentiation was also unaffected when using interpenetrating polymer network of poly(acrylamide-*co*-ethylene glycol/acrylic acid) that had been modified with IKVAV versus laminin[157]. These differences in observations may be attributed to the variations in the density of IKVAV presented on the material or to the mechanical properties of the substrate. The self-assembled nanofibers are estimated to present 7.1×10^{14} IKVAV/cm^2 [155], whereas the phospholipid bilayers are capable of presenting up to 1.64×10^{13} IKVAV/cm^2 [156]. The higher epitope concentration in the self-assembled nanofibers may be required to induce differentiation. Additionally, cell interactions with the synthetic substrate of the material (i.e. peptide amphiphile vs. phospholipid vs the IPN polymer) and source of the neural progenitor cells (cortical- vs.

hippocampal-drived stem cells) may also account for differences in these materials' ability to affect differentiation.

In addition to ECM-derived proteins, the L1 cell adhesion molecule has also been used to modify biomaterials. L1 is primarily expressed in the nervous system – on the surface of Schwann cells, olfactory ensheathing cells, the axon, and the growth cone[158]. L1 has been implicated in the adhesion, neurite outgrowth, and guidance of neurons[159,160]. L1-modified PEO may improve nerve regeneration by supporting the selective attachment of cerebellar neurons over astrocytes and meningeal cells when all three cells were simultaneously seeded[161]. Coatings of PEO that had been activated with pyridyl disulfide were incubated overnight with reduced L1 to create a bioactive surface. Hippocampal neurons and dorsal root ganglia neurons adhered to and extended neurites on the L1-modified substrate. Though the adhesion was assessed at 24 hours after plating, the short-term selective attachment of neurons may be beneficial for retaining surviving neurons following injury.

1.5.4 Conductive Materials

Electrical activity affects both the developing nervous system and the regenerative processes that occur after nerve injury. Immature cerebellar granule cells have been induced to proliferate through the depolarization caused by the neurotransmitter γ-aminobutyric acid[162]. Electrical changes through calcium transients also play a role in growth cone turning[163] and dendrite growth[164,165]. Direct application of electrical fields to neurons also has been shown to guide neurite growth. Neurons responded to field-induced membrane depolarization with neurite initiation and elongation[166,167]. Pre-

exposure to brief electrical stimulation has also converted the repulsive effect of soluble myelin-associated glyocoprotein to a growth-cone attractive molecule in frog neurons[168]. These observations have led researchers to investigate the potential roles of electrical stimulation following nerve injury.

There has been some improvement seen in axonal sprouting and extension in the presence of electrical stimulation. Animals that received direct current electrical stimulation at 0.6 μA and 1.35 V exhibited axons that traveled farther into the lesion site after sciatic nerve injury, when compared the un-stimulated group[169]. Short or long-term electrical stimulation appears to be effective, as continuous electrical stimulation for 1 hour or 2 weeks were both effective at accelerating the re-growth of the femoral motorneurons[170]. Electrical induction may accelerate growth by up-regulating neurotrophic factors or increasing sensitivity to the growth factor by increasing the expression of its receptor. Increased expression of BDNF, mRNA levels of trkB (BDNF receptor), and growth-associated protein 43 have been observed up to 2 days after only 1 hour of stimulation[170,171], and are thought to be involved in electrically-induced axonal regeneration.

In spinal cord injury, voltage gradients also promoted axonal extension into the lesion[172,173], with 60% of animals having regenerating axons present compared to 12% of animals without stimulation[172]. Compared to un-stimulated animals which showed no recovery in muscle reflex after spinal cord hemisection, 25% of animals that received electrical stimulation exhibited recovery[174]. Phase 1 clinical trials evaluating the effect of a human oscillating field stimulator on patients with complete motor and sensory spinal

cord injury also indicate that patients exhibited improved response in light touch, pinprick sensation, and motor status[175].

Conducting polymers have been mostly investigated for improving neural probes and biosensory applications. They are of main interest in nerve tissue engineering as they can provide a substrate that 1) locally delivers electrical stimulation, 2) be employed as a delivery vehicle for neurotrophins or small molecules that can enhance regeneration. Piezoelectric polymers and polypyrroles comprise most conducting materials, the latter of which is more commonly investigated due to the ability to control the amount and duration of electrical stimulation.

1.5.4.1 Piezoelectric Materials

Mechano-electrically stimulated, piezoelectric materials have shown potential as nerve tissue engineering materials by enhancing neurite extension, orientation, and myelination[176]. The polymers polyvinylidenefluoride (PVDF) and poly(lactic-co-glycolic acid) were rendered piezoelectric through a corona poling process (**Figure 1.2**), enabling them to generate an average voltage of 2.5 mV when placed on incubator shelves. Vibrations caused by the incubator were sufficient to generate small deformations and the corresponding electric field; *in vivo* implantation of a PVDF nerve guide is likewise expected to induce a voltage potential. In serum-free media, statistically greater neuroblastoma cultured on poled substrates extended neurites (approximately 59% vs. 42% at 96 hours), and neurites were also statistically longer (an estimated 270 mm vs. 200 mm, as ascertained from presented graphs) than cells cultured on unpoled substrates. Poled PVDF tubular nerve guides used to regenerate a 4 mm sciatic nerve gap have also

exhibited biocompatibility and promoted significantly greater myelination of axons compared to unpoled PVDF, acrylic copolymer, polyethylene, poly tetrafluoroethylene, and silicone elastomer[177,178]. The ability of poled materials to elicit regeneration compared to autograft controls were not reported, nor was functional recovery through behavioral assessment made. The effect of the poling process on increasing myelination *in vivo* has also been observed using poled PLGA[179]. Regeneration on PLGA that was poled at 24 kV for 45 minutes led to significantly more myelinated axons and faster conduction velocity than constructs that were poled at 20 kV for 10 minutes[179].

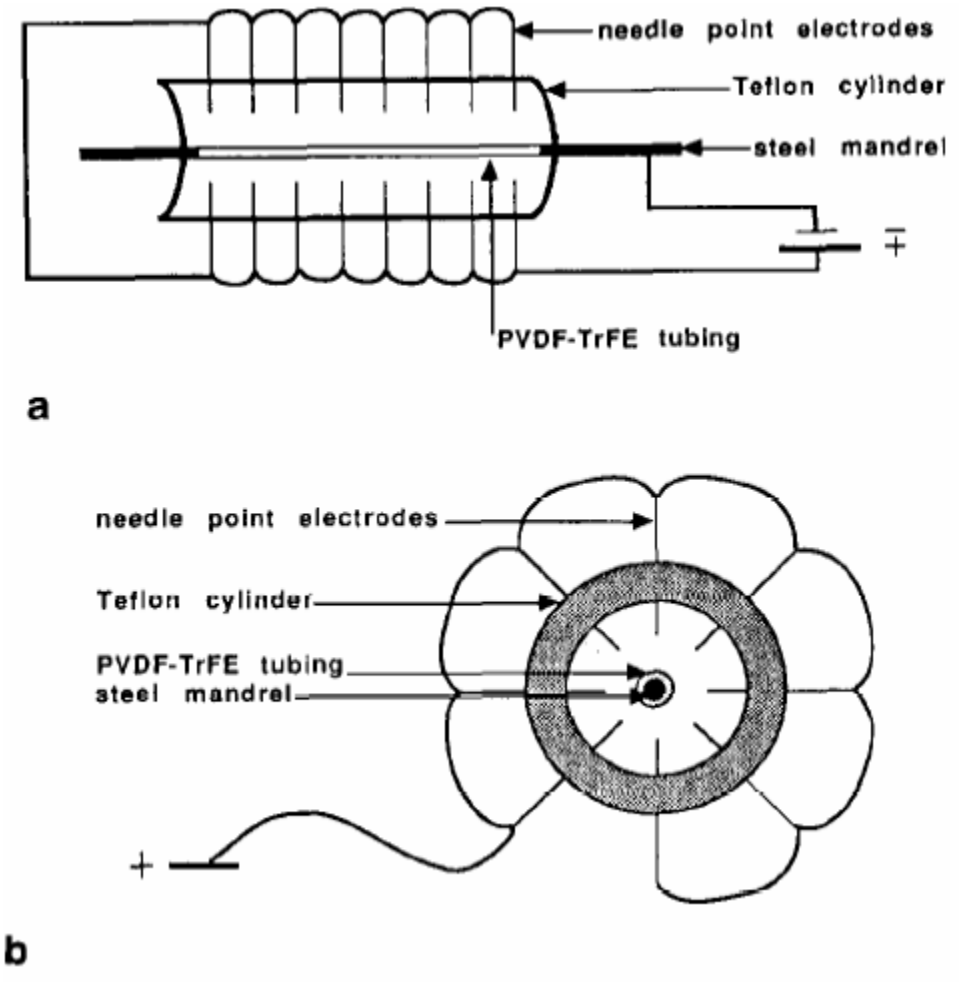

Figure 1.2. Corona poling device for rendering polymer tubes piezoelectric. Appling a high voltage d.c. field across the wall of the channel aligns dipoles within the polymer crystals. A: longitudinal view, B: Cross-sectional view of poling device[178].

1.5.4.2 Polypyrrole

Polypyrrole's conjugated structure of alternating C=C double bonds and C-C single bonds imparts them their electronic properties. Polypyrrole has been used to deliver electrical stimulation to PC12 cells, thereby significantly increasing neurite extension[180,181]. Their biocompatibility is similar to PLGA, eliciting equivalent or less inflammatory response when implanted subcutaneously or intramuscularly[180]. The use of polypyrroles in nerve repair has been limited due to their non cell-adhesive and permanent nature[148], the latter being a concern for long-term, *in vivo* implantation. The synthesis of polypyrroles is also limited to thin films due to the requirement to synthesize it onto an electrode[182].

Many efforts have focused on improving polypyrrole's cell adhesiveness while simultaneously maintaining its conductive properties. Surface-modification of polypyrroles with ECM or ECM-derived epitopes has attempted to enhance cell adhesion. Electrodeposition of polypyrrole with polyglutamic acid (polypyrrole-Glu) enabled the covalent attachment of polylysine and laminin onto its surface[183]. Dorsal root ganglion neurons attached onto the modified surface[183], however the effect of electrical stimulation on neuronal growth was not reported. A second surface modification technique utilized carboxy-endcapped polypyrrole for immobilizing RGD peptide. Polypyrrole was first deposited onto a conductive glass slide, which was then transferred to a solution containing the carboxy-endcapped polypyrrole[147]. RGD was attached to the polypyrrole by activating the carboxylic acids and reacting it with G**RGD**SP peptide. The conductivity of RGD-modified polypyrrole was nearly equivalent to unmodified polypyrrole, but promoted 88% greater endothelial cell adhesion after 3 hours[147].

Endothelial cells were utilized to gauge the general cell response to the bioactive cue; further investigation using neuronal cells are needed to assess its potential in nerve regeneration. RGD has also been non-covalently attached to the polypyrrole. Using a bacteriophage library, a phage clone (T59) that preferentially binds to polypyrrole was identified and synthesized with GRGDS. The resulting polypyrrole-T59-GRGDS enhanced PC12 adhesion compared to substrate without GRGDS[149], but was tested on primary neurons or *in vivo*.

In addition to surface modification techniques, bulk incorporation of ECM-derived components has been used to improve cell adhesion. The laminin B1-derived peptide sequence YIGSR and the laminin B2-derived RNIAEIIKDI have been incorporated into polypyrrole. RNIAEIIKDI-modified polypyrrole displayed lower impedance and had higher neuron density than polypyrrole with YIGSR. Compared to laminin, however, the highest neuron density observed on polypyrrole with any of its epitopes was still 3-fold lower[184].

Polysaccharide ECM components have also been combined with polypyrrole. Thin films of polypyrrole modified with hyaluronic acid were made with conductivity similar to polypyrrole which enabled PC12 neurite sprouting[185]. Chitosan was mixed with different concentrations of polypyrrole in order to create porous, conducting scaffolds[186]. Composites of higher conductivity could be created by adding more polypyrrole, with the maximum value being on the order of 10^{-1} S-cm^{-1}. This is approximately an order of magnitude lower than unmodified polypyrrole or the polypyrrole-hyaluronic acid composite[185], demonstrating the challenge of creating a scaffold that is both conducting and bioactive.

To enhance the regeneration response, neurotrophic factors[95,97,101] or dexamethasone[187] have been co-polymerized with polypyrroles. By adding growth factors during the electrodeposition process, films of polypyrrole with neurotrophin-3 and NGF were used to test the effect of electrical and growth factor stimulation on neurons. The amount of neurotrophin-3 loading was controllable through the polymerization time, while its release could be mediated by applying pulsed voltage, pulsed current, or cyclic voltammetry[96]. Auditory neurons have been cultured on neurotrophin-3 containing polypyrroles, showing significantly greater neurite outgrowth than the unmodified polypyrrole surface[97]. The diffusion of growth factors from the surface likely contributed to the improved sprouting response, since neurons not in direct contact with the neurotrophin-3 containing polypyrrole also grew equally well[97]. Other growth factors may similarly diffuse from polypyrroles, supported by polypyrrole-collagen-NGF substrate improving neurite sprouting from PC12 cells compared to polypyrrole-collagen *in vitro*[95].

The combination of growth factor and electrical stimulation has been investigated by immobilizing NGF onto polypyrrole. To improve neuronal growth, NGF has already been immobilized in non-conducting polymers[98-100]. Similarly, NGF was conjugated to the surface of polypyrrole to assess the effects of an immobilized growth factor with electrical stimulation[101]. An NGF concentration of 0.98 ng/mm^2 was bound to polypyrrole surface and with electrical stimulation, this material increased neurite sprouting and extension from PC12 cells, an effect that was not due to NGF leaching from the surface.

Whereas most delivery approaches using polypyrrole involve growth factors, small molecule drugs can also be delivered. Dexamethasone is a drug that reduces pro-inflammatory cytokines[188] and its binding to receptors mediates the inhibition of astrocyte proliferation and microglial activation[189]. Controlled release of dexamethasone was mediated through incorporation into polypyrrole[187]. To release the drug, the voltage was swept from -0.8 to 1.4 V at a scan rate of 100 mV/s, with one cycle releasing 0.5 $\mu g/cm^2$, and by 30 cycles, 16 $\mu g/cm^2$. The effect of the electrically-released dexamethasone on astrocyte number and neuronal viability was assessed and compared against cells treated with 10^{-6} M soluble dexamethasone. Electrically-released drug did not affect neuronal viability but caused a significant decrease in astrocyte number, similar to the addition of dexamethasone. This may have been caused by reduced astrocyte proliferation, but the potential mechanism was not reported. This approach may help create a more growth-permissive environment by targeting cells that deposit the glial scar following CNS injury.

To change the permanent nature of polypyrroles, erodible and biodegradable polymers based on polypyrrole have been synthesized. Non-biodegradable materials that remain in the body are likely to elicit continuing inflammation, and may also act as a physical barrier to the regeneration response. Conducting polymers have been made that enable erosion and conductivity properties to be controlled. β-substituted polypyrrole monomers were electrochemically or chemically polymerized and showed *in vitro* biocompatibility by supporting the attachment and proliferation of mesenchymal progenitor cells[190]. Erosion of the β-substituted polypyrroles proceeded in a pH-dependent manner and was controllable according to the co-polymer composition.

Tethering pyrrole-thiophene oligomers with degradable ester linkages[191] also resulted in degradable, conducting polypyrroles. Although the ester linkages enable hydrolysis of these polymers, the relatively short conducting oligomers might reduce the electrical conductivity of the material.

1.5.5 Materials with Topographical Cues

Physical contact with the ECM, cells, or synthetic substrates is known to direct cell growth and migration. The organization of ECM fibrils are involved in the migration of neural crest cells[192], while the parallel orientation of neuroblasts to glial fibers suggests contact-mediated cues[193] in the developing nervous system. The presence of radial glia[194] and pioneer axons[195] in the brain influence neuron migration and process orientation. *In vitro*[196,197] and *in vivo*[198] studies indicate that olfactory ensheathing cells and oligodendrocytes provide guidance cues to neurons. Topographical features on polymers or inorganic compounds (gold, titanium, silicon, carbon, silica, lithium niobate, silicon nitride) can also provide guidance to a variety of cells, including mesenchymal cells, oligodendrocytes, neurons, and macrophages[14].

The mechanisms involved in axonal guidance are not fully understood. Substrate adhesiveness[15], shape[16,17], pattern dimensions, and the type and age of the neurons[18-20] influence growth cone motility and neurite alignment. Research is aimed at identifying effective approaches for directing neurite growth. The effects of contact guidance on nerve regeneration are being investigated through utilizing aligned channels or fibers in scaffolds, and in surface patterning techniques for promoting neurite extension and Schwann cell alignment.

1.5.5.1 Aligned Channels in Scaffolds

Scaffolds with multiple channels have been created in an attempt to mimic the endoneurial structure for peripheral nerve repair and to provide topographical guidance for spinal cord regeneration. Aligned channels promote the orientation of Schwann cells and encourage axonal extension. Collagen scaffolds with longitudinally aligned channels have been made by unidirectional freezing[199,200]. Scanning electron microscopy revealed the presence of 20 to 50 μm channels passing through the length of the construct. When seeded with dorsal root ganglia, Schwann cells infiltrated the channels and formed a columnar pattern likened to Bands of Bünger. Schwann cells grew in close association with neurons[199]. Implantation of linear channels within PLA foam scaffolds promoted Schwann cells to line the inner channels and co-localization of axons with the Schwann cells *in vivo* following spinal cord hemisection[21]. No axons were seen in amorphous PLA foams. In another study, PLA scaffolds pre-seeded with Schwann cells also resulted in the co-localization of axons with Schwann cells after implantation into a transected spinal cord[22]. The presence of both topographical cues and Schwann cells, however, did not fully repair the spinal cord, as hindlimb locomotor function was still significantly impaired six weeks after implantation of the construct. Agarose scaffolds containing aligned channels and BDNF have also been made by the unidirectional freezing method[60].

Scaffolds with multiple, aligned channels have also been fabricated via templating methods with stainless steel wires or fibers. In this fabrication method, a solution of polymer is injected into a mold containing the wires or fibers, which are eventually extracted. Agarose scaffolds with channel diameters of 200 μm and 76% porosity have

been implanted after a 2 mm spinal cord lesion in rats[24]. The templated agarose scaffolds promoted linear organization of axons compared to animals without scaffolds, and the inclusion of BDNF-secreting cells increased the presence of axons in such scaffolds[24]. Generating the templates for the agarose scaffolds involved a multi-step process of extruding polystyrene fibers in a matrix of PMMA, dissolving the PMMA matrix, immersing the polystyrene fibers in agarose, and subsequently dissolving the fibers. Peptide modified pHEMA scaffolds with aligned channels have also been made using similar methods. Scaffold porosities ranged from 33 to 37% and were controlled by the number of channels, which ranged from 82 to 132 μm in diameter[26]. Stainless steel wires, ranging from 150 to 660-μm diameter, have also been used to create PLGA[201] and PLG[25] scaffolds with multiple channels. PLGA scaffolds contained 450 or 600 μm-diameter channels, had a wide range of pore sizes (unreported in the literature), and exhibited porosities ranging from 78.7 to 88.6%[201]. PLG scaffolds could be fabricated to contain channels with diameters of 150 or 250 μm at 50% porosity[25].

Micro-patterned channels have been incorporated into the lumen wall to maximize axonal density and maintain contact-guidance[202]. A conduit of poly(D,L-lactide) films with 20/20/3 μm (channel width / spacing / depth) micro-patterns were implanted following a 10 mm sciatic nerve gap. Micro-patterned conduits led to statistically significant enhancement in axonal myelination compared to un-patterned PLA conduits. Micropatterned surfaces have also been used to promote Schwann cell and neuronal cell alignment *in vitro* (See 'Surface Patterning for Promoting Neuronal Growth' and 'Surface Patterning for Glial Alignment' below).

1.5.5.2 Aligned Fibers

Electrospun fibers are desirable for nerve tissue engineering due to their high surface area to volume ratio that may be used to maximize neuronal attachment and growth. Fiber orientation and size are important parameters for guiding cell growth. These fibers may be bundled or packed into a hollow conduit prior to being utilized as a nerve guide. Fiber orientation affects neurite extension; aligned PLA fibers elicited parallel alignment of and significantly longer neurites than random fibers[27]. There may be optimal fiber diameters that are best at eliciting longer and straighter neurite extension, but they are yet to be defined.

Recent developments in electrospun fibers involve the incorporation of growth factors or ECM components into the polymer solution. The resultant fibers can deliver bioactive molecules while providing a substrate that directs axonal extension to the target nerve. A co-polymer of PCL and ethyl ethylene phosphate were co-spun with GDNF in solution, and nerve guides containing one of two different fiber alignments were implanted into a 15 mm sciatic nerve gap[28]. The nerve guide channel was constructed by depositing fibers, having longitudinal or circumferential alignment, onto a film of PCL and ethyl ethylene phosphate, which was then rolled. Total myelinated axons and axonal area were greatest in rats that received scaffolds with longitudinally-aligned fibers and BDNF, compared to scaffolds that contained longitudinal or circumferential alignment without BDNF. Rats which received GDNF-containing fibers were the only group to show significant functional improvement compared to the hollow nerve guide. Compound motor action potential recordings, howeer, indicate that recovery is still incomplete compared to the normal nerve[28]. It was unclear whether the longitudinally

aligned fibers were critical for functional improvement, since circumferentially aligned fibers containing BDNF were not tested.

An additional approach may be to incorporate ECM-derived components. A blend of electrospun PCL and collagen nanofibers induced better guidance of Schwann cells than PCL-only scaffold, but did not affect the neurite length even when neurites grew on the Schwann cells[29]. A close association between Schwann cells, neurites, and fibers was observed, but had little effect on the neurite length even for the neurites on the Schwann cells. While topographical cues presented in the material and Schwann cell appears to direct axonal growth, additional bioactive cues might be needed to enhance the rate of regeneration.

In addition to electrospinning, aligned fibers have been fabricated by melt extrusion and have been induced through magnetic alignment. The effect of fiber curvature on neuronal alignment has been tested using melt-extruded polypropylene fibers[30]. Neurons were cultured onto fibers ranging from 7 to 500 μm in diameter. Neurite outgrowth became more aligned as the diameter became smaller, whereby alignment was always observed at the diameters from 7 to 10 μm[30]. Magnetic alignment may also be used to produce aligned fibers. Magnetically aligned collagen fibrils were created by inducing fibrillogenesis within a 9.4 T magnetic field[31]. Either aligned or non-aligned collagen fibrils filled a collagen nerve guide, which was then implanted into a 6 mm mouse sciatic nerve gap. Nerve guides with aligned fibrils had significantly higher nerve cross-sectional area and myelinated fibers than non-aligned collagen. These results support the role of contact guidance in sciatic nerve regeneration. Further investigation is

necessary to identify the mechanisms and understand how cells (neurons, astrocytes, or non-neural) respond to topographical cues to improve regeneration.

1.5.5.3 Surface Patterning for Promoting Neuronal Growth

Topographical cues have been shown to guide neurite sprouting [18,33]. Different surface morphologies have been created in order to identify critical parameters that can guide and promote neurite growth. The effects of the type and dimensions of the topographical cues on neuronal responses have been investigated using micro-fabrication techniques that allow precise control over surface features. The two types of surface cues reviewed here include pillars and aligned channels, the latter of which is more commonly examined.

Photolithography was used to produce 1 μm-high pillars of varying widths and spacing to assess their effects on hippocampal neurons[32]. Three different gap spaces ranging from 1.5 to 4.5 μm, and two pillar widths (1 and 2 μm) were tested. The 2 μm-wide and 1.5 μm-spaced pillars best enhanced the alignment and extension of neurites among the dimensions tested. These dimensions promoted neurite extension along a straight path for some distance. The presence of gaps between pillars, however, also allowed neurites to turn at ninety degree angles and continue along a new route.

Parallel channels have been fabricated in an attempt to induce polarization and maintain neurite alignment toward a preferred direction[18,33-35]. Using electron beam lithography, 1 and 2 μm-wide channels of 50 to 2000 nm depths have been created with polypyrrole[33]. Although patterning led to a significant increase in the polarization of neurites emanating from hippocampal neurons, the direction of neurite extension was

again either parallel or perpendicular to the channels. The findings of studies utilizing pillar-modified[32] and aligned microchannels[18,33] appear to support the idea that channels of less than 2 μm width allow perpendicular extension of neurites from hippocampal neurons. Alternatively, the feature size may not be sufficient to overcome the surface chemistry, which was isotropic in these cases. Furthermore, the dimensions that permit topographical guidance may vary among neuronal cell types.

Considering the effects of cell-type and the dimensions of surface patterns on the alignment and length of neurites may prove useful in determining effective approaches for nerve regeneration. Because different sizes of growth cones may have varying abilities to sense topographical changes, channel dimensions that effectively promote neurite alignment are likely to depend on the size of the neurites. In a study utilizing mouse sympathetic and sensory ganglia, channel widths of 200 nm were effective at promoting parallel axonal orientation. Researchers reported that the ability of axons to align to parallel channels appeared to be related to the diameter of axons[34]. In addition to the importance of channel spacing in contact guidance, the width of the ridges also appears to be a relevant variable. Narrower groove spacing on PCL promoted better neurite alignment from embryonic cortex neurons[35]. Neurites grew perpendicular to 12.7 μm groove spacing and 4.3 μm ridge width; they extended parallel neurites to the narrower groove spacing of 6.1 and 8.4 μm, and ridge spacing of 2.2 and 3.6 μm[35]. In another study, better alignment of sensory and sympathetic ganglia neurites was observed when the ridge width was decreased while holding the channel width constant, but only when the channel width was 200 nm or less[34].

Micropatterned surfaces have also been investigated in the differentiation of progenitor cells. Co-culturing astrocytes and adult rat hippocampal progenitor cells on a micro-patterned surface significantly increased the expression of a neuron-specific marker, from 15.3% to 35.3%[203]. The presence of astrocytes did not affect expression of the neuron-specific marker when co-cultured on planar surfaces[203], which suggests that topographical cues played a role in differentiation. Further investigations are needed to determine whether the surface patterning affects neurons directly or the effects are mediated by astrocytes.

Depositing bioactive cues in select locations and imprinting patterns of different topographies may be combined to produce micro-patterned surfaces with cell-adhesive domains[183] or immobilized growth factors[98]. Polypyrrole was modified with polyglutamic acid to permit the conjugation of laminin and polylysine. Select electrodeposition of polypyrrole by photolithography, followed by modification with the bioactive cues, permitted the selective attachment of dorsal root ganglia[183]. Another study examined the contribution of topography and NGF immobilization on the polarization and extension of hippocampal neurons. Poly(dimethyl siloxane) microchannels of 1 to 2 μm widths were made, which were subsequently conjugated with NGF. Polarization was more significantly affected by the presence of microchannels rather than 0.1 ng/mm^2 of NGF on the surface, whereas neurite length was increased in a synergistic manner when both NGF and microtopography were presented[98]. Neuronal responses, therefore, can be modulated by the presence of topographical cues presented as patterned surfaces.

1.5.5.4 Surface Patterning for Glial Alignment

Topographies that promote the alignment of Schwann cells or mimic their surfaces have been investigated. Following peripheral injury, Bands of Bünger consisting of columnar Schwann cells form and promote axonal migration along its surface[204]. Re-creating this orientation of Schwann cells may be useful in eliciting axonal regeneration after nerve injury. The physical topography of Schwann cells has been investigated by creating a cell-free surface that mimics its micro- and nano-scale features[205]. After using microfabricated laminin pattern to align Schwann cells, cells were fixed and sputter-coated with gold. A negative imprint of the surface was made onto a PDMS template, which was then used to fabricate a biomimetic substrate containing the cell impressions. The biomimetic surface promoted significantly greater adhesion of dorsal root ganglia and supported the alignment of neurons and Schwann cells[205].

Selectively modifying areas to be cell-adhesive has been used to induce Schwann cell alignment. Micro-patterning of laminin onto PLA[206] and PMMA[207] induced the alignment of Schwann cells on these surfaces. In the study utilizing PLA, compression molding was used to produce polymer films with grooves that adsorbed a higher concentration of laminin within them [206]. In the later study using PMMA, laminin was adsorbed onto the polymer by a PDMS stamp which created parallel lines of the protein, spaced at various distances. Smaller pattern widths increased the alignment of Schwann cells, regardless of interval width[207]. In both studies, the patterning of an ECM component that contains several adhesion-promoting domains promoted Schwann cells to adhere in a columnar manner[206,207]. Schwann cells aligned; however, it was difficult to

assess whether the orientation was caused by the surface topography or the selective deposition of cell adhesive material. Further investigation is needed to decouple the two.

The dimensional variables of channel width, spacing, and depth have been found to affect Schwann cell responses. Silicon chips with microgrooves ranging from 2 to 100 μm widths were created and coated with poly-D-lysine and laminin[204]. Sixty percent of Schwann cells aligned to the microgrooves of 50 and 100 μm widths; 90% oriented themselves parallel when the lanes were between 2 and 20 μm wide. Furthermore, dorsal root ganglia also extended aligned neurites to the patterned surfaces that had been pre-seeded with Schwann cells. A similar effect of groove dimensions on cell alignment was observed in a separate study using PCL coated with poly-L-lysine. In this investigation, astrocytes aligned to grooves that were spaced at 12.5 μm and 25 μm, but exhibited less parallel orientation at larger grooves of 50 to 100 μm[208] (**Figure 1.3**). Grooves spaced less than 25 μm apart were more effective at promoting parallel alignment of astrocytes and neurites. Neurons cultured on aligned astrocytes survived longer than those grown on the patterned polymer, and extended parallel neurites corresponding to the underlying topography for up to 3 weeks[208]. Spinal cord neurons sensed the microgrooves underneath astrocytes, and responded by extending and maintaining neurites parallel to the underlying surface. However, the alignment decreased over time, likely due to the increased proliferation of astrocytes. These studies indicate that groove widths are important. Groove depth has been shown to be significant in promoting alignment as well; changing it from 0.5 μm to 1.5 μm induced a significant increase in Schwann cell alignment[209]. Micro-channels, therefore, can affect the morphology of neurons even when Schwann cells or astrocytes are the cells in direct contact with them.

The potential of micro-patterned surfaces in improving the regenerative response has been demonstrated in a peripheral nerve injury model. PLA film was modified with aligned channels using solvent casting, and rolled into a cylindrical conduit for implantation into a 10 mm sciatic nerve gap in rats. Six weeks later, grooved constructs exhibited significantly greater axonal area, myelination, and angiogenesis than smooth scaffolds[202]. Culturing Schwann cells onto chitosan led to significantly less NGF and BDNF expression compared to PLA[202], indicating that different surface chemistries also impact cell response. The influence of topological guidance *in vivo* still needs to be examined in the regeneration of larger peripheral nerve gaps (20 mm or greater) to determine its efficacy in peripheral nerve regeneration. It may also be useful in promoting regeneration in the spinal cord, using contact guidance alone or in combination with Schwann cells or olfactory ensheathing glial cells.

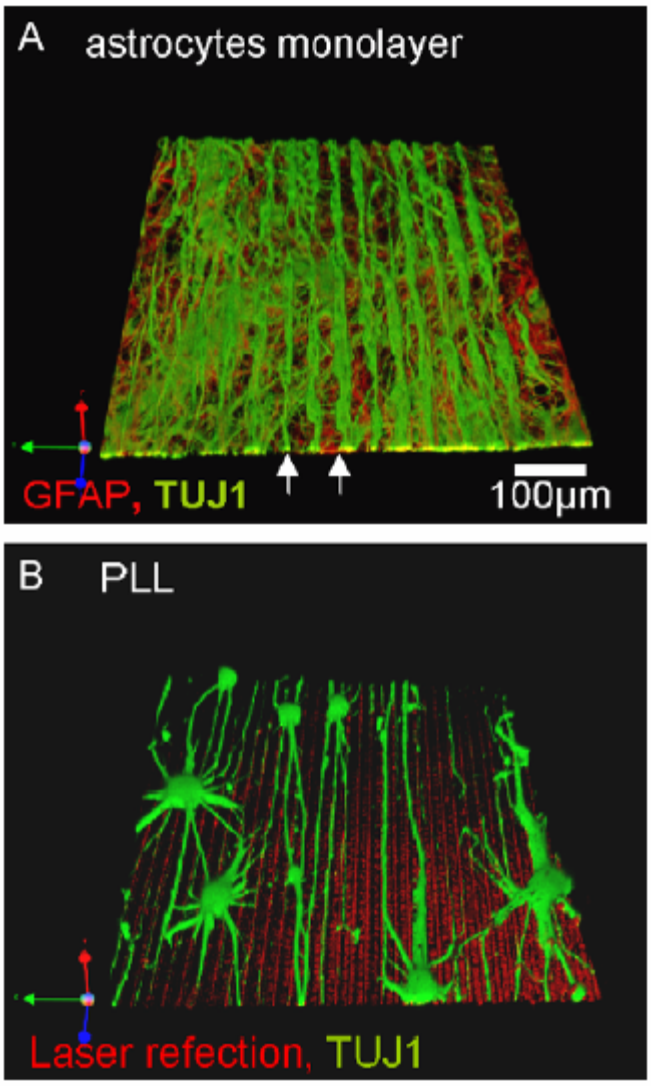

Figure 1.3. Aligned neurite extension on microgrooved substrates that have been preseeded with aligned astrocytes (A) or coated with poly-L-lysine (B). Three-dimensional projection created from confocal z-stack images. A) The astrocyte-specific marker GFAP (red) labels the underlying astrocyte layer, while neurons are labeled by Tuj1 (green). B) Microgrooves were imaged by reflection of the laser line (red). Arrowheads illustrate grooves[208].

Chapter 2. SYNTHESIS OF NEW POLYMERS

2.1 Neurotransmitters and their roles

Neurotransmitters are chemical messengers that propagate the transmission of electrical signals and also influence survival, proliferation, process extension, and differentiation in the nervous system. The effects of neurotransmitters on the developing central nervous system have been thoroughly covered in recent reviews[9,210,211], and some are briefly described here. GABA administration attenuates the cytotoxicity of glutamate in combination with an anti-convulsant[8]; GABA-induced proliferation of neuroblasts has also been observed[9]. In the developing brain, the activation of dopamine receptors affects proliferation and differentiation of progenitor cells[212,213]. Glycine mediates dendritic branching while acetylcholine exerts a chemoattractant influence on embryonic nerve growth cones[9]. The effects of these neurotransmitters on the cell response may depend on the developmental stage[12] and the type[214,215] of neuron that is being studied. The developmental stage and type of neuron used to evaluate the effects of neurotransmitters in nerve repair is an important consideration, as most nerve injuries requiring treatment occur in adults.

Acetylcholine regulates neuronal cytoarchitecture in embryonic and adult neurons and imparts neuroprotection. The activation of acetylcholine receptors induces neurite outgrowth[216-218] and promotes the formation and strengthening of synapses[11,12]. Acetylcholine-mediated axonal growth is believed to occur via an increase in intracellular calcium level[219], which likely initiates intracellular signaling events. Stimulating acetylcholine receptors triggers the influx of extracellular calcium and activates specific gene transcriptions including actin[220], which plays a key role in axon extension. Local

application of acetylcholine induces the nerve growth cone to turn toward the acetylcholine gradient[10]. In addition to its effect on process extension, acetylcholine may also be involved in pathfinding during synapse formation, as suggested by its spontaneous release from embryonic neurons[221]. The stimulation of nicotinic acetylcholine receptors elicits improved behavioral performance in rats and monkeys, and appears to be mediated by the expression of FGF-2[214]. Exposure to nicotine, an acetylcholine agonist, activates the ERK1/2 signaling pathway to protect against the apoptosis of spinal cord neurons isolated from 13-day old mice[222]. Muscarinic receptor activation also protects neuroblastoma cells from DNA damage, oxidative stress, and mitochondrial impairment[223]. Acetylcholine's role in regulating neuronal development, growth, and survival makes it a potential candidate for use in eliciting and directing nerve regeneration after injury.

In addition to mediating neuronal responses, neurotransmitters can also affect astrocytes and oligodendrocytes by changing the expression of neurotransmitter receptors expressed on their surface or stimulating their migration[224-226]. Neurotransmitter stimulation of glial cells promotes neuronal growth, as shown *in vitro* by the improved growth of neurons in response to conditioned media derived from serotonin-stimulated astrocytes[227].

2.2 Rationale for acetylcholine-based materials in nerve repair

Because neurotransmitters play important roles in neural cell activities, neurotransmitter-based materials may be useful. Surface-tethered neurotransmitters[228,229] were shown to activate the corresponding cellular receptors. Dopamine integrated into a

biodegradable polymer has been used to investigate cell recognition and responses[13]. We hypothesize that acetylcholine-based materials may also be used to promote neurite sprouting and extension. We devise a modular design that enables acetylcholine-like motifs to be incorporated within the polymer and control over its concentration. Leucine ethyl ester, having no known specific interaction with neurons, was included in the polymerization to control incorporation of the amount of acetylcholine-like motifs. The polymers are designed to be biodegradable by hydrolysis and possess a flexible polymer backbone to allow presentation of the neurotransmitter motif as a side chain.

2.3 Materials and methods for monomer and polymer synthesis

2.3.1 Diglycidyl sebacate was synthesized by one of two methods: by transesterification of diethyl sebacate (**Figure 2.1**) or by oxidation of diallyl sebacate (**Figure 2.2**). Freshly distilled glycidol (Acros, Geel, Belgium) dried with molecular sieves was refluxed with diethyl sebacate (Acros, Geel, Belgium) in the presence of thallium acetate catalyst (Alfa Aesar, Ward Hill, MA). The following parameters in the transesterification reaction were varied in to maximize the production of diglycidyl sebacate: molar ratios of glycidol and thallium acetate to diethyl sebacate, temperature (55 vs. 110°C), and pressure (60 to 80 torr). The formation of diglycidyl sebacate was monitored by thin layer chromatography.

For the oxidization reaction, diallyl alcohol was first synthesized by refluxing allyl alcohol (20.0 g, 0.100 mole, Alfa Aesar, Ward Hill, MA) and sebacic acid (53.7 ml, 0.800 mole, Alfa Aesar, Ward Hill, MA) at 105°C in 0.1% (v/v) sulfuric acid for 24 hours. Excess sulfuric acid was neutralized with sodium carbonate and unreacted allyl

alcohol was evaporated off at 70°C for 1 hour under vacuum. The product, diallyl sebacate, was extracted with ethyl acetate and dried with anhydrous Na_2SO_4. Diallyl sebacate was oxidized by *m*-chloroperoxybenzoic acid (mCPBA) (70-75% purity, Acros Organics, Geel, Belgium) in methylene chloride refluxed at 40 °C for 8 hours to produce diglycidyl sebacate monomer. The byproduct *m*-chlorobenzoic acid was crystallized at -20 °C overnight and filtered from the solution. The remaining chlorobenzoic acid in solution was removed by buffer extraction or by ionic resin. In the buffer extraction method, remaining acid in solution was neutralized by an aqueous solution of Na_2CO_3 / $NaHCO_3$ (100 ml de-ionized water, 7.69 g Na_2CO_3, 2.86 g $NaHCO_3$), followed by extraction of diglycidyl sebacate using ethyl acetate at 4:1 (v/v) ratio of buffer to ethyl acetate. Chlorobenzoic acid was removed by ionic resin by passing the crude product through an ion exchange column. Afterwards, pure diglycidyl sebacate was isolated by flash chromatography (Buchi Sepacore Flash, Flawil, Switzerland) in a mixture of ethyl acetate and hexane (3:7) on a silica gel column. Separations of crude product less than 400 mg utilized a 12 mm x 150 mm silica column, while separations for up to 1 g of product used a 40 mm x 150 mm silica column. The purity of the final product was characterized using nuclear magnetic resonance spectroscopy (NMR) on a 400-MHz Mercury-400 NMR from Varian, Inc. (Palo Alto, CA).

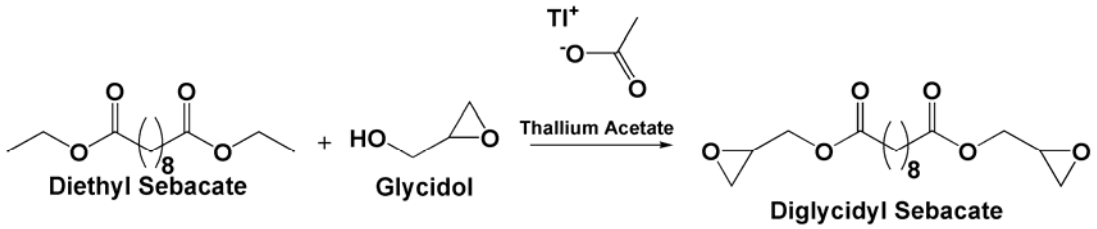

Figure 2.1. Transesterification of diethyl sebacate with glycidol for synthesizing diglycidyl sebacate.

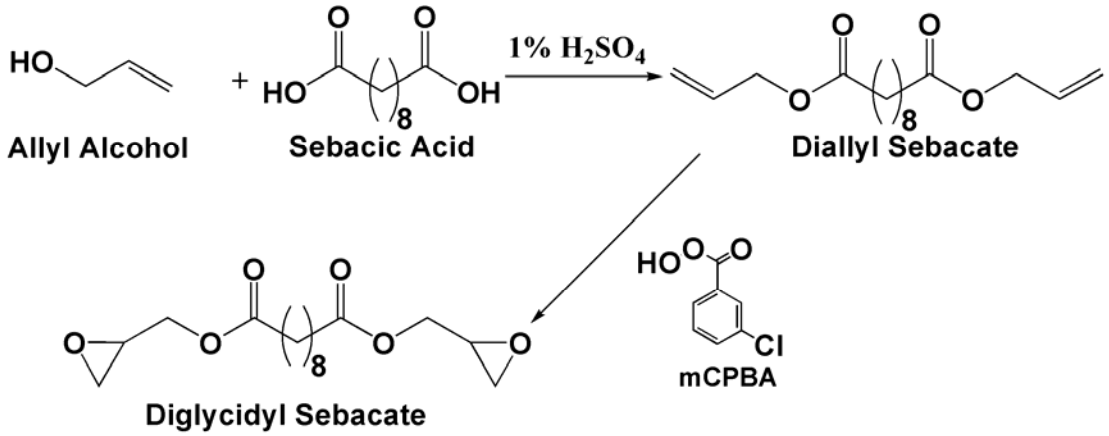

Figure 2.2. Synthesis of diglycidyl sebacate by oxidizing diallyl sebacate.

2.3.2 Liberation of Amines. Aminoethyl acetate was synthesized according to a published procedure,[230] except the reaction flask containing ethanolamine hydrochloride and acetic acid were cooled in ice-water prior to the addition of acetyl chloride. Additionally, 2:1 molar ratio of acetyl chloride to ethanolamine hydrochloride was used. Aminoethyl acetate hydrochloride salt was liberated by one of the following methods: 1) precipitation by using triethylamine; 2) liberation by a solution of NaOH; and 3) dissolving in a basic sodium carbonate-bicarbonate buffer, followed by extraction with ethyl acetate. In the first method, 1 mole of triethylamine was combined with 1 mole of aminoethyl acetate hydrochloride in methanol. The second method also utilized 1 mole of aqueous NaOH (1 ml) to 1 mole of aminoethyl acetate hydrochloride (100 mg),

followed by extraction with ethyl acetate (20 ml). The third method used one of two Na_2CO_3 / $NaHCO_3$ buffers, one at pH 9.7 (100 mg Na_2CO_3, 11 mg $NaHCO_3$, 10 ml de-ionized water) and the other at pH 10.5 (502.6 mg Na_2CO_3, 77.6 mg $NaHCO_3$, 5 ml de-ionized water). The salt was dissolved in the buffer at concentrations ranging from 0.1 to 2.3 grams of aminoethyl acetate hydrochloride salt per 1 ml of buffer, and the aminoethyl acetate was extracted with ethyl acetate at 2 to 200-fold excess over the volume of buffer used.

Leucine ethyl ester hydrochloride (TCI America, Portland, OR) was similarly liberated using a sodium carbonate-bicarbonate buffer. In addition the two buffers mentioned above, a pH 13.0 buffer was also used (3545.29 mg Na_2CO_3, 54.68 mg $NaHCO_3$, 10 ml de-ionized water). Leucine ethyl ester hydrochloride was dissolved in the buffers at concentrations ranging from 0.1 to 2.0 grams of salt per 1 ml of buffer, and the leucine ethyl ester was extracted with ethyl acetate at 2 to 200-fold excess over the volume of buffer used.

2.3.3 Polymer Synthesis

Diglycidyl sebacate, with equimolar $Mg(ClO_4)_2$, appropriate amounts of leucine ethyl ester and aminoethyl acetate were dissolved in DMF and stirred under N_2 at 90 °C. The amounts of leucine ethyl ester and aminoethyl acetate were adjusted accordingly to synthesize the following polymers: $PSA_{100}L_0$, $PSA_{70}L_{30}$, $PSA_{40}L_{60}$, PSA_0L_{100} (A_x = % acetylcholine, L_{1-x} = % leucine ethyl ester) (**Figure 2.3)**. The reaction mixture was heated at 90 °C for 5 days, and any remaining DMF in the resultant viscous liquid was removed with vacuum of 400 mTorr. Ethanol was added to re-dissolve the polymer and

evaporated to hasten removal of DMF. Polymers were precipitated in water and ethyl acetate to remove unreacted monomers and dried. NMR spectra were recorded on a 400-MHz Mercury-400 NMR from Varian, Inc. (Palo Alto, CA). FTIR spectra were recorded on an IR-100 spectrometer from Thermo Nicolet (Waltham, MA). Differential scanning calorimetry was performed on a DSC Q100 from TA Instruments (New Castle, DE). The molecular weights of the polymers were determined using gel permeation chromatography using standard or universal calibration. For standard calibration, polystyrene standards were eluted on a 60 Å YMC-Pack aqueous gel permeation chromatography column connected to a Waters 2690 separations module and Waters 2410 refractive index detector (Milford, MA). For universal calibration, a universally calibrated polystyrene standard was eluted on a Viscotek RImax system connected to a Model 3580 Refractive Index Detector, GPCmax™ Integrated Pump/Autosampler/Degasser Module, and Model 270 Differential Viscometer/Low Angle Light Scattering Dual Detector (Houston, TX).

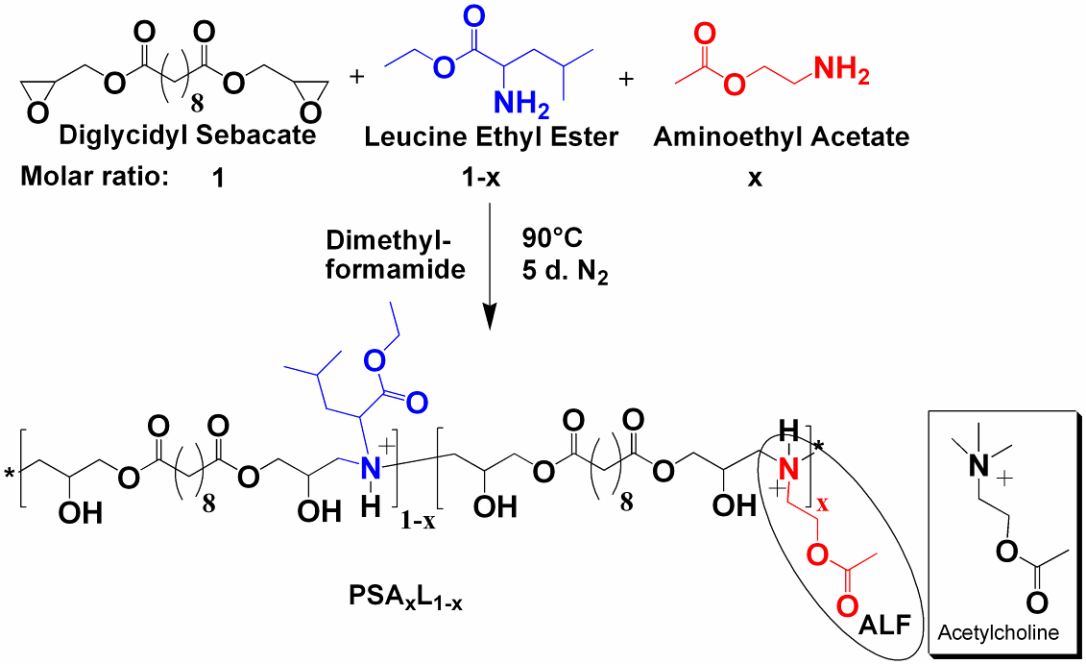

Figure 2.3. Polycondensation of the desired amount of leucine ethyl ester and aminoethyl acetate with diglycidyl sebacate results in biomaterials with varying amounts of acetylcholine motifs. The acetylcholine motif is circled and the structure of acetylcholine is shown for comparison.

2.4 Materials Characterization

2.4.1 Diglycidyl Sebacate. Products from the oxidation of diallyl sebacate were visualized after thin layer chromatography by using a ceric molybdate stain, revealing dark blue spots corresponding to the monoglycidyl sebacate, diglycidyl sebacate, and un-identified by-products of the reaction. The retention factor, the fraction of the total solvent distance traveled by a product, of the diglycidyl sebacate was 0.31.

Diglycidyl sebacate was first synthesized by transesterification (**Table 2.1**). Transesterification synthesis led to a maximum yield of 34%, a yield which was negatively affected by the formation of a clear, insoluble, gel-like by-product. Reaction conditions that were initially chosen did not yield any diglycidyl sebacate (Condition #1). Decreasing the molar ratio of glycidol from 3.6 to 2.4 and lowering the pressure to facilitate ethanol evaporation improved the yield to 14% (Condition #2). The glycidol

and diglycidyl ester appeared to undergo a side reaction, forming the insoluble gel-like by-product. To minimize by-product formation, the reaction time and temperature were decreased to 55°C and 7 hour, increasing the yield to 27% (Condition #3). The temperature was lowered in order to slow the kinetics of by-product formation, but maintained at a level that would permit diglycidyl synthesis. Because an increased yield resulted from lower reaction time and temperature, it was hypothesized that the high temperature favored by-product formation. The reaction temperature was maintained at 55°C, while the molar ratio of glycidol and reaction time was increased to drive formation of diglycidyl sebacate while retarding by-product formation. Performing the transesterification reaction at 4.8:1 molar excess of glycidol to diethyl sebacate at 55°C for 24 hours resulted in 34% yield (Condition #4). The lower temperature and increased availability of glycidol contributed to an improved yield.

Table 2.1. Purified yields of diglycidyl sebacate by transesterification.

	Molar Ratio					
Condition	**Diethyl Sebacate**	**Glycidol**	**Time (hr)**	**Temperature (°C)**	**Pressue (Torr)**	**Purified Yield**
1	1	3.6	13	110	80	0 %
2	1	2.4	14	110	60	14 %
3	1	2.4	7	55	60	27 %
4	1	4.8	24	55	60	34 %

Diglycidyl sebacate was also synthesized by the oxidation of diallyl sebacate. Synthesis yield was greater than 90%, assessed by NMR of the crude product immediately following the reaction. The purity of the mCPBA and the separations processes significantly affected the yield of purified diglycidyl sebacate (**Table 2.2**). Oxidizing diallyl sebacate for 6 hours at 40 °C with a 3:1 molar ratio of mCPBA to

diallyl sebacate resulted in yields of 77% and 91%. Using lower purity of mCPBA negatively affected the yield, where yield of 47% was obtained. The molar ratio of mCPBA to diallyl sebacate was kept constant between conditions 1 and 2. Because mCPBA is commercially available only as a mixture of peroxy and reduced acids, a lower purity product required more of the oxidizing mixture to be added to compensate for the difference in purity. The higher amount of the chlorobenzoic acid likely caused degradation of diglycidyl sebacate when mCPBA extraction by sodium carbonate - sodium bicarbonate buffer was performed.

The separations method used to extract mCPBA and by-products affected the purified yields. To prevent degradation of the ester by acid hydrolysis, chlorobenzoic acid was separated from the reaction mixture by ionic resin extraction instead of extraction by sodium carbonate-sodium bicarbonate buffer. Utilizing ionic resin resulted in an increased yield from 47% to roughly 60% (Condition #3). mCPBA extraction by ionic resin minimized the exposure of diglycidyl sebacate to water, unlike the buffer extraction method that likely cleaved the ester linkage by hydrolysis. Following mCPBA extraction, pure diglycidyl sebacate was isolated from by-products using normal phase, liquid chromatography. Conditions 1-3 utilized a smaller silica column, capable of separating up to 400 mg of crude product. During the attempt to scale up the synthesis and purification of diglycidyl sebacate, a larger silica column was used to separate up to 1 g of crude product. Using a larger silica column decreased yield to 22% to 30% (Condition #4), which likely was due to degradation on the larger column. Degradation was confirmed by the additional presence of by-products which had not appeared prior to liquid chromatography separation.

Table 2.2. Purified yields of diglycidyl sebacate by oxidation reaction. * indicates a batch of lower purity mCPBA was used.

Condition	Diallyl Sebacate	mCPBA	Time (hr)	Temperature (°C)	Separations Process	Purified Yield
1	1	3	6	40	mCPBA extraction by buffer	77% 91%
2	1	3*	6	40	mCPBA extraction by buffer	47%
3	1	3*	6	40	mCPBA extraction by ionic resin	60% 65% 65%
4	1	3*	6	40	Larger scale separation by liquid chromato-graphy	22% 30%

^{1}H NMR spectrum of digylcydiyl sebacate in chloroform-*d*: δ 4.40 (m, 2H), 3.90 (m, 2H), 3.20 (m, 2H), 2.84 (t, 2H), 2.64 (m, 2H), 2.34 (t, 4H), 1.63 (t, 4H), 1.30 (s, 8H), **(Figure 2.4)**.

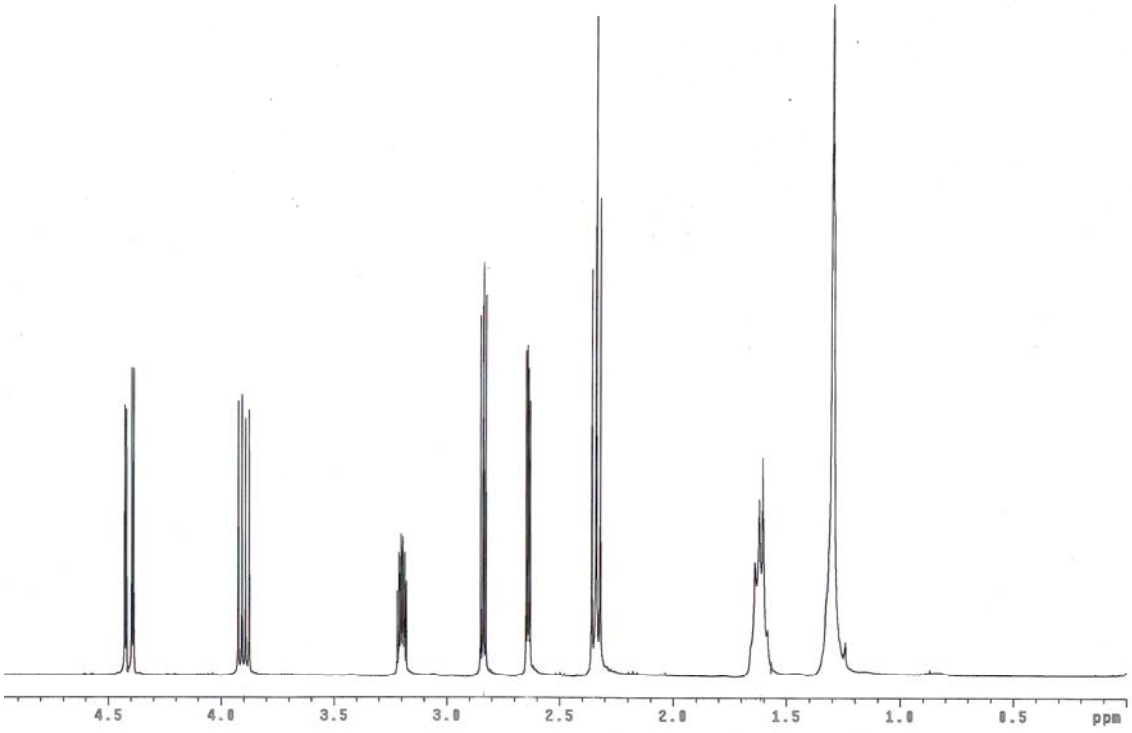

Figure 2.4. NMR spectrum of diglycidyl sebacate.

2.4.2 Liberated aminoethyl acetate and leucine ethyl ester were clear liquids at room temperature, compared to white crystalline powder in their unliberated states. A summary of conditions for liberating the amine monomers are listed in **Tables 2.3 and 2.4**. Using sodium carbonate-sodium bicarbonate ($Na_2CO3/NaHCO_3$) buffer was most effective for liberating both amine monomers.

The ratio of ethyl acetate to buffer was the most influential factor for isolating high yields of aminoethyl acetate. Approximately 83% of aminoethyl acetate's theoretical yield was isolated using a pH 10.5 buffer and a 200:1 (v/v) ratio of ethyl acetate to the buffer. The high ratio of organic solvent to buffer is necessary because of aminoethyl acetate's solubility in water, while the pH 10.5 buffer with sufficient buffering capacity maintained aminoethyl acetate in its liberated state. ^{1}H NMR of aminoethyl acetate in chloroform-*d*: δ 3.69 (t, 2H), 3.39 (m, 2H), 2.00 (s, 3H), **(Figure 2.5)**.

The pH of the organic solvent to buffer affected isolation yields for leucine ethyl ester. A pH 10.5 buffer was sufficient at isolating leucine ethyl ester at 60% and 71% yields at ethyl acetate to buffer ratio of 20 to 1. Increasing the pH of the buffer to 13.0 improved the yields to 81% and 82%. Leucine ethyl ester's solubility in water is less than that of aminoethyl acetate due to the presence of the isopropyl group. Leucine ethyl ester was isolated at similar yield to aminoethyl acetate using lower ratios of ethyl acetate to buffer. Leucine ethyl ester was distilled after liberation at 120°C and 72 torr. ^{1}H NMR for leucine ethyl ester in chloroform-*d*: δ 4.16 (m, 2H), 3.44 (m, 1H), 1.77 (m, 1H), 1.48 (m, 2H), 1.27 (t, 3H), 0.92 (t, 6H), **(Figure 2.6)**.

Table 2.3. Isolated yields of aminoethyl acetate.

Liberation method	pH of $Na_2CO_3/NaHCO_3$ buffer	Ethyl Acetate : Buffer (vol/vol)	Isolated Yield
Precipitation by triethylamine	n/a	n/a	0%
Aqueous NaOH	14.0	20:1	2%
$Na_2CO3/NaHCO_3$ buffer #1	9.7	2:1	0%
$Na_2CO_3/NaHCO_3$ buffer #2	10.5	5:1	8%
$Na_2CO_3/NaHCO_3$ buffer #2	10.5	50:1	68%
$Na_2CO_3/NaHCO_3$ buffer #2	10.5	200:1	86%, 80%, 84%

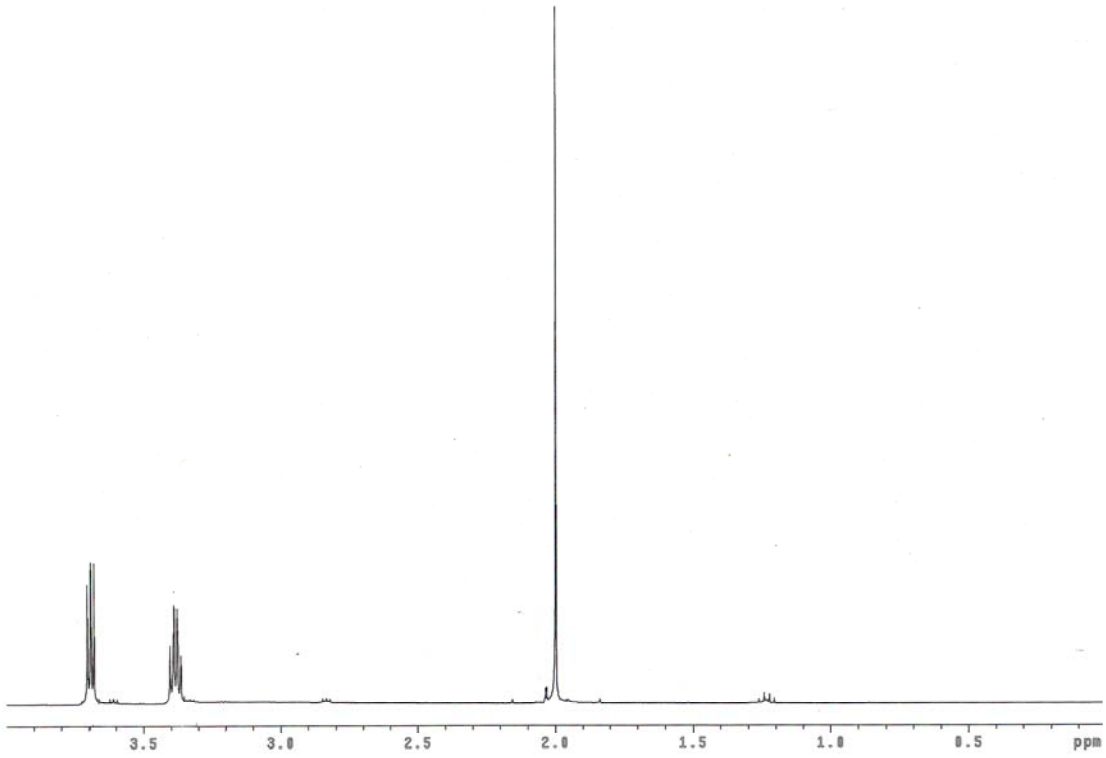

Figure 2.5. NMR spectrum of aminoethyl acetate.

Table 2.4. Isolated yields of leucine ethyl ester.

pH of $Na_2CO_3/NaHCO_3$ buffer	Ethyl Acetate : Buffer (vol/vol)	Isolated Yield
9.7	2:1	0 %
10.5	20:1	60%, 71%
13.0	20:1	81%, 82%

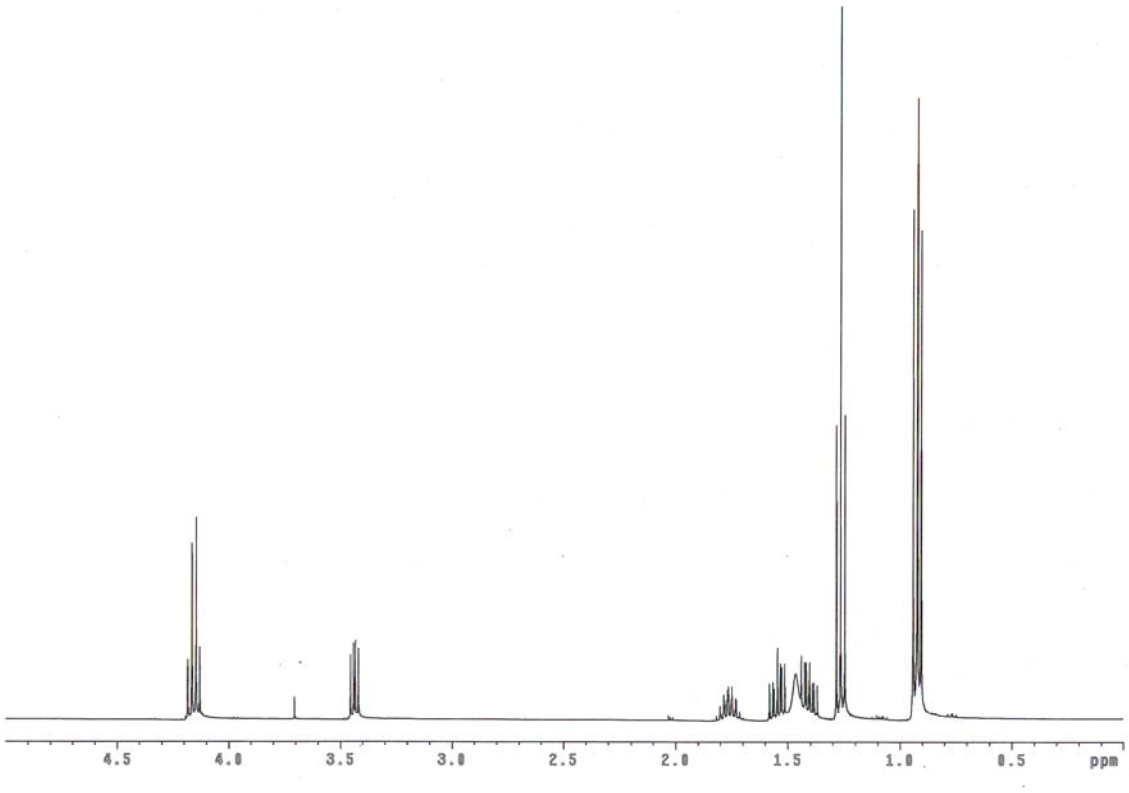

Figure 2.6. NMR spectrum of leucine ethyl ester.

2.4.3 Polymers containing different concentrations of acetylcholine motif. After removal of DMF and unreacted monomers, most polymers were isolated at approximately 25% yield (**Table 2.5**). The summary of polymer yields is not listed in any particular order, except for increasing concentration of acetylcholine motif. The primary goal of polymer synthesis was to obtain sufficient amount of polymer for *in vitro* evaluation, with a secondary goal of maximizing polymer yield. Future optimization studies could be performed by testing each process variable may be tested at two levels (low vs. high value) to identify trends and potential interactive effects. Assuming that three variables (concentration, time, and temperature) are to be tested at two values, optimization would require 8 experiments per acetylcholine motif concentration, and 40 total experiments for 5 concentrations.

Due to time constraints, optimization studies were not performed. The results presented here may highlight potential trends for optimizing polymer yield. For example, when synthesizing polymers having the same acetylcholine motif concentration, increasing both the concentration and the duration of the reaction appeared to increase yield. When synthesizing PSA_0L_{100} at 90°C, increasing the concentration of reactants from 300 to 1100 mg/ml and lengthening the reaction time from 4 to 6 days led to a 56% increase in purified yield (Reactions 1 and 2).

Identifying optimal polymerization conditions that are applicable to the synthesis of all polymers are difficult, since such conditions are likely to be specific to polymer composition. Yield may also depend on the polymer type; utilizing identical reaction conditions for two different polymer types result in different yields. Obtaining high yield is important in order to obtain sufficient amounts of the material; however it is also

important to preserve the polymer's properties that are useful for its application. For example, highly concentrating the monomers during the polymerization may lead to high yield, but the resulting polymer may be more cross-linked. Although a higher yield may be achieved, changing this polymer property could affect cellular responses to the polymer by affecting the presentation of the acetylcholine motifs.

The polymers' compositions were determined using standard analytical methods. The content of acetylcholine motifs in each polymer was evaluated by comparing NMR peak integrations corresponding to the isopropyl group of leucine ethyl ester at δ 0.84 to the ethylene groups of sebacate at δ 1.23 (**Figure 2.7**). Once polymerized, these peaks shifted slightly from the corresponding positions in the monomers. The area ratios corresponding to PSA_0L_{100} were determined for three different batches of the polymer and these averaged to provide an empirically-derived baseline value. **Table 2.6** provides the corresponding leucine ethyl ester and acetylcholine motif concentrations, and lists the polymer designation for each polymer.

Fourier transformed infrared (FTIR) spectra of the bulk polymers revealed an intense C=O stretch at 1725 cm^{-1}, confirming the presence of ester bonds along the backbone of the polymer. The subsequent peaks at 1650 cm^{-1} and 1557 cm^{-1} are shifts in the C=O stretch due to hydrogen bonding within the polymer. Polymers containing the acetylcholine motif also indicated the presence of the acetate ester C-O bond at 1241 cm^{-1} and confirmed the incorporation of aminoethyl acetate in polymers containing the acetylcholine motif (**Figure 2.8**).

Table 2.5. Summary of polymerization yields.

Reaction	Polymer	Concentration (mg diglycidyl/ ml solvent)	Time (days)	Temperature (°C)	Purified Yield
1	PSA_0L_{100}	300	4	90	15%
2	PSA_0L_{100}	1100	6	90	71%
3	$PSA_{40}L_{60}$	300	3	90	25%
4	$PSA_{60}L_{40}$	300	4	90	23%
5	$PSA_{60}L_{40}$	1600	11	60	30%
6	$PSA_{70}L_{30}$	300	6	90	26%
7	$PSA_{70}L_{30}$	1100	6	90	23%
8	$PSA_{100}L_0$	300	6	90	33%

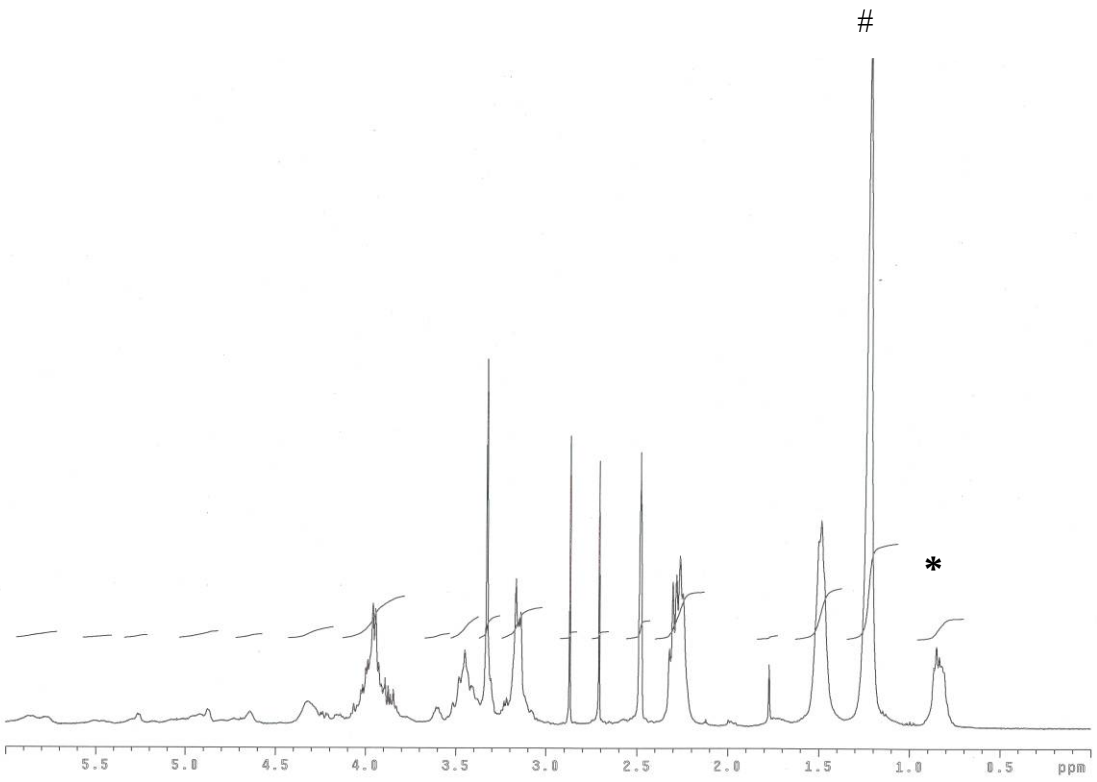

Figure 2.7. NMR characterization of polymers. NMR spectrum of $PSA_{70}L_{30}$ with the isopropyl group of leucine ethyl ester at δ 0.84 (*) and the ethylene groups of sebacate at δ 1.23 (#).

Table 2.6. Acetylcholine contents of polymers were empirically derived according to ratios of the areas corresponding to the isopropyl and ethylene groups at 0.84 and 1.23 ppm, respectively.

Area of peak associated with					
0.84 ppm	1.23 ppm	Area Ratio	Calculated Leu%	Calculated Ach motif%	Polymer Designation
15.18	22.35	0.679195	101.7%	-1.7%	PSA0L100
15.96	23.51	0.67886	101.6%	-1.6%	PSA0L100
17.11	26.49	0.645904	96.7%	3.3%	PSA0L100
12.02	23.26	0.516767	77.4%	22.6%	PSA20L80
9.02	23.22	0.388458	58.2%	41.8%	PSA40L60
6.95	27.02	0.257217	38.5%	61.5%	PSA60L40
4.46	19.38	0.230134	34.5%	65.5%	PSA70L30
5.12	23.68	0.216216	32.4%	67.6%	PSA70L30
4.22	22.26	0.189578	28.4%	71.6%	PSA70L30
1.73	9.31	0.185822	27.8%	72.2%	PSA70L30
3.55	24.1	0.147303	22.1%	77.9%	PSA80L20
1.96	15.18	0.129117	19.3%	80.7%	PSA80L20
0	22.39	0	0.0%	100.0%	PSA100L0
0	25.06	0	0.0%	100.0%	PSA100L0
0	10.56	0	0.0%	100.0%	PSA100L0

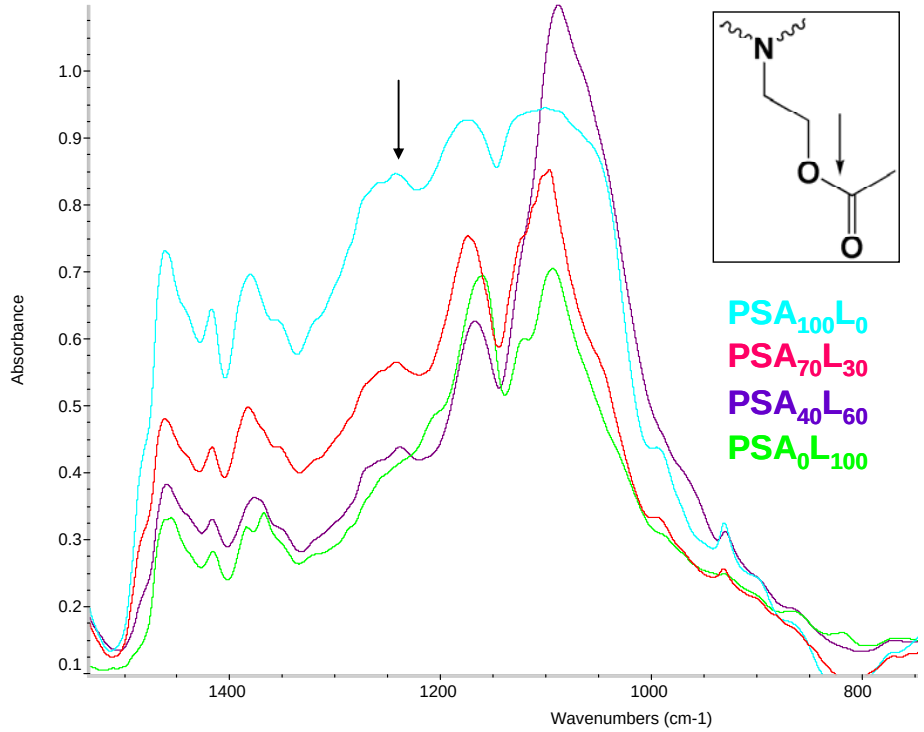

Figure 2.8 FTIR spectra of polymers with acetylcholine motifs display the presence of acetate ester C-O bonds at 1244 cm^{-1} (arrow). As expected, this absorption is absent in PSA_0L_{100}.

The polymers' molecular weights and glass transition temperatures (T_g) are reported in **Table 2.6**. Tg values were not reported for all polymers analyzed by GPC due to limited availability of the polymers. The polymer containing only acetylcholine motifs ($PSA_{100}L_0$) exhibited lower molecular weight and the lowest T_g than all other polymers. The acetylcholine motifs or undetectable impurities contained in aminoethyl acetate may have acted as plasticizers to lower the T_g of polymers having more motifs. All of the polymers were soluble in DMF, slightly soluble in ethyl acetate, acetone, ethanol, and methanol, and insoluble in water.

Table 2.7. Glass transition temperatures and molecular weights of polymers. *Polymer batch used in neurite sprouting studies. §Determination of molecular weight by universal calibration.

Polymer	Molecular Weight		T_g (ºC)
	M_n	M_w	
PSA_0L_{100}	13,701	14,324*	3.6
	6,796	7,981	n/a
$PSA_{20}L_{80}$	4,574	7,315	n/a
$PSA_{40}L_{60}$	21,303	22,371*	0.3
$PSA_{70}L_{30}$	6,744	7,966*	-6.1
	7,803	10,307	n/a
	18,049	22,272§	n/a
	24,517	36,411§	n/a
$PSA_{100}L_0$	4,774	5,141*	-24.4
	5,429	5,770	n/a

2.5 Discussion, conclusions, and future studies in synthesizing polymers

The abilities to increase the yield of diglycidyl sebacate, optimize the solvent amount for the polymerization, and control the molecular weight of the polymers are important objectives that can significantly affect the availability of such polymers for nerve tissue engineering applications.

One way of potentially increasing the yield of diglycidyl sebacate is to utilize an alternative synthesis scheme that does not depend on *m*-chloroperoxybenzoic acid (mCPBA). In the synthesis of diglycidyl sebacate, the use of mCPBA significantly increases time and labor, while also causing the isolated yield to be susceptible to the purity of the oxidizer. When sufficient amount of mCPBA is used to oxidize the diallyl sebacate, synthesis yield of diglycidyl sebacate is >90% according to NMR of the crude product. The mCPBA, however, must be crystallized overnight and eliminated through multiple filtrations using an ionic resin column, adding 13-17 hours of time to obtain diglycidyl sebacate. The mCPBA comes as a mixture of peroxy acid and the reduced

benzoic acid. Because the molar amount of mCPBA required to oxidize diallyl sebacate to diglycidyl sebacate is fixed, a lower purity mCPBA requires greater addition of the mCPBA-benzoic acid mixture. This tends to negatively affect isolated yield, since diglycidyl sebacate appears to be lost or degraded in the presence of more benzoic acid.

Optimizing the solvent amount for the polymerizations may lead to increased polymer yield and higher molecular weights while preserving the presentation of the acetylcholine motif. Minimizing the use of DMF may lessen the loss of polymer that occurs during post-synthesis purification. Because DMF is toxic to cells, it must be thoroughly eliminated from the polymer before *in vitro* or *in vivo* use with cells. Its high boiling point (153 ºC) requires the application of high vacuum, heating, induction of azeotropes using alternate organic solvents, and washes with water or ether. The greater DMF to eliminate, the more of the polymer is lost due to degradation or increased washing steps needed to remove it. Although the polymerization does proceed in the absence of DMF and leads to polymers of increased molecular weight, the resultant polymers may also be cross-linked. This can affect the presentation of the acetylcholine motif and cell responses to the material.

Polymers of a range of molecular weights may be isolated by controlling the duration of the polymerization and utilizing fractional solubilities in organic solvents. Characterizing the effect of reaction time on changes in molecular weights may enable polymers within a molecular weight range to be isolated. The longer the reaction time, the larger the polymers are expected to become. However, there may be a bi-phasic response of molecular weight with time, since degradation with longer reaction time is also possible. To circumvent this problem, polymers of particular molecular weight

ranges may be isolated by fractional solubilities within different organic solvents. Lower molecular weight oligomers may be more soluble low molecular weight alcohols or ethyl acetate, while higher molecular weight polymers are likely to precipitate out of such solvents.

In our study, we incorporated leucine ethyl ester into the polymer in order to control the concentration of acetylcholine motifs within the polymer. The concentration of leucine ethyl ester, though it has no known effects on neurite sprouting, may mediate neurite sprouting. Instead of leucine ethyl ester, other amino acids with no known effects on sprouting, such as isoleucine, alanine, or asparagine, could be used to vary the amount of acetylcholine motifs in the polymer. Instead of acetylcholine motifs, a different neurotransmitter motif could be tested. Another neurotransmitter, such as glutamate or glycine, may be incorporated into the polymer to determine whether each provides an additional effect that is useful for nerve tissue engineering. Glutamate would be a candidate neurotransmitter for incorporation into the polymer, since its application as a soluble gradient induces growth cone turning[231]. It would be interesting to determine the effect of incorporating glycine into a polymer; unlike acetylcholine, glycine is an inhibitory neurotransmitter that attenuates the propagation of the action potential. The neuron's excitability may play a role in neurite sprouting or other regeneration-related responses, such as up-regulation of growth factor receptors or actin polymerization. Since cell excitability is affected by neurotransmitter type, polymers based on excitatory or inhibitory neurotransmitters may also differentially affect excitability.

The modular design of synthesizing the acetylcholine-based polymers permits the investigation of 1) interactive effects between two or more types of neurotransmitter

motifs, and 2) effect of the physicochemical properties of the polymer backbone. The presence of both serotonin and acetylcholine involves interactive effects that mediate neurite sprouting[218]. Similarly, one can examine the effect of different combinations of two or more neurotransmitter motifs in polymers. Combinations of two or more neurotransmitters may be created to determine whether interactive effects exist between them that synergistically enhance neurite growth. In addition to the presence of different types and amounts of neurotransmitter motif, another factor that may affect neurite sprouting is the polymer backbone. In this study, we utilized a sebacate backbone to permit flexible presentation of the acetylcholine motif. The backbone can be varied so that the polymer is more hydrophilic or hydrophobic, possesses mechanical properties closer to the native nerve, or permits cross-linking which can affect the time scale of polymer degradation. Using the same type and amount of neurotransmitter motif, polymers based on different linkers can be synthesized to assess how the physicochemical properties of the backbone affect neurite sprouting.

Chapter 3. APPLICATION OF ACETYLCHOLINE-BASED POLYMERS IN NERVE TISSUE ENGINEERING

3.1 Examining the role of Acetylcholine-based materials

Acetylcholine-based materials may be useful in nerve tissue engineering, as acetylcholine influences neurite sprouting, synapse formation, and growth cone turning, among other neural cell activities (see Chapter 2, Sections 2.1 and 2.2). To explore the potential of acetylcholine-based materials, we set out to modulate neuronal responses by controlling the composition of acetylcholine motifs in a series of polymers. We synthesized and characterized polymers containing different concentrations of acetylcholine-like motifs (Chapter 2).

The interactions between these polymers and neurons are characterized using rat dorsal root ganglia (DRG) explants. DRG relay peripheral stimuli to spinal nerves[232] and can respond to acetylcholine via multiple cholinergic receptors that are expressed during embryonic and postnatal development[216,233,234]. Undissociated DRG explants are used since this model maintains the three-dimensional relationship between the neurons and associated cells within the DRG, providing a more similar environment found in nerve regeneration. We hypothesize that acetylcholine motifs incorporated in a polymer modulate neurite sprouting from dorsal root ganglia. We screened the potential application of these materials in nerve tissue engineering using the following criteria: 1) neurite sprouting, 2) neurite length, and 3) distribution of the neurite lengths.

3.2 Materials and methods for in vitro evaluation of acetylcholine-based materials

3.2.1 Preparation of Surfaces for DRG Culture. Glass coverslips were washed overnight in 1% Alconox detergent, rinsed with deionized water and ethanol, and dried. They were coated with 20 μl of the corresponding polymer solution (4.62 mg/ml) in DMF and dried overnight at 600 mTorr. The coated coverslips were then placed in non-tissue culture treated 24-well plates that were transferred to a vacuum oven at 60°C to remove any remaining DMF and to create an even coating. On the day of DRG isolation, each polymer-coated coverslip was sterilized by UV exposure for 30 minutes, and then soaked in 1ml of phosphate buffered saline on an orbital shaker (20 rpm) for 30 min (6x). A twenty-four well plate was coated with 150 μl of laminin (66.7 μg/ml) (BD Biosciences, San Jose, CA) in molecular grade water and placed on an orbital shaker (20 rpm) overnight prior to seeding.

3.2.2 Dorsal Root Ganglia Culture and Analysis. DRG from spinal levels L4-L6 of postnatal day-3 Sprague Dawley rats were dissected and collected in Hanks' balanced salt solution (Mediatech, Inc., Herndon, VA). The ganglia were washed with Hanks' balanced salt solution twice and seeded in neurobasal medium supplemented with B-27 (2%; Invitrogen, Carlsbad, CA), 2 mM L-glutamine, 20 μg/ml gentamycin, and 50 ng/ml nerve growth factor onto a pre-coated 24-well plate at one ganglion per well. Glial proliferation was inhibited with 5-fluorodeoxyuridine (7.5 μg/ml) and uridine (17.5 μg/ml) (MP Biomedicals, Solon, OH). Half of the medium was first changed at day 3, and every third day after. To test the effect of soluble acetylcholine on the neurite length of DRG grown on laminin and PSA_0L_{100}, a stock solution of acetylcholine chloride (MP

Biomedicals, Solon, OH) was added to the media to maintain a final concentration of 1 mM. For the antagonist studies, stock solutions of atropine (MP Biomedicals, Solon, OH) and mecamylamine (USP, Rockville, MD) in neurobasal medium were first made, then diluted to create a final concentration of 100 μM. The culture was maintained in a humid 5% CO_2 incubator at 37°C. DRG were fixed and stained for synaptophysin using rat anti-synaptophysin monoclonal antibody (Biomeda Corp., Foster City, CA) and Alexa Fluor 594 fluorescently labeled goat anti-mouse IgG antibody (Invitrogen, Carlsbad, CA).

The area of neurite outgrowth was photographed using an inverted phase contrast microscope [Nikon TE-2000U microscope (Melville, NY) equipped with a 4 MP Diagnostics Spot Flex digital camera (Sterling Heights, MI)]. Adobe Photoshop CS2 (San Jose, CA) was used to merge the photos and outline the neurites using the 'find edge' function. DRG exhibiting one or more neurites were considered to be sprouting. DRG with no neurites were considered 'not sprouting'. Day 4 neurite length measurements were performed on each 'sprouting' ganglion whose growth was unimpeded by the well's perimeter. Neurite length was measured by tracing the path of a neurite from the boundary of the dorsal root ganglion to the tip of the neurite. Upon reaching a branching point, length was traced along the path yielding the greater length. No neurites with the same branching points were measured. The 10 longest neurites of each ganglion were measured with ImageJ (NIH, Bethesda, MD).

3.2.3 Statistical Analysis. Binary logistic regression was used to assess and determine the nature of the relationship between acetylcholine-motif concentration and probability

of sprouting. Because the neurite sprouting response can be considered to be a binary response, the logit transformation was used:

$$\ln\left(\frac{\pi_i}{1-\pi_i}\right) = b_0 + b_1 * (Ach\%)_i + b_2 * (Ach\%)_i^2, \qquad \textbf{Equation 1}$$

where π_i is the probability of sprouting and $(Ach\%)_i$ is the concentration of acetylcholine-motifs of the polymer. Maximum likelihood estimates of the coefficients b_0, b_1, and b_2 were found using the statistical software program Minitab 15 (State College, PA). Coefficients were considered to be statistically significant at p-values less than 0.05.

Error bars for adherent and sprouting percentages were calculated as the 95% confidence interval for the proportion being estimated using the normal approximation to the binomial distribution. Chi-squared homogeneity testing was used to evaluate statistical significance of the difference in substrates' ability to promote neurite sprouting. Analysis of variance was used to determine whether differences in neurite sprouting area were statistically significant.

3.3 In vitro responses of DRG to acetylcholine-based polymers

3.3.1 Neurite sprouting. To investigate how ALFs modulate neurite sprouting, the polymers were coated onto glass coverslips. Neurite growth was monitored daily. Measurement of neurite length was reliable up to approximately 4-6 days because extensive networks of neurites formed beyond 6 days. The data on neurite sprouting was obtained on day 4. All polymer-coated coverslips were sterilized with UV light. ATR-

FTIR spectra of each polymer before and after UV exposure showed no change, indicating that the integrity of the polymer was preserved.

DRG cultured on the polymer-coated coverslips exhibited growth of one or more neurites, or no neurites at all **(Figure 3.1)**. 'Sprouting' DRG exhibited one or more neurites, while those with no neurites were considered to be 'non-sprouting.' The neurite sprouting area response varied considerably on a polymer of a given acetylcholine motif concentration **(Figure 3.2)**. Measuring the neurite sprouting area of DRG with one or more neurites revealed that there was not a statistically significant difference in neurite area when DRG were cultured on different polymer surfaces ($p = 0.166$). There was no difference in neurite sprouting area when DRG were cultured on laminin and the polymer surfaces ($p = 0.118$). Arbitrary segmentation of the data is averted by utilizing a general definition to characterize DRG responses to the polymers and using the classification 'sprouting' vs. 'non-sprouting' as an indicator of growth.

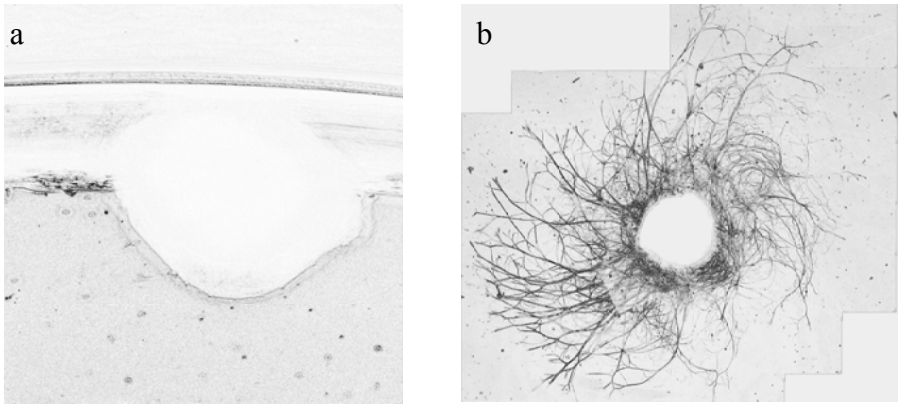

Figure 3.1. DRG were considered to be either non-sprouting (a) or sprouting (b).

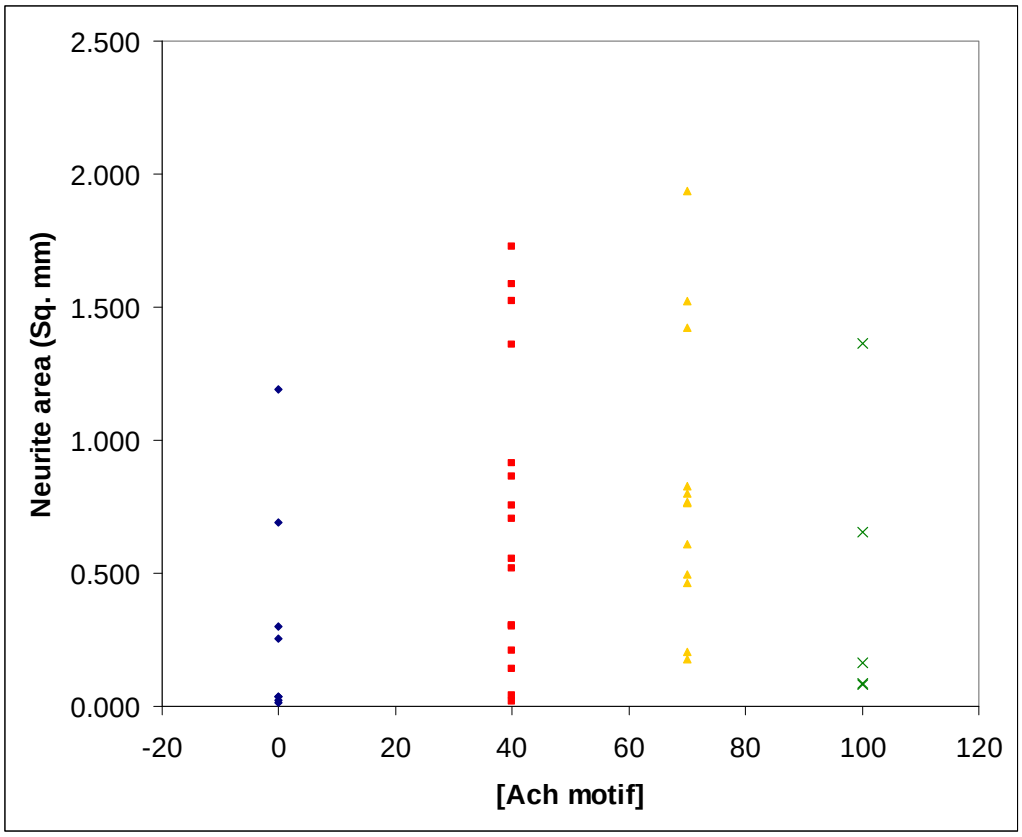

Figure 3.2. Neurite sprouting area on polymers containing various acetylcholine motif concentrations. Observations were made from 8, 16, 12, 5 DRG cultured on PSA_0L_{100}, $PSA_{40}L_{60}$, $PSA_{70}L_{30}$, and $PSA_{100}L_0$, respectively.

Logistic regression revealed that the sprouting ability of DRG was influenced by the concentration of acetylcholine motifs of the polymer. This analysis considers each DRG as an independent trial that exhibits either a sprouting or non-sprouting response (**Figure 3.1**). Because the sprouting response can be considered to be a binary response, the logit transformation was used:

$$\ln\left(\frac{\pi_i}{1-\pi_i}\right) = b_0 + b_1 * (Ach\%)_i + b_2 * (Ach\%)_i^2 \qquad \textbf{Equation 1}$$

where π_i is the probability of sprouting, $(Ach\%)_i$ is the concentration of acetylcholine-motifs of the polymer, i corresponds to the ith DRG, and b_0, b_1, and b_2 are

coefficients determined by maximum likelihood estimation. After running a binary logistic regression package on the data, the values corresponding to the acetylcholine motif terms, b_1, and b_2, were determined to be statistically different from zero at the p-values listed (**Table 3.1**). The model is significant, and therefore, concludes that the probability of neurite sprouting depends on the concentration of acetylcholine motifs. Substituting the coefficient values into Equation 1 gives the fitted response function:

$$\ln\left(\frac{\hat{\pi}_i}{1-\hat{\pi}_i}\right) = b_0 + b_1 * (Ach\%)_i + b_2 * (Ach\%)_i^2 \qquad \textbf{Equation 2}$$

where $\hat{\pi}_i$ is the average sprouting response corresponding to a concentration of acetylcholine motif. Goodness of fit tests were performed using the statistical package, and included Pearson, Deviance, and Hosmer-Lemeshow tests. All tests indicated that the data was modeled adequately.

Table 3.1. Estimates of the coefficients for logistic regression.

Parameter	Value	p-value (non-zero parameter)
b_0	-0.695662	0.111
b_1	0.0540668	0.006
b_2	-0.0006091	0.001

DRG sprouting on polymers containing-acetylcholine motifs were compared with responses observed on laminin and with the addition of soluble acetylcholine. Within the family of synthesized polymers, $PSA_{70}L_{30}$ was the most efficient at promoting neurite sprouting, with 59.1 ± 20.5% of DRG having sprouted at least 20 neurites, which is comparable to 60.0 ± 21.5% on laminin (**Figure 3.3**). $PSA_{40}L_{60}$ also prompted considerable growth with 57.1 ± 18.3% of DRG sprouting neurites. $PSA_{100}L_0$ and PSA_0L_{100} both showed markedly decreased sprouting compared to $PSA_{70}L_{30}$ and $PSA_{40}L_{60}$. Sprouting on $PSA_{100}L_0$ and PSA_0L_{100} may have been induced by positive charges, due to the amines on the polymer backbone, that are known to encourage neurite extension.[180,235] Alternatively, the DRG that sprouted may have been the most robust DRG that were capable of sprouting irrespective of the surface condition.

To assess whether solution-phase acetylcholine affects neurite sprouting, DRG were cultured on PSA_0L_{100} and laminin in the presence of 1 mM of the neurotransmitter. The addition of acetylcholine increased the fraction of DRG exhibiting neurite sprouting on PSA_0L_{100} from 34.8 ± 19.5% to 38.1 ± 20.8% (**Figure 3.3**). This difference, however, was not statistically significant. Soluble acetylcholine may mediate its effects differently from the acetylcholine motif, which is covalently bound to the polymer until hydrolysis. Binding of acetylcholine to the receptor can cause internalization of the

neurotransmitter[236,237] whereas it is yet unknown whether the acetylcholine motif interacts with the acetylcholine receptor and is processed in the same manner. The addition of solution-phase acetylcholine did not significantly alter neurite sprouting on laminin. Laminin's ability to promote outgrowth is well-established and involves specific growth-promoting domains,[118,120] integrin-binding domain,[121] and a heparin-binding domain.[114] Addition of 1 mM acetylcholine may not have significantly impacted neurite growth on laminin because of the existence of many other neurite sprouting cues.

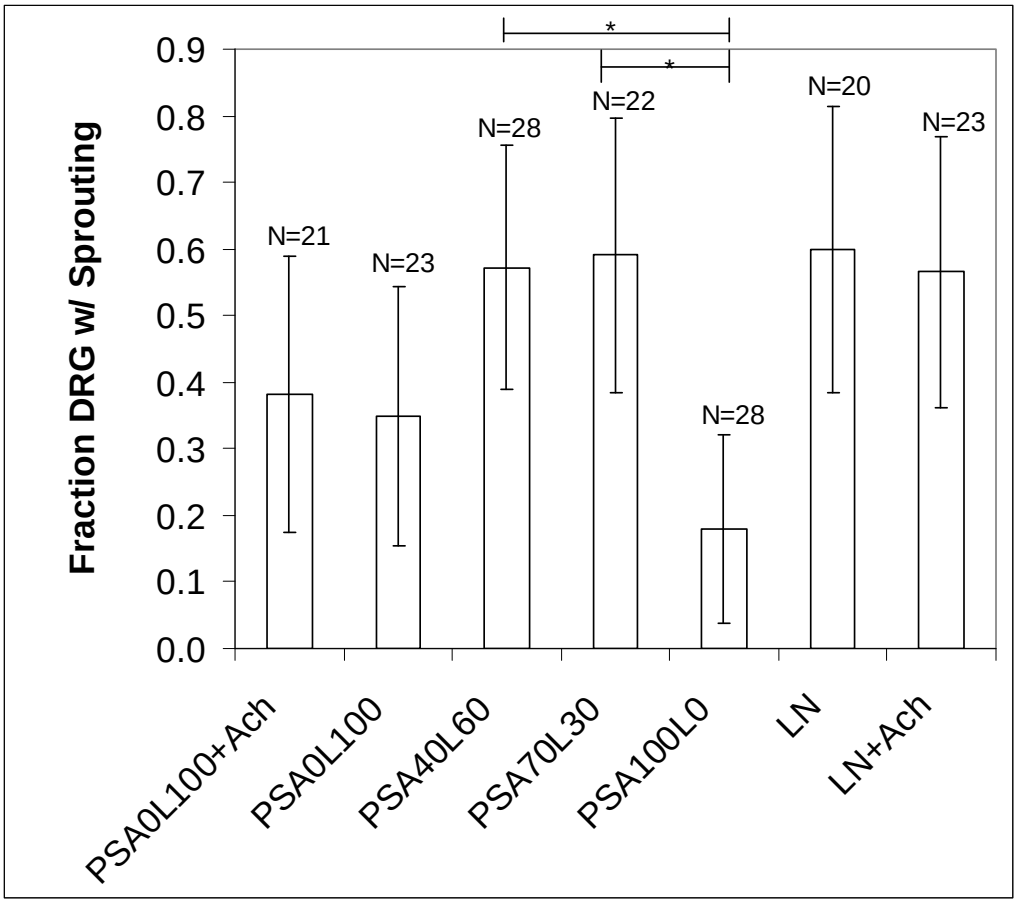

Figure 3.3. Effect of polymer composition and soluble acetylcholine on DRG sprouting. DRG were cultured on polymers containing acetylcholine motifs or laminin, and with soluble acetylcholine added to a final concentration of 1 mM (+ Ach). Error bars indicate 95% confidence interval. DRG sprouting responses on polymers that do not have overlapping 95% confidence intervals are statistically different, * $p<0.05$. N: total number of DRG cultured.

3.3.2 Neurite length. For nerves to regenerate successfully, a biomaterial should support the extension of the sprouted neurites. The activation of acetylcholine receptors by the addition of acetylcholine agonists significantly increased neurite outgrowth and length[217]. Acetylcholine motifs within a biomaterial could also affect neurite extension. To assess extension of neurites on the polymers, we measured the 10 longest neurites per ganglion, pooled the data from the sprouting DRG on each substrate, and compared the distribution of neurite lengths.

Long neurites grew on all surfaces and the acetylcholine motif content affected the distribution of the longest neurites. DRG on both PSA_0L_{100} and $PSA_{70}L_{30}$ exhibited long neurites at 2.93 mm and 2.77 mm, respectively (**Table 3.2**). However, more DRG adhered to and sprouted on $PSA_{70}L_{30}$ than PSA_0L_{100} (**Figure 3.3**). Additionally, a greater fraction of neurites grew longer than 2.0 mm on $PSA_{70}L_{30}$ than the other polymers (**Table 3.3**). It is possible that the neurite lengths were affected by the number of neurons within a DRG, and the existence of this potential measurement artifact was checked. Neurite density measurements, normalized to the area of the DRG, revealed neurite densities were similar among DRG considered to be 'sprouting'. Furthermore, within the same group of DRG, the neurite area was not statistically different. Therefore, the different neurite length distributions were not likely due to differences in the sizes of the DRG or population distribution of the neurites.

The growth rate of the longest neurite, when averaged over four days, on $PSA_{70}L_{30}$ was 692 μm/day. The rigor of this growth rate is maintained up to 6 days, and decreased slightly to 601 μm/day by day 8. This appears to be higher than the DRG growth rates of 250 μm[238] to 370 μm[128,239] per day calculated from data reported in the

literature. Nerve growth *in vivo* is much more complicated than culturing DRG explants; *in vitro* neurite growth rate nonetheless provides a measure of the material's propensity to promote nerve growth. Adding acetylcholine to the culture medium of DRG on PSA_0L_{100} and laminin appears to have a positive effect on neurite extension. The maximum observed neurite length of DRG seeded onto laminin increased from 3.49 mm to 4.59 mm. On PSA_0L_{100}, the addition of acetylcholine nearly doubled the fraction of neurites with lengths between 2.0 to 2.5 mm (**Table 3.2**).

Table 3.2. Distribution of longest neurite lengths. DRG were cultured on polymers containing acetylcholine motifs or laminin, and with soluble acetylcholine added to a final concentration of 1 mM (+ Ach).

		% neurite with length [mm]					
	Max neurite length [mm]	> 3.5 mm	3.0 - 3.5	2.5 - 3.0	2.0 - 2.5	1.5 - 2.0	< 1.5 mm
PSA_0L_{100} + Ach	2.61	-	-	5	30	33	32
PSA_0L_{100}	2.93	-	-	7	17	33	43
$PSA_{40}L_{60}$	2.54	-	-	1	5	40	54
$PSA_{70}L_{30}$	2.77	-	-	7	31	36	26
$PSA_{100}L_0$	2.28	-	-	-	20	65	15
Laminin	3.49	-	4	20	34	16	26
Laminin + Ach	4.59	2	2	19	14	7	56

3.3.3 Neuronal phenotype. Functional restoration after nerve injury requires synapse formation between neurons and their target tissue and, in certain cases, between neurons as well. We examined the presence of synaptic vessicle proteins on all polymers in order to evaluate the maintenance of neuronal phenotype. DRG seeded on $PSA_{70}L_{30}$ and laminin both expressed synaptophysin (**Figure 3.4**), an established neuronal marker, up to 21 days in culture.[240] DRG on the remaining polymers also stained positive for synaptophysin. This indicates that neurons grown on ALF-containing polymers can retain phenotypic protein expression.

3.3.4 Neurite sprouting in the presence of acetylcholine antagonists. The sebacate polymer backbone is designed to permit flexible presentation of the acetylcholine motif, which may interact with acetylcholine receptors expressed on DRG[233,234]. Acetylcholine binds to two types of receptors, nicotinic and muscarinic receptors. Nicotinic receptors are ligand-gated ion channels that upon binding of two acetylcholine molecules, open to allow the passage of sodium ions. The depolarization caused by the influx of sodium then leads to the opening of voltage-gated calcium channels, subsequently leading to the influx of calcium into the cell[241]. Muscarinic receptors are G-protein coupled receptors that have two main activities associated with them. Binding of acetylcholine to muscarinic receptors may activate phospholipase C activity or the inhibition of adenylyl cyclase activity[242].

To examine interactions between acetylcholine receptors and polymers containing acetylcholine-motifs, DRG were cultured in the presence of nicotinic and muscarinic antagonists. One-hundred micro-molar of each antagonist were added separately to DRG cultured on polymers and on laminin. Addition of nicotinic and muscarinic receptor antagonists, mecamylamine or atropine, respectively, to polymers with acetylcholine motifs decreased neurite sprouting in a statistically significant manner **(Figure 3.5)**. Addition of the antagonists to DRG culture on laminin, in the same concentration, did not significantly affect neurite sprouting. These results suggest that the acetylcholine receptor mediates neurite sprouting on polymers containing acetylcholine-motifs. Activation of acetylcholine receptors has been shown to enhance neurite outgrowth in previous studies[217,243], and application of antagonists in the presence of acetylcholine agonists similarly led to attenuation of neurite sprouting and extension[217,243].

a

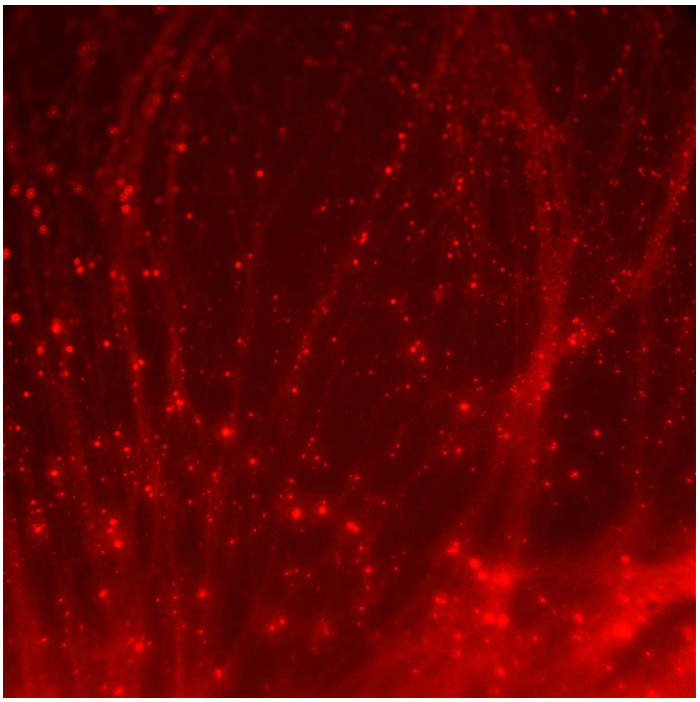

b

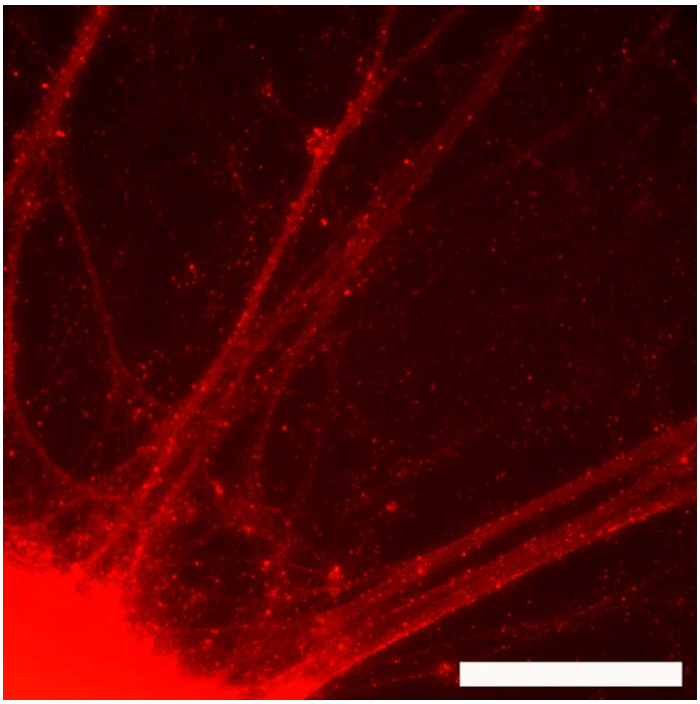

Figure 3.4. DRG were stained for the synaptic vesicle protein synaptophysin when cultured on polymers containing acetylcholine motif (a) and laminin (b). The presence of numerous synaptic vesicles is indicated by punctate red spots along the neurites. Day 21, 200 x, scale bar = 200 μm.

a

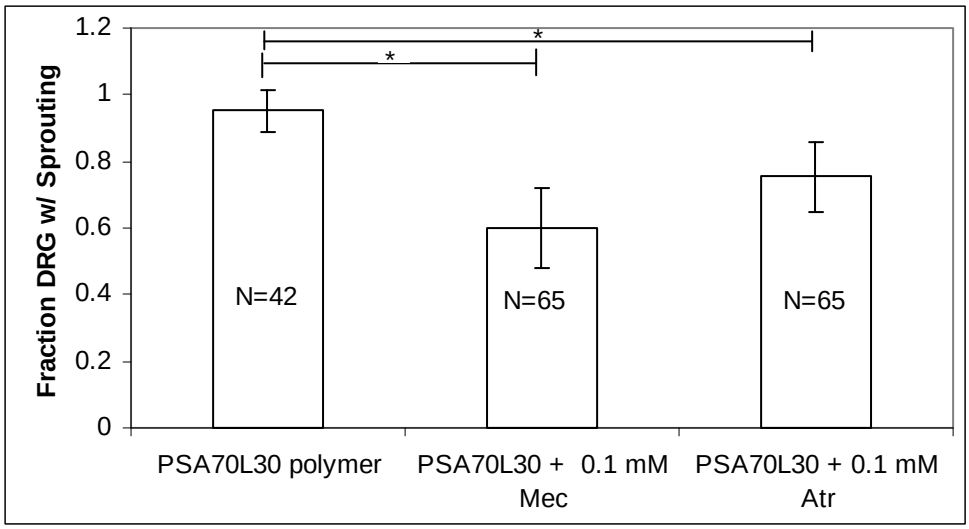

b

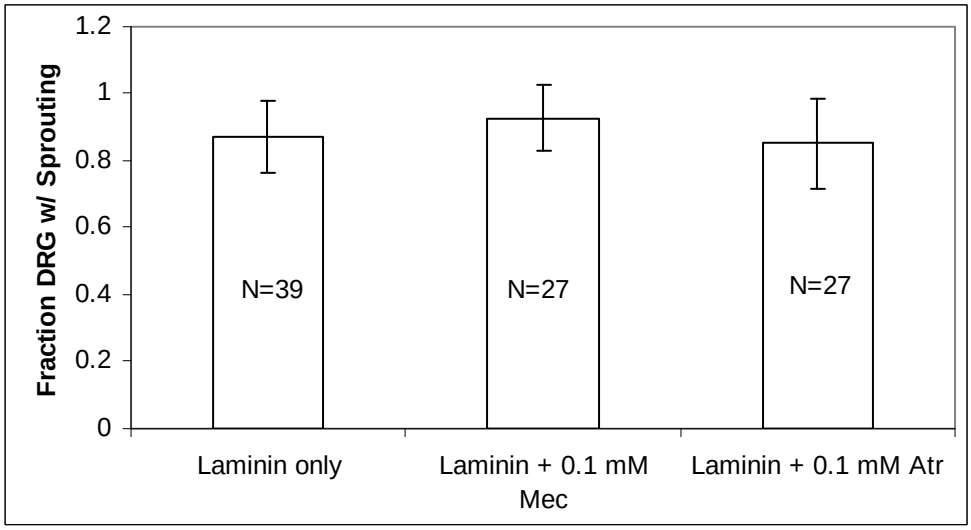

Figure 3.5. Addition of acetylcholine antagonists significantly decreases DRG sprouting on polymers with acetylcholine motifs (a) but not on laminin (b). Error bars indicate 95% confidence interval. DRG sprouting responses on polymers that do not have overlapping 95% confidence intervals are statistically different, * $p<0.05$. N: total number of DRG cultured.

3.4 Discussion, conclusions and future studies in the evaluation of new polymers for nerve tissue engineering

The studies presented here indicate acetylcholine motifs in materials modulate neurite sprouting from DRG. Among the polymers that were tested, polymers of

intermediate concentrations of acetylcholine motifs were most effective at promoting sprouting. All polymers permitted neurite extension and maintained the neuronal phenotype. Antagonist binding studies suggest that acetylcholine motifs interact with receptors to mediate neurite sprouting. Addition of acetylcholine agonists have similarly induced a significant increase in fiber outgrowth in chick DRG, an effect which was also abolished in the presence of receptor antagonists[217]. These studies suggest the potential use of acetylcholine-based polymers in nerve tissue engineering. Future studies for assessing the their applicability involve understanding cell-material interactions between neurons and the polymers and examining how acetylcholine motifs may play a role in other relevant responses involved in nerve regeneration.

The antagonist binding study suggests the polymer interacts with the acetylcholine receptor; further studies are required to establish this interaction. Downstream events following acetylcholine receptor activation may be assessed, such as the activation of phospholipase C, inhibition of adenylyl cyclase, changes in intracellular calcium levels, or differences in electrical activity of neurons. These studies will compare whether acetylcholine motifs can induce changes in cell activities that are similar to acetylcholine (or its agonists), and whether these activities can be abolished by the presence of competing antagonists.

The acetylcholine motif may interact with muscarinic or nicotinic acetylcholine receptors. Phospholipase C activity, which is associated with the Gq activity of a subset of muscarinic receptors[242], can be monitored by the amount of inositol phosphate produced as a function of the concentration of acetylcholine motifs. Another subset of muscarinic receptors may also be involved – those having a Gi activity that inhibits

adenylyl cyclase activity[242] – and can be examined similarly by monitoring changes in cAMP levels when the concentration of acetylcholine motifs is increased. Controls for each study would involve assessing the baseline level of phospholipase C in the cells, the baseline level of cAMP in unstimulated neurons, cAMP levels when its production is induced, and the effect of adding increasing concentration of an acetylcholine agonist, such as carbachol, on phospholipase C and adenylyl cyclase activities.

Upon the binding of acetylcholine to neuronal, nicotinic acetylcholine receptors, the ion channels are permeated by extracellular calcium[241]. Influx of extracellular calcium have been shown to activate actin transcription in neuron-like PC12 cells[220], while the resulting depolarization from the influx of calcium stimulates lamellipodia formation and axonal branching in cerebral cortex neurons[167]. Calcium transients also play a role in inducing axon branching in cortical neurons by targeting the calcium/calmodulin-dependent protein kinase II[164]. The acetylcholine motifs may interact with acetylcholine receptors through similar mechanisms involving changes in calcium levels.

Cell excitability, measured by intracellular calcium imaging or electrophysiological recordings, may be used to assess the involvement of acetylcholine receptors. The intracellular calcium levels of neurons cultured on acetylcholine-based polymers can be monitored with fluorescent probes that are sensitive to free calcium in the cell, and compared with cells cultured on laminin or PSA_0L_{100}. If acetylcholine motifs activate nicotinic receptors on neurons, there is likely to be a greater magnitude of changes in the levels and frequency of calcium influxes on cells cultured on the polymers with acetylcholine motifs compared to laminin or $PSA_0L_{100.}$ Whole-cell patch clamping

can also be used to evaluate whether neurons' electrical activity are affected by the substrate on which they are cultured. Extracellular patch clamp is useful in assessing whether an ionic current can be induced when cells expressing acetylcholine receptors are exposed to the acetylcholine motif. Additionally, the increasing concentration of the acetylcholine motif may be applied to determine whether changes in cell excitability are proportional to the concentration.

Hydrolysis of the polymer's ester bonds is likely to result in an amine-containing degradation product (**Figure 3.6)**, referred to as the 'tentative active component.' Isolating and testing it on neurons could further elucidate how acetylcholine-based polymers affect neurite sprouting. It is unknown whether acetylcholine motifs bound to the sebacate backbone, those free in solution as the tentative active component, or both, can activate acetylcholine receptors. A preliminary study would be to investigate if acetylcholine motifs as oligomers or as the tentative active component elicit cell responses (those mentioned above) associated with acetylcholine receptor activation. Different magnitudes of cell responses may be observed that depend on the presentation of the motif as an oligomer or the tentative active component. To evaluate which is more effective at activating the acetylcholine receptor, cell responses as a function of time can be compared when equivalent concentrations of acetylcholine, oligomer, or tentative active component are added. Determining how the presentation of acetylcholine motifs affects receptor activation, and subsequent signaling pathways, could be useful for re-designing the polymer to optimize neurite growth.

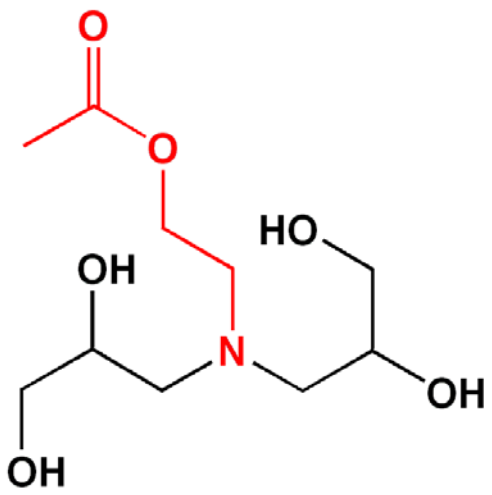

Figure 3.6. Tentative active component of acetylcholine-based polymers resulting from the hydrolysis of ester bonds on the polymer backbone.

The acetylcholine-based polymers may be used to study effects on other responses that are relevant to nerve tissue engineering – such as neurite guidance and synaptogenesis. The role of acetylcholine in growth cone guidance has been shown, as growth cones secrete the neurotransmitter[221] and turn toward acetylcholine gradients[10]. To test whether acetylcholine-based polymers can induce growth cone turning, polymers containing the motif can be selectively patterned onto a growth permissive substrate. Observations of the neurite morphology can be made to assess whether neurite growth coincides with regions containing the acetylcholine-based polymer. It would also be of interest to see whether acetylcholine-based polymers can promote and guide neurite growth in the presence of myelin or myelin-associated inhibitors, since *in vivo* nerve regeneration in the central nervous system is likely to occur in their presence. The soluble form of the polymer, either as a tentative active component (**Figure 3.6)** or a low molecular weight oligomer, may also affect growth cone turning that was similarly seen with gradients of acetylcholine. Identifying whether the growth cone can be induced to

turn towards gradients of the soluble polymer may provide an alternative strategy to guide neurite extension using soluble, neurotransmitter-based motifs.

The spontaneous secretion of acetylcholine in developing neurons[221] implicates acetylcholine's role in synapse formation. The potential role of acetylcholine motifs in synaptogenesis may be investigated by quantifying the number of synapses formed on acetylcholine-based polymers vs. PSA_0L_{100} (or other substrate lacking acetylcholine motifs) using immunohistochemistry for pre-synaptic and post-synaptic markers. More importantly, the formation of *functional* synapses should also be assessed by eliciting an action potential and determining the efficiency of its propagation. *In vitro* evaluation of functional synapse formation may be performed by applying a current to one neuron, then measuring the speed and the magnitude of the current's propagation through other neurons interacting with it using voltage clamping. Similarly, an *in vivo* evaluation of functional synapse formation may be performed by quantifying the speed of propagating an action potential along a nerve regenerated using the acetylcholine-based material vs. a control polymer lacking the motif, such as PLGA or PSA_0L_{100}.

Acetylcholine-motifs may also play a role in cell differentiation and apoptosis. Activation of acetylcholine receptors have been shown to induce actin transcription[220] and neuro-filament expression[217], and protect cells from apoptosis induced by DNA damage, oxidative stress, and mitochondrial impairment[223]. Acetylcholine-based polymers might also affect these processes, and may be useful in differentiating stem cells or preventing extensive cell death that usually results from nerve injuries. Differentiation of stem cells on the acetylcholine-based polymers can be assessed by monitoring the expression of the neuronal proteins neurofilament, tau, or

synaptophysin[240], and comparing those levels to cells cultured on on PSA_0L_{100}. Evaluating the potential of acetylcholine-based polymers in preventing apoptosis may be achieved by assessing their effect on promoting survival in response to an insult through cell number of differences in the expression of apoptosis-related proteins (such as caspase, bcl-2, bax).

Future studies discussed so far involve examining the role of acetylcholine motifs on neurons; glial cells expressing acetylcholine receptors may also respond to the neurotransmitter motif. Muscarinic acetylcholine receptors on are involved in cell cycle progression[244], proliferation[245,246], and progenitor cell survival[247] of Schwann cells[248], astrocytes[245], and oligodendrocytes[249]. Activation of nicotinic acetylcholine receptors on astrocytes also significantly increases intracellular calcium ions[250]. Furthermore, glial cells may indirectly modulate neuronal responses by secreting acetylcholine-binding protein[251].

Acetylcholine-based polymers may directly affect glial cell processes and their functional abilities in expediting nerve regeneration after injury. Glial cells can be cultured onto polymers with acetylcholine motifs to assess its effects on proliferation or on cell survival in the presence of apoptosis-inducing factors. Cell excitability, caused by the influx of ions, may play a role in modulating astrocyte reactivity *in vivo*. Because such proteins are upregulated in reactive astrocytes, GFAP and ezrin immunoreactivity in spinal cord lesions treated with scaffolds containing the acetylcholine motif polymer may elucidate whether such polymers can affect astrocyte reactivity[252]. Potentially modulating astrocyte activity through interactions with the acetylcholine motif could be useful for myelination, as astrocytes can modulate the myelinating ability of

oligodendrocytes[36]. Direct interactions between the acetylcholine motifs and oligodendrocytes might also influence whether acetylcholine motifs affect growth factor production, and can be assessed by assaying neurotrophic content of conditioned media isolated from cells grown on the polymer.

Chapter 4. SCAFFOLD FABRICATION TECHNIQUE OF NERVE GUIDANCE CHANNELS

4.1 Fabrication of nerve guidance scaffolds

Nerve guidance channels may be used to enhance regeneration after injury by providing a physical substrate, delivering growth factors, facilitating the arrangement of cells, or a combination of these functions. The material, growth factors, and cells included in the scaffolds influence neuronal and the overall regenerative responses (Sections 1.4.1 to 1.4.4). Additionally, the topographical cues presented in the scaffold's dimensions[253], microtopography[254], and porosity[255-258] affect *in vivo* responses as well, although the exact relationship between scaffold properties and responses are not fully determined. This is due in part to confounding variables wherein the effect of the topographical cue was not completely isolated – for example, cases in which two different materials were used to investigate a topographical effect. Controlling the scaffold properties within the same material may enable an improved understanding of how such properties affect neurite extension, myelination, functional synapse formation, and functional recovery.

Scaffolds of aligned fibers or having longitudinally oriented channels are being investigated for their ability to direct growth. Their increased surface area and uni-directional nature are designed to promote cell adhesion and guide regeneration toward the target of nerve re-innervation. Evaluation of aligned fibers in peripheral nerve regeneration models indicate an enhancement of myelination, axonal area[28,31,259], and muscle innervation[259] compared to un-aligned fibers. Electrospinning has most often

been used to produce these aligned fibers, though solvent precipitation technique has also been employed[260].

An alternative approach for inducing topographical guidance involves scaffolds with multiple channels. These have been designed to mimic the endoneurial structure found in peripheral nerves. Scaffolds containing multiple, longitudinally oriented channels have been fabricated using laser ablation[261], induced phase separation[23,60,200,262], and fiber templating[24,25,201,263-266]. While these methods are capable of producing channels, there is difficulty in controlling processing parameters to achieve the desired scaffold properties. The laser ablation technique was used to create channel impressions onto a porous polymer of 100 μm depth[261]; scaffolds for peripheral nerve regeneration would likely be much longer than such depths. The induced phase separation method does not ensure that channels go through the entire length of the scaffold. Fiber templating has been successful at creating scaffolds with longitudinal channels. This method, however, provides little control over pore sizes and distribution, which are important parameters influencing the diffusion of nutrients or in the migration of cells into the scaffold.

We present a method for fabricating macroporous scaffolds with longitudinal channels using a combination of salt leaching and fiber templating. We tested the effects of the size of the salt particles and the number of fibers on average pore size and channel volume, respectively. Scaffolds were fabricated from poly(glycerol sebacate), since this polymer has comparable mechanical properties to the peripheral nerve and is biocompatible in nerve regeneration applications[267]. The fabrication method presented here may also be used to control porosity and channel dimensions.

4.2 Materials and methods for creating and characterizing scaffolds

4.2.1 Preparation of scaffolds. Poly(glycerol sebacate) was synthesized according to previously published method[268]. Salt particles were ground using a mechanical grinder and sifted according to particle size using 25-32 μm and 25 μm sieves (ASTM Nos. 450 and 500, respectively) then stored in a dessicator to prevent aggregation. Teflon fibers were soaked in a saturated salt solution, frozen, and then lyophilized in order to coat the fibers with a layer of salt. Teflon molds, each consisting of half a cylinder cut along its longitudinal axis **(Figure 4.1)**, were filled with alternating layers of salt and fibers. 250 mg of salt was used per mold, with 25 or 50 salt-coated Teflon fibers. The salt and fibers were gently packed into the mold using the flat edge of a metal spatula. Molds with salt and fibers were placed in a 37°C, humidified chamber for 1 or 2 hours, and then into a 37°C vacuum chamber overnight. 250 μl of 0.2 g/ml of poly(glycerol sebacate) in tetrahydrofuran was added to each mold, and the solvent was allowed to evaporate in a chemical hood for at least 30 minutes. The molds were transferred to a 150°C vacuum oven and the polymer was cured for 48 hours. Salt leaching was performed by immersing 6-8 scaffolds in 2L of agitated, de-ionized water, which was changed every 12 hours for 48 hours. Teflon fibers were gently extracted from the wet scaffold by holding it between the index finger and thumb and pulling out fibers one at a time.

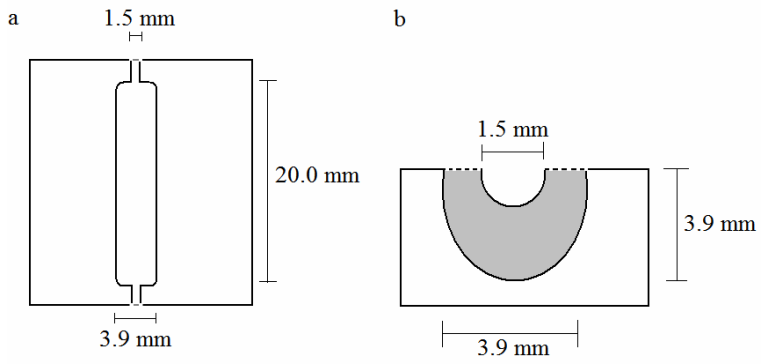

Figure 4.1. Schematic of Teflon mold used to create scaffolds. Top view (a) and side view (b).

4.2.2 Topographical analysis by cryo-sectioning, SEM, and micro-CT. Cross sectional micro-structure was analyzed on randomly-selected scaffold segments using a scanning electron microscope (SEM). Scaffold samples were attached to aluminum mounts with carbon tape, sputter-coated with gold using a Polaron SC7640 High Resolution Sputter Coater (Quorum Technologies, Newhaven, United Kingdom), and observed with a Leo 1550 SEM (20 kV, 3-5 nm spot size). The presence of channels in the scaffold was examined by embedding the scaffold in Tissue-Tek Optimal Cutting Temperature (OCT) Compound (Sakara Finetek U.S.A., Torrance, CA) and cryosectioning a 10 mm section of the scaffold into 100 μm-thick sections. Sections were imaged by bright field microscopy on an inverted microscope [Nikon TE-2000U microscope (Melville, NY) equipped with a 4 MP Diagnostics Spot Flex digital camera (Sterling Heights, MI)]. Micro-CT analysis was performed on a Scanco Medical μCT 40 micro-computed tomography scanner (Southeastern, PA), and used to determine the porosity, average pore size, and pore size distributions of the scaffolds with a voxel size of 6 μm.

4.2.3 Statistical Analysis. Analysis of variance was applied to determine whether differences in average pore size and channel volume were significant ($p < 0.05$).

4.3 Results of Topographical Analysis

4.3.1 Image Analyses. Imaging by micro-CT revealed that longitudinally oriented fibers were embedded throughout the length of the scaffold **(Figure 4.2).** Analyses by SEM and cryo-sectioning were performed to assess the presence of micro-pores and longitudinal channels once the fibers were removed. Cross-sectional images of the scaffold show that micro-pores were present throughout it **(Figure 4.3)** and that extraction of the fibers led to open channels **(Figure 4.4).** Comparing an area on one picture with the same area on a subsequent section shows that channels remain open, with the possibility of separation or merging of channels.

Micro-CT, SEM, and cryosections of the scaffold indicate that micro-porous scaffolds with longitudinally oriented channels were formed with the salt fusion and fiber templating method. Fibers maintained their alignment to the axis of the scaffold mold through salt packing and salt fusion steps. Teflon fibers were successfully extracted from scaffolds of 10 mm length. There was no observed breakage of fibers during extraction, as determined by examining each of their lengths and comparing it with the length of the scaffold. The salt leaching step allowed micropores to form within scaffolds, as revealed by SEM analysis. Holes smaller than the salt particle sizes employed were also observed, and can be attributed to the evaporation of glycerol formed during the polymer curing process.

Open channels remained after Teflon fibers were extracted. Because the fibers were not exactly parallel to one another during the fabrication process, one channel could merge with another. This may affect regeneration *in vivo* by causing neuronal processes to cross paths, and may lead to inexact reconnection of the nerve bundles at the distal and proximal ends of the nerve gap. It is also possible that merging nerve bundles may lead to paracrine stimulation that could further enhance neurite elongation. The effects of crossed channels on the regenerative response are still unknown. Further improvements on ensuring channel separation could be used to fabricate scaffolds with completely separated channels, and gauge differences in biological responses in the future. Meanwhile, topographical cues' influence on nerve regeneration through scaffold dimensions can be investigated.

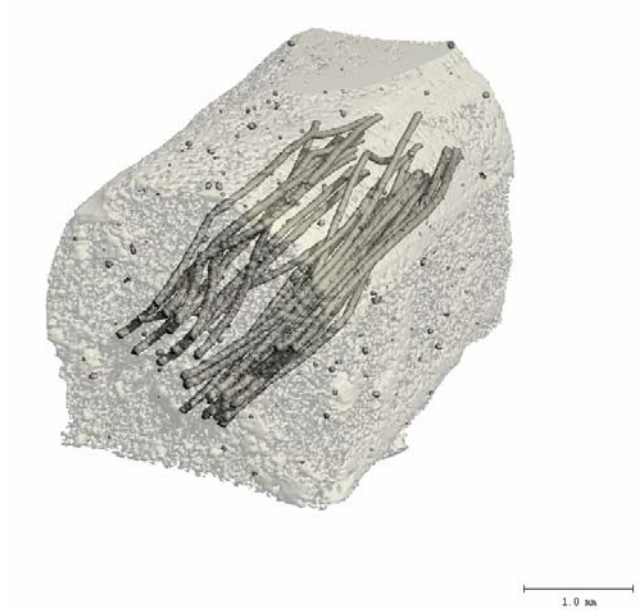

Figure 4.2. Micro-CT analysis of PGS scaffold containing Teflon fibers.

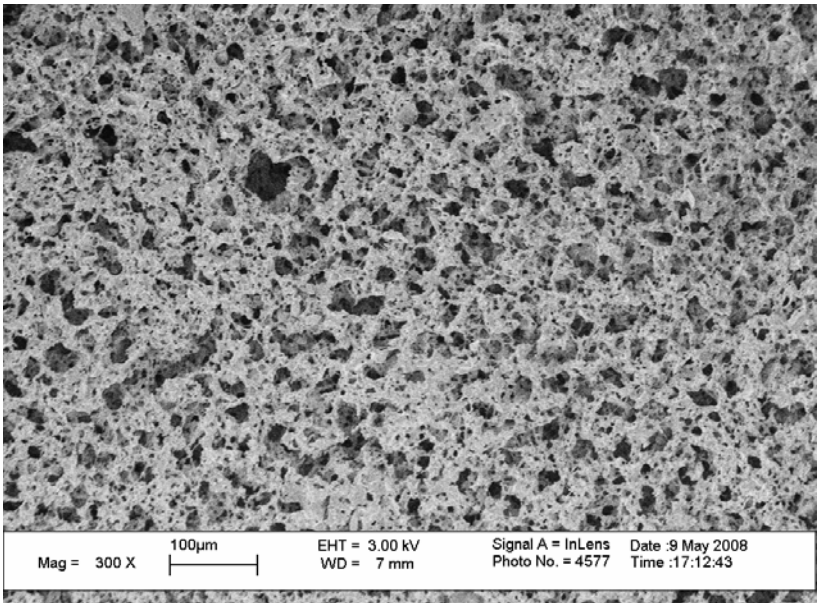

Figure 4.3. SEM image of scaffold cross-section showing its porous nature. A salt template consisting of 32 – 45 µm particles were fused and 100 fibers were embedded for the production this particular scaffold.

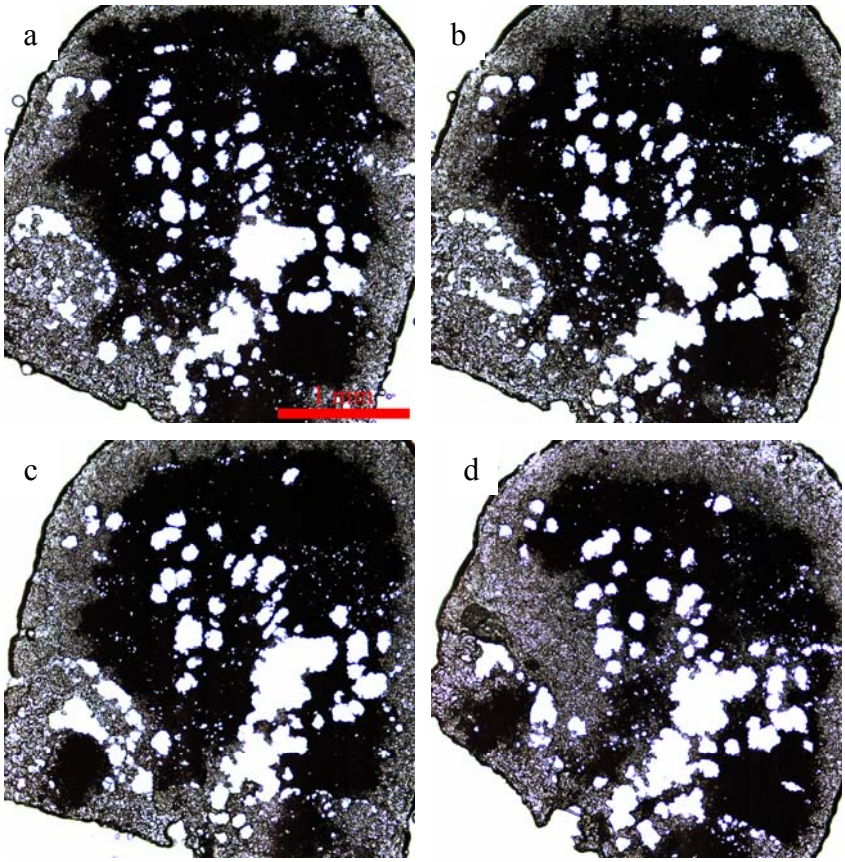

Figure 4.4. Longitudinally-oriented channels remain after the extraction of fibers. Images were obtained by cryosectioning scaffolds into 100 µm-thick slices. Consecutive sections (a-d) along the length of the scaffold. Scale bar = 1 mm.

4.3.2 Analysis of Scaffold dimensions by micro-CT. We attempted to control the channel volume, pore size, and pore distribution by varying the number of fibers, salt particle sizes, and salt fusion time used during the scaffold fabrication. Micro-CT scans were used to determine the volume occupied by fibers, the average pore size, the distribution of the pore sizes, and the volume fraction occupied by the polymer scaffold.

Volume occupied by the channels is proportional to the number of fibers embedded in the scaffold. Doubling the number of fibers increased the channel volume by roughly 2-fold **(Figure 4.5)**. Twenty five fibers occupied 1.3 % of the total scaffold volume, compared with 2.7% occupied by 50 fibers.

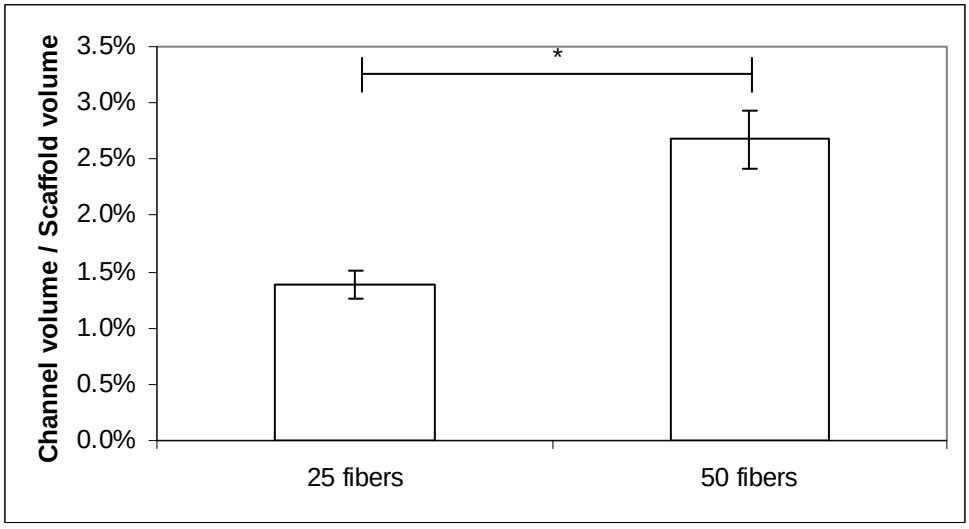

Figure 4.5. Channel volume as a fraction of scaffold volume. Scaffolds made with 50 fibers had approximately twice the channel volume as scaffolds made with 25 fibers. *$p < 0.05$. Error bars = standard deviation. N = 6 samples per condition.

In order to control average pore size and pore size distribution, different-sized salt particles and fusion times were tested. Salt particles of two different distributions were obtained by sieving – less than 25 μm or particles between 25 and 32 μm. After fibers

and salt were added to a mold, the salt was fused for 1 or 2 hrs. The salt particle size had a statistically significant effect on the average pore size of the scaffolds at fusion times of 2 hours **(Figure 4.6)**. The salt particle size did not have an effect on average pore size when salt was fused for 1 hour. Increasing the fusion time from 1 to 2 hours greatly decreased the variance of the average pore size in statistically significant manner **(Figure 4.6).** The average pore size depends largely on the salt particle size and while distribution of particle sizes can be affected by the salt fusion time.

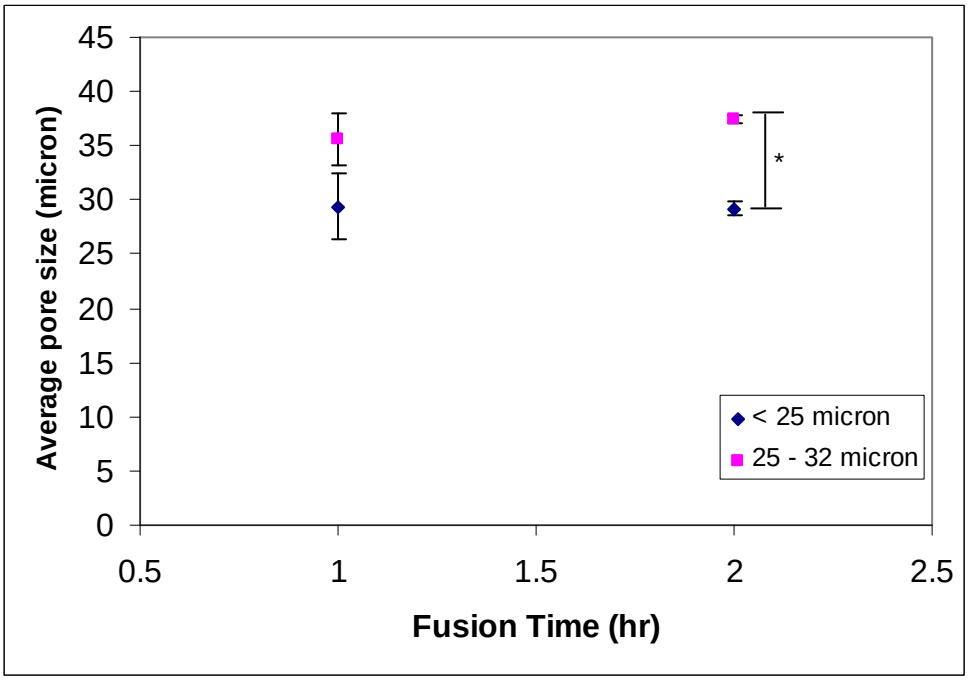

Figure 4.6. Two hour fusion time enhances differences between average pore sizes due to salt particle size. Longer fusion time decreases variance associated with salt particles,*$p<0.05$

4.4 Discussions, conclusions and future studies in the fabrication of microporous scaffolds with longitudinally aligned channels

We have presented a fabrication method for a micro-porous scaffold containing longitudinally oriented channels. We showed that the channel volume, average pore size, and distribution of the pore sizes can be controlled through the fiber number, salt particle size, and salt fusion time, respectively. Although it was not examined in this study, there are other scaffold dimensions that may be controlled using this fabrication method. Porosity is likely to be influenced by the amount of salt added to the mold and the number of channels. Channel diameter is controllable through the fiber diameter. Methods that have been previously used to create aligned channels in scaffolds include unidirectional freezing[199,200] and templating[24-26]. Compared to these techniques, the scaffold fabrication technique presented here allows additional control over pore size, porosity, channel volume and dimensions while enabling the presentation of aligned channels.

Future process improvements involve ensuring channel separation and decreasing fabrication time. Because channels' merging could cause regenerating nerves to intertwine and lead to incorrect reconnection of the nerve ends, a scaffold with separate, longitudinal channels may be more ideal. To improve separation of the fibers, a mold with fully open ends could be used **(Figure 4.7)**. The fully open ends would not confine fibers as closely as the current mold and allow them to disperse more evenly. Furthermore, salt particles and fibers may be more easily layered into this space, which can decrease the fabrication time. Much of the effort in the current fabrication method is

spent ensuring that salt particles are interspersed between fibers, which is more difficult when fibers are so closely associated together using the current mold.

Testing the scaffolds of varying dimensional properties *in vivo* nerve regeneration may give a better understanding on how scaffold properties affect regeneration. Observing how the channel volume or diameter affects the rate of axonal extension or infiltration of Schwann cells into the scaffold is useful in the design of a nerve guidance channel. The effect of pore size and pore distribution on the ability to different cell types to enter the scaffold may also be used to facilitate growth. For example, the presence of reactive astrocytes in a spinal nerve guidance channel would be undesirable, whereas successful migration of endothelial cells into a peripheral nerve guidance channel could encourage vascularization. Topographical cues, in the presence of other growth-promoting stimuli, could also have synergistic effects. Scaffolds may be combined with neurotrophic factors, extracellular matrix cues, neurotransmitter-based materials, or all of these, to maximize the regeneration response.

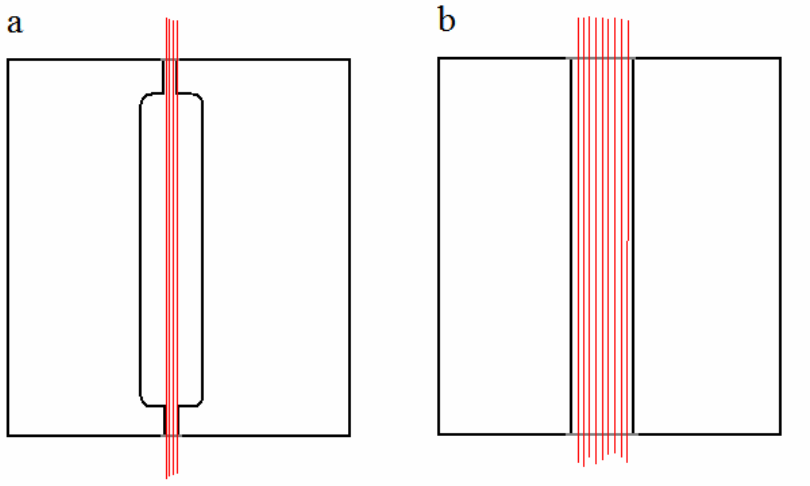

Figure 4.7. Design of molds for nerve guidance scaffolds may be used to control spacing of channels within scaffold. Top view of a) Current mold for fabrication b) Mold with open configuration

Topographical guidance may exert its various influences on cells through cell adaption mechanisms or by inducing alterations in protein adsorption[269]. Filopodial interactions with materials suggest that they play a role in sensing topographical surroundings. Differences in interfacial forces could be interpreted by cells by influencing focal adhesion formation and cytoskeleton structure[270]. Cells may then adapt to local environments by controlling the secretion of extracellular matrix proteins[271]. Another possible mechanism for topographical guidance involves alterations in adsorbed proteins, which could result from differential wetting of surfaces, surface energy differences, or changes in surface area. Local concentrations of adsorbed proteins can vary according to wetting of surfaces[272], potentially through changes in hydrophobicity along patterned surfaces[273]. Proteins may also preferentially adsorb to topographical surfaces with increased surface energy[274,275] or higher surface areas[14,276].

Chapter 5. CONCLUSIONS, PERSPECTIVES AND FUTURE STUDIES

5.1 Conclusions

The goals of this thesis were to: 1) synthesize polymers with control over the polymer backbone and amount of acetylcholine-like motifs; 2) assess the effect of acetylcholine motif concentration on neurite sprouting *in vitro*; and 3) fabricate nerve guidance channel that is both microporous and contains longitudinally oriented channels. A modular synthesis design enabled materials to be made that possess covalently-bound acetylcholine motifs within the polymer. This differs with previous studies which have focused on avidin-biotin interactions to tether a derivatized form of GABA to surfaces[228,229]. The synthesis scheme allowed neurotransmitter motifs and polymer backbones to be varied. The scheme also permits the ability to synthesize a variety of polymers, with the potential to study the effects of 2 or more neurotransmitters, polymer degradation, or mechanical properties that can be affected by the neurotransmitter motifs and polymer backbone. This study is the first to demonstrate that neurite sprouting *in vitro* of DRG is affected in a biphasic manner by the concentration of the acetylcholine motifs presented by a polymer. This subtle distinction suggests that maximizing the amount of chemical cues do not necessarily lead to maximized neurite growth. By fabricating a microporous scaffold with channels from poly(glycerol sebacate), the effect of presenting biochemical and physical cues may be investigated in peripheral nerve injury models.

5.2 Potential and Limitations of Acetylcholine-based Polymers

It is yet unknown whether the acetylcholine-based polymers interact with the neurotransmitter's receptors. Incorporating aminoethyl acetate and leucine ethyl ester in the polymer may have affected surface chemistry or molecular topology, thereby influencing neurite sprouting. The concentration of leucine ethyl ester, though it has no known effects on neurite sprouting, may also play a role in neurite growth. Instead of leucine ethyl ester, other single amino acids with no known effects on sprouting, such as isoleucine, alanine, or asparagine, could also be used to investigate the effect of acetylcholine motifs in the polymer. If these alternatives all show the same trend as what is observed in this study, then it is likely that the acetylcholine motif and not leucine ethyl ester is the bioactive moiety of the polymer. While the antagonist binding studies suggest acetylcholine receptors are involved neurite sprouting, further assessments using electrophysiological recordings and molecular assays are needed to determine this.

The concentration dependence of neurite sprouting observed on the acetylcholine-based polymers could be caused by changes in protein adsorption pattern on the materials' surface. No serum was added to the DRG culture and NGF was the only protein added to the system. Cells may secrete their own proteins during culture, and their adsorption on the polymer can depend on surface chemistry and morphology. Different materials will likely yield different adsorption patterns and different protein configurations. Protein adsorption may be investigated by methods such as ellipsometry, atomic force microscopy, or fluorescence spectroscopy, but these methods do not indicate conformation of the adsorbed proteins. More sophisticated tools are required in addition

to these conventional techniques, as it is currently difficult to assess the protein configurations as they exist on the material surface within cell culture media.

If the acetylcholine motifs interact with the receptors, these interactions could be used to elicit changes in electrical activity, extracellular matrix production, and cell cycle progression. These changes can impact cells of the nervous system, as well as immune[277] and inflammatory cells[278,279] that express acetylcholine receptors. Given the potential interactions with acetylcholine receptors, the possibilities of using the acetylcholine-based polymers will be discussed below.

Activation of the acetylcholine receptor can modulate the cell's electrical activity through the influx of calcium through voltage-gated calcium channels or the release of intracellular calcium stores. These electrical changes through calcium transients play a role in growth cone turning[163] and dendrite growth[164,165]. Influx of calcium stimulates lamellipodia formation and axonal branching in cerebral cortex neurons[167]. Calcium transients also play a role in inducing axon branching in cortical neurons by targeting the calcium/calmodulin-dependent protein kinase II[164]. Electric field-induced membrane depolarization can similarly cause neurite initiation and elongation[166,167].

Depolarization may also convert the repulsive effect of soluble myelin-associated glyocoprotein to a growth-cone attractive molecule, which has been shown in frog neurons[168]. Myelin-associated glycoprotein is a key inhibitory component that prevents axon regeneration after spinal cord injury. By depolarizing the neurons with a potassium ion solution, higher intracellular calcium levels could be obtained, which then mediated attractive turning toward myelin-associated glycoprotein[280]. If the acetylcholine-based polymer can modulate neurons' depolarizations, it may be useful for inducing neurite

initiation and elongation, as well as promiting growth even in the presence of growth-inhibitory cues.

Acetylcholine motifs on polymers may affect nerve regeneration through interactions with glial cells, since Schwann cells[248], astrocytes[245], and oligodendrocytes[249] express acetylcholine receptors. Activating these receptors on glial cells can increase the proliferation of cortical astrocytes[245] and oligodendrocyte progenitors[281], though the mechanism is not fully understood. If the same effect is seen with use of the acetylcholine-based polymers, the mitogenic effect of muscarinic receptor activation may be detrimental in repairing spinal cord injury since reactive astrocytes and oligodendrocytes are responsible for secreting growth-inhibitory proteins. It is unknown whether the acetylcholine-based polymers will affect the production of chondroitin sulfate proteoglycans or myelin associated inhibitors.

Though astrocytes produce the glial scar and chondroitin sulfate proteoglycans after central nerve injury, stimulating their acetylcholine receptors could induce neurite formation and modulate extracellular matrix production. Astrocytes that have been stimulated with carbachol (an acetylcholine agonist) are capable of inducing neuritogenesis in hippocampal neurons[282]. Carbachol stimulation induced astrocytes to produce and release fibronectin, laminin-1, and plasminogen activator inhibitor-1. If the acetylcholine-based polymers are able to similarly induce extracellular matrix production and neuritogenesis, one could take advantage of the astrocytes' presence at the injury site. Plasminogen activator inhibitor-1 inhibits the activity of plasminogen activators that are responsible for the formation of plasmin, a proteolytic enzyme that degrades many components of the extracellular matrix including laminin and fibronectin. Plasminogen

activator inhibitor-1 has also been found to induce neurite outgrowth by directly phosphorylating Trk A receptors and activating ERK1/2 and c-Jun in PC12 cells[282,283]. Activation of the ERK1/2 pathway has also been implicated in neurite elongation of hippocampal neurons[284], as well as protecting against arachidonic acid induced-apoptosis of spinal cord neurons[222].

This research presents one of the first studies to utilize covalent linkage of neurotransmitter motifs within polymers. This approach contrasts to other materials utilized in nerve tissue engineering because acetylcholine-based polymers have the potential to directly affect the cell's electrical activity by changing levels of calcium, a molecule that is ubiquitously used by cells in controlling a variety of cell processes. Activation of the acetycholine receptor mobilizes calcium signals, which can activate or deactivate calcium-sensitive processes (**Table 5.1**)[285]. Neurons can respond to calcium signals by triggering exocytosis of neurotransmitters or inducing entry of calcium, which has numerous targets including: adenylyl cyclase I or II that control cyclic AMP production, proline-rich tyrosine kinase, mitogen-activated protein kinase, calcium/calmodulin-dependent kinase II, and calmodulin-calcineurin.

Potential interactions between the acetylcholine motifs and nicotinic and muscarinic receptors on neurons and glia could mediate changes in calcium levels. Calcium's regulatory role in a multitude of processes can have associated advantages and disadvantages. This property could provide multiple targets of intervention for directing cell behavior, while competing effects may also exist between processes. **Figure 5.1** illustrates calcium's role in signalling pathways[285] that have been implicated in nerve

regeneration. The following paragraphs provide examples on how the polymer could potentially affect regeneration via calcium levels.

Table 5.1. Calcium-sensitive processes that affect cell behaviors that may play a role in nerve regeneration[285].

Calcium-sensitive process	Cell behavior affected
Troponin C Calmodulin activation of myosin-light chain kinase	Contraction
Ca2+/calmodulin-dependent protein kinase Transcription factors	Learning and Memory
Adenylyl cyclase Cyclic AMP phosphodiesterase Nitric oxide synthase Protein kinase C Proline-rich kinase 2 Inositol-1,4,5-trisphosphate	Cross-talk with other signaling pathways
Ion channels	Membrane excitability, Secretion
Synaptotagmin	Secretion
Mitochondrial enzymes	ATP synthesis, Steroid Synthesis
Caspases	Apoptosis

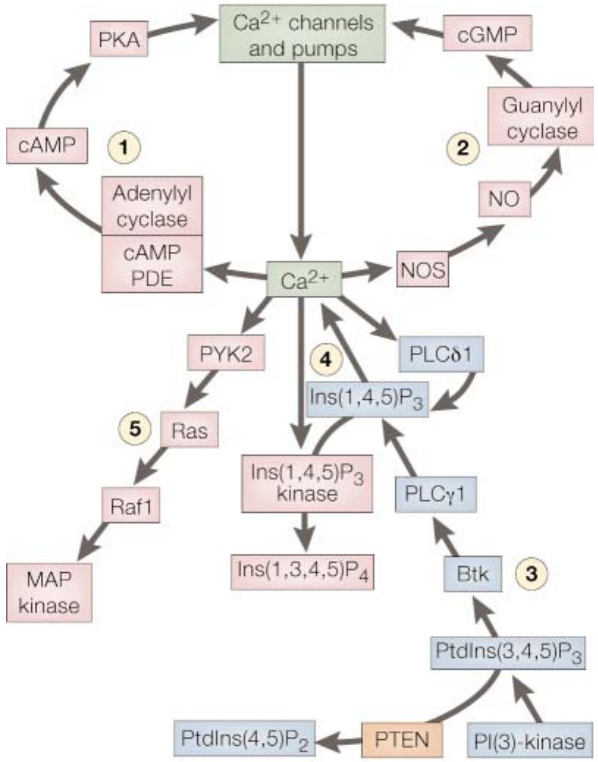

Figure 5.1. Calcium interacts with: 1) cAMP; 2) Nitric oxide synthase; 3) phosphatidylinositol-3-OH kinase; 4) PLC; and 5) mitogen-activated protein kinase[285].

The polymer may increase calcium levels, which subsequently could increase cyclic adenosine monophosphate (cAMP) levels to facilitate nerve regeneration. Adenylyl cyclase can be activated by calcium to increase cAMP production. Elevation of cyclic AMP levels may be particularly useful in regenerating the spinal cord by overcoming inhibition of myelin, promoting neuronal survival, and encouraging axonal extension beyond the spinal cord lesion.

Transversing the injury site is a major challenge in regenerating the spinal cord; the presence of inhibitory proteins and the glial scar prevent growth across this boundary. Microinjecting a membrane-permeable analog of cyclic AMP increased regrowth of sensory neurons into the spinal cord lesion and could overcome myelin *in vitro*[286]. Elevating cAMP levels also prolong the survival of spinal motor neurons in culture, in a distinct manner from the addition of growth factors. Spinal motor neurons cultured in the presence of multiple growth factors of BDNF, CNTF, FGF, GDNF, and HGF only transiently promoted survival, and most cells had died after 7 days in culture[287]. In contrast, the majority of neurons cultured with cAMP survived in the same period and could do so even at low density. Growth factors and cAMP could synergistically prolong survival[287] as well as improve regeneration beyond the spinal cord lesion[288]. Furthermore, increasing cAMP levels can also increase expression of trk B (BDNF receptor)[289], which can increase neurons' sensitivity to the growth factor.

Another effect of calcium activation is to increase nitric oxide synthase (NOS), which can affect levels of nitric oxide, a mediator of inflammation and thrombosis. Following spinal cord injury, neuronal NOS in spinal cord cells is up-regulated[290]. High levels of NOS are neurotoxic to spinal cord cells, and there is evidence in peripheral

nerve injury models that inhibiting NOS enhances myelination and survival of axons[291]. Mice with sciatic nerve injury that were treated with NOS inhibitors exhibited electrophysiological recovery earlier and had larger, myelinated fibers than control mice. Inflammation may damage cells but can also promote regeneration[292-294]; inflammation may be controlled by NOS levels according to calcium activation of the cell. The potential upregulation of NOS via calcium-signalling events and corresponding increase the inflammatory response should be balanced against the potential anti-inflammatory effects that could also be mediated through acetylcholine receptors. Macrophages express nicotinic[278] and muscarinic[279] acetylcholine receptors. Nicotinic receptor activation inhibits the release of tumor necrosis factor by macrophages[278] by supressing phosphorylation of I-kappa B and inhibiting the transcriptional activity of nuclear factor-kappa B[295].

Acetylcholine motifs have the potential to activate the receptor, which could induce changes in calcium levels that play a role in mediating cAMP and NOS levels. In addition, the calcium transients could also activate the mitogen-activated protein kinase (MAPK) signalling pathway. The ERK1/2 and c-Jun MAPK pathways have been implicated in neurite elongation[282-284] following stimulation of the acetylcholine receptors of astrocytes and hippocampal neurons. Growth factors, such as NGF, BDNF, and GDNF also activate MAPK[296-298]. The acetylcholine-based polymers may exert their effects through the MAPK pathways, in addition to mediating cAMP and NOS.

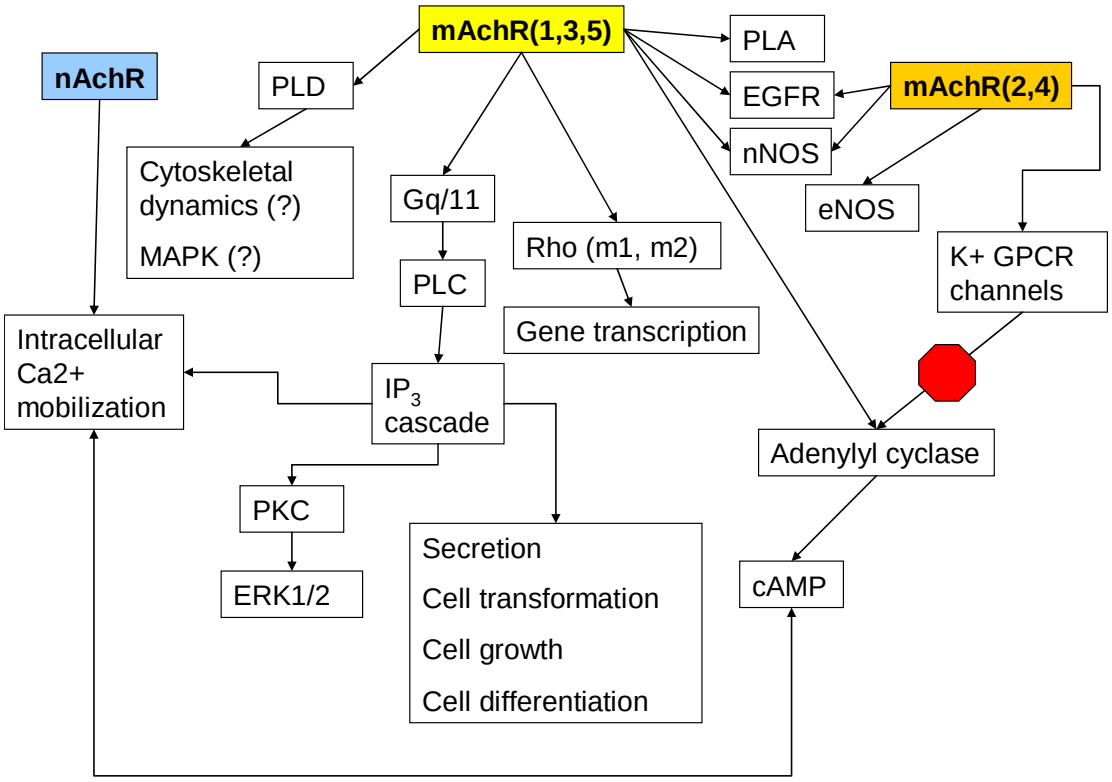

Figure 5.2. Signalling events following acetylcholine receptor activation[299]. Activating nicotinic acetylcholine receptor (nAchR) mobilizes calcium transients, which can modulate cAMP levels in the cell. There are two subtypes of muscarinic acetylcholine receptors (mAchR). m1, m3, and m5 mAchRs are associated with activating phospholipase C (PLC), while m2 and m4 mAchRs inhibit adenylyl cyclase activity. PLA: phospholipase A, PLD: phospholipase D, PKC: protein kinase C, nNOS: neuronal nitric oxide synthase, IP_3: inositol triphosphate, EGFR: epidermal growth factor receptor. '?' indicates that studies suggest PLD mediates these events.

Activation of acetylcholine receptors may lead to downstream signalling events that ultimately could affect cell processes, including gene transcription, cytoskeletal dynamics, growth, and secretion[242,299]. **Figure 5.2** summarizes signalling pathways that may become involved, depending on whether nicotinic or muscarinic acetylcholine receptors are activated. To assess whether acetylcholine-based polymers activate either of the two muscarinic receptor subtypes, measurement of downstream effectors can be performed.

Activation of phospholipase C catalyzes inositol triphosphate and diacylglycerol to form; this cascade mobilizes intracellular calcium, activates protein kinase C, and affects cell growth. Inositol triphosphate production in response to stimulation with acetylcholine motifs can be performed, with and without the presence of subtype selective agonists that will block m1, m3, and m5 receptors. Changes in inositol triphosphate levels would likely elicit corresponding changes on the downstream effectors.

Transactivation of the epidermal growth factor receptor (EGFR) is another mechanism potentially activated by acetylcholine motifs. Activation of muscarinic acetylcholine receptors activates the extracellular activity of a transmembrane metalloproteinase, which processes the EGFR and activates it. Measuring metalloproteinase activity of the cell in response to exposure to the acetylcholine motif could be used to indicate this pathway's involvement. Selective antagonist to nicotinic receptors is not expected affect this activity.

5.3 Evaluation of materials for nerve regeneration

Nerve repair is likely to be a complex process, involving multiple cell interactions. While the main interest is usually to assess how materials may promote growth, inflammatory and immune responses to the material are also very relevant and could determine the materials' effectiveness *in vivo*. Implantion of the materials in the body often involve protein adsorption and desorption, blood-material interactions, acute inflammation, and can further progress to chronic inflammation, granulation tissue development, foreign body reaction, and fibrosis/fibrous capsule development[300].

Numerous proteins (such as those involved in the coagulation pathway) and non-neural cells (i.e. platelets, macrophages, leukocytes) are present and can interact with the materials' surface. Furthermore, the procedure of implanting scaffolds into the injury site could heighten the acute inflammatory response, since the implantation procedure would be invasive and likely damage existing vasculature. In the case of implanting acetylcholine-based polymers for nerve regeneration, the deposition of proteins and cells could sufficiently obscure neurons or glia from interacting with the acetylcholine motif. Degradation product of the acetylcholine-based polymer into sebacic acid and a component containing the acetylcholine motif (see Section 3.4) could release the 'tentative active product' into the site, with the potential to stimulate the neurons and glia in soluble form.

Non-neural cells may also respond to acetylcholine motifs, which could affect their roles in the inflammation and immune responses. As outlined in Section 5.1, macrophages express the acetylcholine receptor[278,279], which when activated, can inhibit the release of tumor necrosis factor[278]. Stimulating nicotinic acetylcholine receptors *in vitro* in mice-derived macrophages also caused increase proliferation of macrophages[279]. Potential activation of nicotinic receptors by the acetylcholine motif may quicken the formation of foreign body giant cells, since fusion of macrophages is involved in this process.

Leukocytes, which are involved in the chronic inflammatory response and immune response to materials, also express muscarinic acetylcholine receptors[301]. Immunologic stimulation of T- and B- lymphocytes can lead to up-regulation of muscarinic receptors on their surfaces[277], though it is unclear whether their activation

induces calcium transients[302,303]. Leukocytes also play roles in thrombosis, acute inflammatory response, and foreign body giant cell formation. It would be of interest if acetylcholine receptor activation of these cells plays a role in these responses.

Evaluation of biomaterials in treating nerve injury mostly has focused on neuronal responses *in vitro*, quantification of the regenerated axon's properties, or functional recovery that is assessed through behavioral testing. There is no standard method or animal model to assess regeneration efficiency, making it difficult to identify effective strategies. Several methods have been used for measuring neurite length alone, and many more exist for quantifying the extent of regeneration through a scaffold. A method has been developed to assess functional recovery after spinal cord injury in rodents[304], but it is not always utilized. Because there is no universal test to assess functional recovery, distinctions and advantages associated with various treatment are difficult to determine.

Additionally, there is no standard animal model for nerve injury. Different experimental treatments studying their effects on nerve regeneration have been investigated in mice, rats, humans, and other animals. Any resulting nerve regeneration may be dependent on variations between the recovery abilities of the animals and not wholly on the treatment. Although it may be difficult to determine them at first, creating standard protocols and evaluation techniques will be of great value to the field of nerve regeneration. The ability to compare nerve regeneration among the different materials that are used could give insights on effective approaches.

REFERENCES

[1] Fan, W. *et al.*, Repairing a 35-mm-long median nerve defect with a chitosan/PGA artificial nerve graft in the human: a case study. *Microsurgery* 28 (4), 238-242 (2008).

[2] National Institute of Neurological Disorders and Stroke, N.I.H., Spinal cord injury: hope through research, Available at http://www.ninds.nih.gov/disorders/sci/detail_sci.htm, (2008).

[3] Anderson, K.D., Targeting recovery: priorities of the spinal cord-injured population. *J Neurotrauma* 21 (10), 1371-1383 (2004).

[4] Berkowitz, M., O'Leary, P., Kruse, D., & Harvey, C., *Spinal cord injury: An analysis of medical and social costs.* (Demos Medical Publishing Inc., New York, 1998).

[5] Chalfoun, C.T., Wirth, G.A., & Evans, G.R., Tissue engineered nerve constructs: where do we stand? *J Cell Mol Med* 10 (2), 309-317 (2006).

[6] Fawcett, J., Repair of spinal cord injuries: where are we, where are we going? *Spinal Cord* 40 (12), 615-623 (2002).

[7] Schmidt, C.E. & Leach, J.B., Neural tissue engineering: strategies for repair and regeneration. *Annu Rev Biomed Eng* 5, 293-347 (2003).

[8] Mattson, M.P. & Kater, S.B., Excitatory and inhibitory neurotransmitters in the generation and degeneration of hippocampal neuroarchitecture. *Brain Res* 478 (2), 337-348 (1989).

[9] Nguyen, L. *et al.*, Neurotransmitters as early signals for central nervous system development. *Cell Tissue Res* 305 (2), 187-202 (2001).

[10] Zheng, J.Q., Felder, M., Connor, J.A., & Poo, M.M., Turning of nerve growth cones induced by neurotransmitters. *Nature* 368 (6467), 140-144 (1994).

[11] Roerig, B., Nelson, D.A., & Katz, L.C., Fast synaptic signaling by nicotinic acetylcholine and serotonin 5-HT3 receptors in developing visual cortex. *J Neurosci* 17 (21), 8353-8362 (1997).

[12] Aramakis, V.B. & Metherate, R., Nicotine selectively enhances NMDA receptor-mediated synaptic transmission during postnatal development in sensory neocortex. *J Neurosci* 18 (20), 8485-8495 (1998).

[13] Gao, J. *et al.*, A neuroinductive biomaterial based on dopamine. *Proc Natl Acad Sci U S A* 103 (45), 16681-16686 (2006).

[14] Curtis, A. & Wilkinson, C., Topographical control of cells. *Biomaterials* 18 (24), 1573-1583 (1997).

[15] Letourneau, P.C., Possible roles for cell-to-substratum adhesion in neuronal morphogenesis. *Dev Biol* 44 (1), 77-91 (1975).

[16] Clark, P., Connolly, P., Curtis, A.S., Dow, J.A., & Wilkinson, C.D., Topographical control of cell behaviour. I. Simple step cues. *Development* 99 (3), 439-448 (1987).

[17] Clark, P., Connolly, P., Curtis, A.S., Dow, J.A., & Wilkinson, C.D., Topographical control of cell behaviour: II. Multiple grooved substrata. *Development* 108 (4), 635-644 (1990).

[18] Rajnicek, A., Britland, S., & McCaig, C., Contact guidance of CNS neurites on grooved quartz: influence of groove dimensions, neuronal age and cell type. *J Cell Sci* 110 (Pt 23), 2905-2913 (1997).

[19] Rajnicek, A. & McCaig, C., Guidance of CNS growth cones by substratum grooves and ridges: effects of inhibitors of the cytoskeleton, calcium channels and signal transduction pathways. *J Cell Sci* 110 (Pt 23), 2915-2924 (1997).

[20] Clark, P., Connolly, P., Curtis, A.S., Dow, J.A., & Wilkinson, C.D., Cell guidance by ultrafine topography in vitro. *J Cell Sci* 99 (Pt 1), 73-77 (1991).

[21] Cai, J., Ziemba, K.S., Smith, G.M., & Jin, Y., Evaluation of cellular organization and axonal regeneration through linear PLA foam implants in acute and chronic spinal cord injury. *J Biomed Mater Res A* 83 (2), 512-520 (2007).

[22] Hurtado, A. *et al.*, Poly (D,L-lactic acid) macroporous guidance scaffolds seeded with Schwann cells genetically modified to secrete a bi-functional neurotrophin implanted in the completely transected adult rat thoracic spinal cord. *Biomaterials* 27 (3), 430-442 (2006).

[23] Patist, C.M. *et al.*, Freeze-dried poly(D,L-lactic acid) macroporous guidance scaffolds impregnated with brain-derived neurotrophic factor in the transected adult rat thoracic spinal cord. *Biomaterials* 25 (9), 1569-1582 (2004).

[24] Stokols, S. *et al.*, Templated agarose scaffolds support linear axonal regeneration. *Tissue Engineering* 12 (10), 2777-2787 (2006).

[25] Yang, Y. *et al.*, Neurotrophin releasing single and multiple lumen nerve conduits. *J Control Release* 104 (3), 433-446 (2005).

[26] Yu, T.T. & Shoichet, M.S., Guided cell adhesion and outgrowth in peptide-modified channels for neural tissue engineering. *Biomaterials* 26 (13), 1507-1514 (2005).

[27] Yang, F., Murugan, R., Wang, S., & Ramakrishna, S., Electrospinning of nano/micro scale poly(L-lactic acid) aligned fibers and their potential in neural tissue engineering. *Biomaterials* 26 (15), 2603-2610 (2005).

[28] Chew, S.Y., Mi, R., Hoke, A., & Leong, K.W., Aligned protein-polymer composite fibers enhance nerve regeneration: a potential tissue-engineering platform. *Advanced Functional Materials* 17, 1288-1296 (2007).

[29] Schnell, E. *et al.*, Guidance of glial cell. migration and axonal growth on electrospun nanofibers of poly-epsilon-caprolactone and a collagen/poly-epsilon-caprolactone blend. *Biomaterials* 28 (19), 3012-3025 (2007).

[30] Smeal, R.M., Rabbitt, R., Biran, R., & Tresco, P.A., Substrate curvature influences the direction of nerve outgrowth. *Ann Biomed Eng* 33 (3), 376-382 (2005).

[31] Ceballos, D. *et al.*, Magnetically aligned collagen gel filling a collagen nerve guide improves peripheral nerve regeneration. *Exp Neurol* 158 (2), 290-300 (1999).

[32] Dowell-Mesfin, N.M. *et al.*, Topographically modified surfaces affect orientation and growth of hippocampal neurons. *J Neural Eng* 1 (2), 78-90 (2004).

[33] Gomez, N., Lee, J.Y., Nickels, J.D., & Schmidt, C.E., Micropatterned polypyrrole: A combination of electrical and topographical characteristics for the stimulation of cells. *Advanced Functional Materials* 17 (10), 1645-1653 (2007).

[34] Johansson, F., Carlberg, P., Danielsen, N., Montelius, L., & Kanje, M., Axonal outgrowth on nano-imprinted patterns. *Biomaterials* 27 (8), 1251-1258 (2006).

[35] Tsuruma, A. *et al.*, Topographical control of neurite extension on stripe-patterned polymer films. *Colloids and Surfaces A: Physicochemical and Engineering Aspects* 284-285, 470-474 (2006).

[36] Vernadakis, A., Glia-neuron intercommunications and synaptic plasticity. *Prog Neurobiol* 49 (3), 185-214 (1996).

[37] David, S. & Aguayo, A.J., Axonal elongation into peripheral nervous system "bridges" after central nervous system injury in adult rats. *Science* 214 (4523), 931-933 (1981).

[38] Fu, S.Y. & Gordon, T., The cellular and molecular basis of peripheral nerve regeneration. *Molecular Neurobiology* 14 (1-2), 67-116 (1997).

[39] Filbin, M.T., Myelin-associated inhibitors of axonal regeneration in the adult mammalian CNS. *Nature Reviews Neuroscience* 4 (9), 703-713 (2003).

[40] Hughes, P.E. *et al.*, Activity and injury-dependent expression of inducible transcription factors, growth factors and apoptosis-related genes within the central nervous system. *Progress in Neurobiology* 57 (4), 421-450 (1999).

[41] Stichel, C.C. & Muller, H.W., The CNS lesion scar: new vistas on an old regeneration barrier. *Cell and Tissue Research* 294 (1), 1-9 (1998).

[42] Vargas, M.E. & Barres, B.A., Why is Wallerian degeneration in the CNS so slow? *Annu Rev Neurosci* 30, 153-179 (2007).

[43] Purves, D. *et al.*, *Neuroscience*, 3rd ed. (Sinauer Associates, Inc., Sunderland, 2004).

[44] McDonald, J.W. *et al.*, Transplanted embryonic stem cells survive, differentiate and promote recovery in injured rat spinal cord. *Nat Med* 5 (12), 1410-1412 (1999).

[45] Ogawa, Y. *et al.*, Transplantation of in vitro-expanded fetal neural progenitor cells results in neurogenesis and functional recovery after spinal cord contusion injury in adult rats. *J Neurosci Res* 69 (6), 925-933 (2002).

[46] Karimi-Abdolrezaee, S., Eftekharpour, E., Wang, J., Morshead, C.M., & Fehlings, M.G., Delayed transplantation of adult neural precursor cells promotes remyelination and functional neurological recovery after spinal cord injury. *J Neurosci* 26 (13), 3377-3389 (2006).

[47] Andrews, M.R. & Stelzner, D.J., Evaluation of olfactory ensheathing and schwann cells after implantation into a dorsal injury of adult rat spinal cord. *J Neurotrauma* 24 (11), 1773-1792 (2007).

[48] Pearse, D.D. *et al.*, Transplantation of Schwann cells and/or olfactory ensheathing glia into the contused spinal cord: Survival, migration, axon association, and functional recovery. *Glia* 55 (9), 976-1000 (2007).

[49] Xu, X.M., Zhang, S.X., Li, H., Aebischer, P., & Bunge, M.B., Regrowth of axons into the distal spinal cord through a Schwann-cell-seeded mini-channel implanted into hemisected adult rat spinal cord. *Eur J Neurosci* 11 (5), 1723-1740 (1999).

[50] Pinzon, A., Calancie, B., Oudega, M., & Noga, B.R., Conduction of impulses by axons regenerated in a Schwann cell graft in the transected adult rat thoracic spinal cord. *J Neurosci Res* 64 (5), 533-541 (2001).

[51] Blesch, A., Yang, H., Weidner, N., Hoang, A., & Otero, D., Axonal responses to cellularly delivered NT-4/5 after spinal cord injury. *Mol Cell Neurosci* 27 (2), 190-201 (2004).

[52] Tuszynski, M.H. *et al.*, NT-3 gene delivery elicits growth of chronically injured corticospinal axons and modestly improves functional deficits after chronic scar resection. *Exp Neurol* 181 (1), 47-56 (2003).

[53] Richardson, P.M., McGuinness, U.M., & Aguayo, A.J., Axons from CNS neurons regenerate into PNS grafts. *Nature* 284 (5753), 264-265 (1980).

[54] Asada, Y., Kawaguchi, S., Hayashi, H., & Nakamura, T., Neural repair of the injured spinal cord by grafting: comparison between peripheral nerve segments and embryonic homologous structures as a conduit of CNS axons. *Neurosci Res* 31 (3), 241-249 (1998).

[55] Mori, F., Himes, B.T., Kowada, M., Murray, M., & Tessler, A., Fetal spinal cord transplants rescue some axotomized rubrospinal neurons from retrograde cell death in adult rats. *Exp Neurol* 143 (1), 45-60 (1997).

[56] Choi, B.-H. *et al.*, Nerve repair using a vein graft filled with collagen gel. *Journal of Reconstructive Microsurgery* 21 (4), 267-272 (2005).

[57] Foidart-Dessalle, M. *et al.*, Sciatic nerve regeneration through venous or nervous grafts in the rat. *Exp Neurol* 148 (1), 236-246 (1997).

[58] Miyoshi, Y., Date, I., Ohmoto, T., & Iwata, H., Histological analysis of microencapsulated dopamine-secreting cells in agarose/poly(styrene sulfonic acid) mixed gel xenotransplanted into the brain. *Exp Neurol* 138 (1), 169-175 (1996).

[59] Batorsky, A., Liao, J., Lund, A.W., Plopper, G.E., & Stegemann, J.P., Encapsulation of adult human mesenchymal stem cells within collagen-agarose microenvironments. *Biotechnol Bioeng* 92 (4), 492-500 (2005).

[60] Stokols, S. & Tuszynski, M.H., Freeze-dried agarose scaffolds with uniaxial channels stimulate and guide linear axonal growth following spinal cord injury. *Biomaterials* 27 (3), 443-451 (2006).

[61] Paino, C.L. & Bunge, M.B., Induction of axon growth into Schwann cell implants grafted into lesioned adult rat spinal cord. *Exp Neurol* 114 (2), 254-257 (1991).

[62] Zhang, X. *et al.*, Co-transplantation of neural stem cells and NT-3-overexpressing Schwann cells in transected spinal cord. *J Neurotrauma* 24 (12), 1863-1877 (2007).

[63] Evans, G.R. *et al.*, Bioactive poly(L-lactic acid) conduits seeded with Schwann cells for peripheral nerve regeneration. *Biomaterials* 23 (3), 841-848 (2002).

[64] Teng, Y.D. *et al.*, Functional recovery following traumatic spinal cord injury mediated by a unique polymer scaffold seeded with neural stem cells. *Proc Natl Acad Sci U S A* 99 (5), 3024-3029 (2002).

[65] Novikov, L.N. *et al.*, A novel biodegradable implant for neuronal rescue and regeneration after spinal cord injury. *Biomaterials* 23 (16), 3369-3376 (2002).

[66] Kalbermatten, D.F. *et al.*, Fibrin matrix for suspension of regenerative cells in an artificial nerve conduit. *J Plast Reconstr Aesthet Surg* (2008).

[67] Mosahebi, A., Wiberg, M., & Terenghi, G., Addition of fibronectin to alginate matrix improves peripheral nerve regeneration in tissue-engineered conduits. *Tissue Eng* 9 (2), 209-218 (2003).

[68] Xu, X.M., Chen, A., Guenard, V., Kleitman, N., & Bunge, M.B., Bridging Schwann cell transplants promote axonal regeneration from both the rostral and caudal stumps of transected adult rat spinal cord. *J Neurocytol* 26 (1), 1-16 (1997).

[69] Guest, J.D., Rao, A., Olson, L., Bunge, M.B., & Bunge, R.P., The ability of human Schwann cell grafts to promote regeneration in the transected nude rat spinal cord. *Exp Neurol* 148 (2), 502-522 (1997).

[70] Bamber, N.I. *et al.*, Neurotrophins BDNF and NT-3 promote axonal re-entry into the distal host spinal cord through Schwann cell-seeded mini-channels. *Eur J Neurosci* 13 (2), 257-268 (2001).

[71] Iannotti, C. *et al.*, Glial cell line-derived neurotrophic factor-enriched bridging transplants promote propriospinal axonal regeneration and enhance myelination after spinal cord injury. *Exp Neurol* 183 (2), 379-393 (2003).

[72] Kwon, B.K. *et al.*, Brain-derived neurotrophic factor gene transfer with adeno-associated viral and lentiviral vectors prevents rubrospinal neuronal atrophy and stimulates regeneration-associated gene expression after acute cervical spinal cord injury. *Spine* 32 (11), 1164-1173 (2007).

[73] Taylor, L., Jones, L., Tuszynski, M.H., & Blesch, A., Neurotrophin-3 gradients established by lentiviral gene delivery promote short-distance axonal bridging

beyond cellular grafts in the injured spinal cord. *J Neurosci* 26 (38), 9713-9721 (2006).

[74] Thuret, S., Moon, L.D., & Gage, F.H., Therapeutic interventions after spinal cord injury. *Nat Rev Neurosci* 7 (8), 628-643 (2006).

[75] Tsai, E.C. & Tator, C.H., Neuroprotection and regeneration strategies for spinal cord repair. *Curr Pharm Des* 11 (10), 1211-1222 (2005).

[76] Willerth, S.M. & Sakiyama-Elbert, S.E., Approaches to neural tissue engineering using scaffolds for drug delivery. *Advanced Drug Delivery Reviews* 59 (4-5), 325-338 (2007).

[77] Zhang, N., Yan, H., & Wen, X., Tissue-engineering approaches for axonal guidance. *Brain Res Brain Res Rev* 49 (1), 48-64 (2005).

[78] Putney, S.D. & Burke, P.A., Improving protein therapeutics with sustained-release formulations. *Nat Biotechnol* 16 (2), 153-157 (1998).

[79] Krewson, C.E., Dause, R., Mak, M., & Saltzman, W.M., Stabilization of nerve growth factor in controlled release polymers and in tissue. *J Biomater Sci Polym Ed* 8 (2), 103-117 (1996).

[80] Vogelin, E. *et al.*, Effects of local continuous release of brain derived neurotrophic factor (BDNF) on peripheral nerve regeneration in a rat model. *Exp Neurol* 199 (2), 348-353 (2006).

[81] Jain, A., Kim, Y.T., McKeon, R.J., & Bellamkonda, R.V., In situ gelling hydrogels for conformal repair of spinal cord defects, and local delivery of BDNF after spinal cord injury. *Biomaterials* 27 (3), 497-504 (2006).

[82] Cao, X. & Shoichet, M.S., Defining the concentration gradient of nerve growth factor for guided neurite outgrowth. *Neuroscience* 103 (3), 831-840 (2001).

[83] Dodla, M.C. & Bellamkonda, R.V., Differences between the effect of anisotropic and isotropic laminin and nerve growth factor presenting scaffolds on nerve regeneration across long peripheral nerve gaps. *Biomaterials* 29 (1), 33-46 (2008).

[84] Chen, M.H., Chen, P.R., Chen, M.H., Hsieh, S.T., & Lin, F.H., Gelatin-tricalcium phosphate membranes immobilized with NGF, BDNF, or IGF-1 for peripheral nerve repair: an in vitro and in vivo study. *J Biomed Mater Res A* 79 (4), 846-857 (2006).

[85] Deister, C. & Schmidt, C.E., Optimizing neurotrophic factor combinations for neurite outgrowth. *J Neural Eng* 3 (2), 172-179 (2006).

[86] Uebersax, L. *et al.*, Silk fibroin matrices for the controlled release of nerve growth factor (NGF). *Biomaterials* 28 (30), 4449-4460 (2007).

[87] Sterne, G.D., Brown, R.A., Green, C.J., & Terenghi, G., Neurotrophin-3 delivered locally via fibronectin mats enhances peripheral nerve regeneration. *Eur J Neurosci* 9 (7), 1388-1396 (1997).

[88] Sun, W. *et al.*, Promotion of peripheral nerve growth by collagen scaffolds loaded with collagen-targeting human nerve growth factor-beta. *J Biomed Mater Res A* 83 (4), 1054-1061 (2007).

[89] Sakiyama-Elbert, S.E. & Hubbell, J.A., Controlled release of nerve growth factor from a heparin-containing fibrin-based cell ingrowth matrix. *J Control Release* 69 (1), 149-158 (2000).

[90] Sakiyama-Elbert, S.E. & Hubbell, J.A., Development of fibrin derivatives for controlled release of heparin-binding growth factors. *J Control Release* 65 (3), 389-402 (2000).

[91] Taylor, S.J., McDonald, J.W., 3rd, & Sakiyama-Elbert, S.E., Controlled release of neurotrophin-3 from fibrin gels for spinal cord injury. *J Control Release* 98 (2), 281-294 (2004).

[92] Taylor, S.J., Rosenzweig, E.S., McDonald, J.W., 3rd, & Sakiyama-Elbert, S.E., Delivery of neurotrophin-3 from fibrin enhances neuronal fiber sprouting after spinal cord injury. *J Control Release* 113 (3), 226-235 (2006).

[93] Willerth, S.M. *et al.*, Rationally designed peptides for controlled release of nerve growth factor from fibrin matrices. *Journal of Biomedical Materials Research Part A* 80A (1), 13-23 (2007).

[94] Piotrowicz, A. & Shoichet, M.S., Nerve guidance channels as drug delivery vehicles. *Biomaterials* 27 (9), 2018-2027 (2006).

[95] Kim, D.H., Richardson-Burns, S.M., Hendricks, J.L., Sequera, C., & Martin, D.C., Effect of immobilized nerve growth factor on conductive polymers: Electrical properties and cellular response. *Advanced Functional Materials* 17 (1), 79-86 (2007).

[96] Thompson, B.C. *et al.*, Optimising the incorporation and release of a neurotrophic factor using conducting polypyrrole. *Journal of Controlled Release* 116 (3), 285-294 (2006).

[97] Richardson, R.T. *et al.*, The effect of polypyrrole with incorporated neurotrophin-3 on the promotion of neurite outgrowth from auditory neurons. *Biomaterials* 28 (3), 513-523 (2007).

[98] Gomez, N., Lu, Y., Chen, S.C., & Schmidt, C.E., Immobilized nerve growth factor and microtopography have distinct effects on polarization versus axon elongation in hippocampal cells in culture. *Biomaterials* 28 (2), 271-284 (2007).

[99] Kapur, T.A. & Shoichet, M.S., Immobilized concentration gradients of nerve growth factor guide neurite outgrowth. *J Biomed Mater Res A* 68 (2), 235-243 (2004).

[100] Moore, K., Macsween, M., & Shoichet, M., Immobilized concentration gradients of neurotrophic factors guide neurite outgrowth of primary neurons in macroporous scaffolds. *Tissue Engineering* 12 (2), 267-278 (2006).

[101] Gomez, N. & Schmidt, C.E., Nerve growth factor-immobilized polypyrrole: Bioactive electrically conducting polymer for enhanced neurite extension. *Journal of Biomedical Materials Research Part A* 81A (1), 135-149 (2007).

[102] Whittlesey, K.J. & Shea, L.D., Nerve growth factor expression by PLG-mediated lipofection. *Biomaterials* 27 (11), 2477-2486 (2006).

[103] Houchin-Ray, T., Swift, L.A., Jang, J.H., & Shea, L.D., Patterned PLG substrates for localized DNA delivery and directed neurite extension. *Biomaterials* 28 (16), 2603-2611 (2007).

[104] Hubbell, J.A., Materials as morphogenetic guides in tissue engineering. *Curr Opin Biotechnol* 14 (5), 551-558 (2003).

[105] Armstrong, S.J., Wiberg, M., Terenghi, G., & Kingham, P.J., ECM molecules mediate both Schwann cell proliferation and activation to enhance neurite outgrowth. *Tissue Engineering* 13 (12), 2863-2870 (2007).

[106] Sierpinski, P. *et al.*, The use of keratin biomaterials derived from human hair for the promotion of rapid regeneration of peripheral nerves. *Biomaterials* 29 (1), 118-128 (2008).

[107] Bourguignon, L.Y.W., Gilad, E., Peyrollier, K., Brightman, A., & Swanson, R.A., Hyaluronan-CD44 interaction stimulates Rac1 signaling and PKN gamma kinase activation leading to cytoskeleton function and cell migration in astrocytes. *Journal of Neurochemistry* 101 (4), 1002-1017 (2007).

[108] Borkenhagen, M., Clemence, J.F., Sigrist, H., & Aebischer, P., Three-dimensional extracellular matrix engineering in the nervous system. *Journal of Biomedical Materials Research* 40 (3), 392-400 (1998).

[109] Sanes, J.R., Extracellular matrix molecules that influence neural development. *Annu Rev Neurosci* 12, 491-516 (1989).

[110] Reichardt, L.F. & Tomaselli, K.J., Extracellular matrix molecules and their receptors: functions in neural development. *Annu Rev Neurosci* 14, 531-570 (1991).

[111] Gundersen, R.W., Response of sensory neurites and growth cones to patterned substrata of laminin and fibronectin in vitro. *Dev Biol* 121 (2), 423-431 (1987).

[112] Powell, S.K. & Kleinman, H.K., Neuronal laminins and their cellular receptors. *Int J Biochem Cell Biol* 29 (3), 401-414 (1997).

[113] Ichikawa, N. *et al.*, Identification of neurite outgrowth active sites on the laminin alpha4 chain G domain. *Biochemistry* 44 (15), 5755-5762 (2005).

[114] Edgar, D., Timpl, R., & Thoenen, H., The heparin-binding domain of laminin is responsible for its effects on neurite outgrowth and neuronal survival. *EMBO J* 3 (7), 1463-1468 (1984).

[115] Kuhn, T.B., Schmidt, M.F., & Kater, S.B., Laminin and fibronectin guideposts signal sustained but opposite effects to passing growth cones. *Neuron* 14 (2), 275-285 (1995).

[116] Kuhn, T.B., Williams, C.V., Dou, P., & Kater, S.B., Laminin directs growth cone navigation via two temporally and functionally distinct calcium signals. *J Neurosci* 18 (1), 184-194 (1998).

[117] Bonner, J. & O'Connor, T.P., The permissive cue laminin is essential for growth cone turning in vivo. *J Neurosci* 21 (24), 9782-9791 (2001).

[118] Tashiro, K. *et al.*, A synthetic peptide containing the IKVAV sequence from the A chain of laminin mediates cell attachment, migration, and neurite outgrowth. *J Biol Chem* 264 (27), 16174-16182 (1989).

[119] Jucker, M., Kleinman, H.K., & Ingram, D.K., Fetal rat septal cells adhere to and extend processes on basement membrane, laminin, and a synthetic peptide from the laminin A chain sequence. *J Neurosci Res* 28 (4), 507-517 (1991).

[120] Liesi, P., Narvanen, A., Soos, J., Sariola, H., & Snounou, G., Identification of a neurite outgrowth-promoting domain of laminin using synthetic peptides. *FEBS Lett* 244 (1), 141-148 (1989).

[121] Luckenbill-Edds, L., Laminin and the mechanism of neuronal outgrowth. *Brain Res Brain Res Rev* 23 (1-2), 1-27 (1997).

[122] Graf, J. *et al.*, A pentapeptide from the laminin B1 chain mediates cell adhesion and binds the 67,000 laminin receptor. *Biochemistry* 26 (22), 6896-6900 (1987).

[123] Bellamkonda, R., Ranieri, J.P., & Aebischer, P., Laminin oligopeptide derivatized agarose gels allow three-dimensional neurite extension in vitro. *J Neurosci Res* 41 (4), 501-509 (1995).

[124] Borkenhagen, M., Clemence, J.F., Sigrist, H., & Aebischer, P., Three-dimensional extracellular matrix engineering in the nervous system. *J Biomed Mater Res* 40 (3), 392-400 (1998).

[125] Dhoot, N.O., Tobias, C.A., Fischer, I., & Wheatley, M.A., Peptide-modified alginate surfaces as a growth permissive substrate for neurite outgrowth. *J Biomed Mater Res A* 71 (2), 191-200 (2004).

[126] Schense, J.C., Bloch, J., Aebischer, P., & Hubbell, J.A., Enzymatic incorporation of bioactive peptides into fibrin matrices enhances neurite extension. *Nat Biotechnol* 18 (4), 415-419 (2000).

[127] Dodla, M.C. & Bellamkonda, R.V., Anisotropic scaffolds facilitate enhanced neurite extension in vitro. *J Biomed Mater Res A* 78 (2), 213-221 (2006).

[128] Luo, Y. & Shoichet, M.S., A photolabile hydrogel for guided three-dimensional cell growth and migration. *Nat Mater* 3 (4), 249-253 (2004).

[129] Liu, H. *et al.*, Porous poly (DL-lactic acid) modified chitosan-gelatin scaffolds for tissue engineering. *J Biomater Appl* 19 (4), 303-322 (2005).

[130] Madihally, S.V. & Matthew, H.W., Porous chitosan scaffolds for tissue engineering. *Biomaterials* 20 (12), 1133-1142 (1999).

[131] Yu, L.M., Kazazian, K., & Shoichet, M.S., Peptide surface modification of methacrylamide chitosan for neural tissue engineering applications. *J Biomed Mater Res A* 82 (1), 243-255 (2007).

[132] Itoh, S. *et al.*, Effects of a laminin peptide (YIGSR) immobilized on crab-tendon chitosan tubes on nerve regeneration. *Journal of Biomedical Materials Research Part B-Applied Biomaterials* 73B (2), 375-382 (2005).

[133] Suzuki, M. *et al.*, Tendon chitosan tubes covalently coupled with synthesized laminin peptides facilitate nerve regeneration in vivo. *J Neurosci Res* 72 (5), 646-659 (2003).

[134] Levesque, S.G. & Shoichet, M.S., Synthesis of cell-adhesive dextran hydrogels and macroporous scaffolds. *Biomaterials* 27 (30), 5277-5285 (2006).

[135] Musoke-Zawedde, P. & Shoichet, M.S., Anisotropic three-dimensional peptide channels guide neurite outgrowth within a biodegradable hydrogel matrix. *Biomedical Materials* 1 (3), 162-169 (2006).

[136] Stabenfeldt, S.E., Garcia, A.J., & LaPlaca, M.C., Thermoreversible laminin-functionalized hydrogel for neural tissue engineering. *J Biomed Mater Res A* 77 (4), 718-725 (2006).

[137] Ahmed, M.R., Venkateshwarlu, U., & Jayakumar, R., Multilayered peptide incorporated collagen tubules for peripheral nerve repair. *Biomaterials* 25 (13), 2585-2594 (2004).

[138] Itoh, S. *et al.*, Evaluation of cross-linking procedures of collagen tubes used in peripheral nerve repair. *Biomaterials* 23, 4475-4481 (2002).

[139] Ahmed, M.R., Basha, S.H., Gopinath, D., Muthusamy, R., & Jayakumar, R., Initial upregulation of growth factors and inflammatory mediators during nerve regeneration in the presence of cell adhesive peptide-incorporated collagen tubes. *Journal of the Peripheral Nervous System* 10 (1), 17-30 (2005).

[140] Akassoglou, K., Akpinar, P., Murray, S., & Strickland, S., Fibrin is a regulator of Schwann cell migration after sciatic nerve injury in mice. *Neurosci Lett* 338 (3), 185-188 (2003).

[141] Akassoglou, K., Yu, W.M., Akpinar, P., & Strickland, S., Fibrin inhibits peripheral nerve remyelination by regulating Schwann cell differentiation. *Neuron* 33 (6), 861-875 (2002).

[142] Duan, X.D., McLaughlin, C., Griffith, M., & Sheardown, H., Biofunctionalization of collagen for improved biological response: Scaffolds for corneal tissue engineering. *Biomaterials* 28 (1), 78-88 (2007).

[143] Rafiuddin Ahmed, M. & Jayakumar, R., Peripheral nerve regeneration in RGD peptide incorporated collagen tubes. *Brain Res* 993 (1-2), 208-216 (2003).

[144] Shaw, D. & Shoichet, M.S., Toward spinal cord injury repair strategies: peptide surface modification of expanded poly(tetrafluoroethylene) fibers for guided neurite outgrowth in vitro. *J Craniofac Surg* 14 (3), 308-316 (2003).

[145] Tong, Y.W. & Shoichet, M.S., Enhancing the neuronal interaction on fluoropolymer surfaces with mixed peptides or spacer group linkers. *Biomaterials* 22 (10), 1029-1034 (2001).

[146] Clemence, J.F., Ranieri, J.P., Aebischer, P., & Sigrist, H., Photoimmobilization of a bioactive laminin fragment and pattern-guided selective neuronal cell attachment. *Bioconjug Chem* 6 (4), 411-417 (1995).

[147] Lee, J.W., Serna, F., & Schmidt, C.E., Carboxy-endcapped conductive polypyrrole: Biomimetic conducting polymer for cell scaffolds and electrodes. *Langmuir* 22 (24), 9816-9819 (2006).

[148] Guimard, N.K., Gomez, N., & Schmidt, C.E., Conducting polymers in biomedical engineering. *Progress in Polymer Science* 32 (8-9), 876-921 (2007).

[149] Sanghvi, A.B., Miller, K.P., Belcher, A.M., & Schmidt, C.E., Biomaterials functionalization using a novel peptide that selectively binds to a conducting polymer. *Nat Mater* 4 (6), 496-502 (2005).

[150] Plant, G.W., Woerly, S., & Harvey, A.R., Hydrogels containing peptide or aminosugar sequences implanted into the rat brain: influence on cellular migration and axonal growth. *Exp Neurol* 143 (2), 287-299 (1997).

[151] Woerly, S., Pinet, E., de Robertis, L., Van Diep, D., & Bousmina, M., Spinal cord repair with PHPMA hydrogel containing RGD peptides (NeuroGel). *Biomaterials* 22 (10), 1095-1111 (2001).

[152] Biran, R., Webb, K., Noble, M.D., & Tresco, P.A., Surfactant-immobilized fibronectin enhances bioactivity and regulates sensory neurite outgrowth. *J Biomed Mater Res* 55 (1), 1-12 (2001).

[153] Ahmed, I. *et al.*, Three-dimensional nanofibrillar surfaces covalently modified with tenascin-C-derived peptides enhance neuronal growth in vitro. *Journal of Biomedical Materials Research Part A* 76A (4), 851-860 (2006).

[154] Meiners, S., Nur-e-Kamal, M.S., & Mercado, M.L., Identification of a neurite outgrowth-promoting motif within the alternatively spliced region of human tenascin-C. *J Neurosci* 21 (18), 7215-7225 (2001).

[155] Silva, G.A. *et al.*, Selective differentiation of neural progenitor cells by high-epitope density nanofibers. *Science* 303 (5662), 1352-1355 (2004).

[156] Thid, D. *et al.*, Supported phospholipid bilayers as a platform for neural progenitor cell culture. *J Biomed Mater Res A* 84 (4), 940-953 (2008).

[157] Saha, K., Irwin, E.F., Kozhukh, J., Schaffer, D.V., & Healy, K.E., Biomimetic interfacial interpenetrating polymer networks control neural stem cell behavior. *J Biomed Mater Res A* 81 (1), 240-249 (2007).

[158] Kenwrick, S. & Doherty, P., Neural cell adhesion molecule L1: relating disease to function. *Bioessays* 20 (8), 668-675 (1998).

[159] Chaudhry, N., de Silva, U., & Smith, G.M., Cell adhesion molecule L1 modulates nerve-growth-factor-induced CGRP-IR fiber sprouting. *Exp Neurol* 202 (1), 238-249 (2006).

[160] Honig, M.G., Camilli, S.J., & Xue, Q.S., Effects of L1 blockade on sensory axon outgrowth and pathfinding in the chick hindlimb. *Dev Biol* 243 (1), 137-154 (2002).

[161] Webb, K. *et al.*, Substrate-bound human recombinant L1 selectively promotes neuronal attachment and outgrowth in the presence of astrocytes and fibroblasts. *Biomaterials* 22 (10), 1017-1028 (2001).

[162] Fiszman, M.L., Borodinsky, L.N., & Neale, J.H., GABA induces proliferation of immature cerebellar granule cells grown in vitro. *Brain Res Dev Brain Res* 115 (1), 1-8 (1999).

[163] Nishiyama, M. *et al.*, Cyclic AMP/GMP-dependent modulation of Ca2+ channels sets the polarity of nerve growth-cone turning. *Nature* 423 (6943), 990-995 (2003).

[164] Tang, F. & Kalil, K., Netrin-1 induces axon branching in developing cortical neurons by frequency-dependent calcium signaling pathways. *J Neurosci* 25 (28), 6702-6715 (2005).

[165] Lohmann, C., Myhr, K.L., & Wong, R.O., Transmitter-evoked local calcium release stabilizes developing dendrites. *Nature* 418 (6894), 177-181 (2002).

[166] Palmer, A.M., Messerli, M.A., & Robinson, K.R., Neuronal galvanotropism is independent of external Ca(2+) entry or internal Ca(2+) gradients. *J Neurobiol* 45 (1), 30-38 (2000).

[167] Ramakers, G.J. *et al.*, Depolarization stimulates lamellipodia formation and axonal but not dendritic branching in cultured rat cerebral cortex neurons. *Brain Res Dev Brain Res* 108 (1-2), 205-216 (1998).

[168] Ming, G., Henley, J., Tessier-Lavigne, M., Song, H., & Poo, M., Electrical activity modulates growth cone guidance by diffusible factors. *Neuron* 29 (2), 441-452 (2001).

[169] Kerns, J.M., Fakhouri, A.J., Weinrib, H.P., & Freeman, J.A., Electrical stimulation of nerve regeneration in the rat: the early effects evaluated by a vibrating probe and electron microscopy. *Neuroscience* 40 (1), 93-107 (1991).

[170] Al-Majed, A.A., Neumann, C.M., Brushart, T.M., & Gordon, T., Brief electrical stimulation promotes the speed and accuracy of motor axonal regeneration. *J Neurosci* 20 (7), 2602-2608 (2000).

[171] Geremia, N.M., Gordon, T., Brushart, T.M., Al-Majed, A.A., & Verge, V.M., Electrical stimulation promotes sensory neuron regeneration and growth-associated gene expression. *Exp Neurol* 205 (2), 347-359 (2007).

[172] Borgens, R.B., Electrically mediated regeneration and guidance of adult mammalian spinal axons into polymeric channels. *Neuroscience* 91 (1), 251-264 (1999).

[173] Borgens, R.B. & Bohnert, D.M., The responses of mammalian spinal axons to an applied DC voltage gradient. *Exp Neurol* 145 (2 Pt 1), 376-389 (1997).

[174] Borgens, R.B., Blight, A.R., & McGinnis, M.E., Behavioral recovery induced by applied electric fields after spinal cord hemisection in guinea pig. *Science* 238 (4825), 366-369 (1987).

[175] Shapiro, S. *et al.*, Oscillating field stimulation for complete spinal cord injury in humans: a phase 1 trial. *J Neurosurg Spine* 2 (1), 3-10 (2005).

[176] Valentini, R.F., Vargo, T.G., Gardella, J.A., Jr., & Aebischer, P., Electrically charged polymeric substrates enhance nerve fibre outgrowth in vitro. *Biomaterials* 13 (3), 183-190 (1992).

[177] Aebischer, P., Valentini, R.F., Dario, P., Domenici, C., & Galletti, P.M., Piezoelectric guidance channels enhance regeneration in the mouse sciatic nerve after axotomy. *Brain Res* 436 (1), 165-168 (1987).

[178] Fine, E.G., Valentini, R.F., Bellamkonda, R., & Aebischer, P., Improved nerve regeneration through piezoelectric vinylidenefluoride-trifluoroethylene copolymer guidance channels. *Biomaterials* 12 (8), 775-780 (1991).

[179] Bryan, D.J. *et al.*, Enhanced peripheral nerve regeneration through a poled bioresorbable poly(lactic-co-glycolic acid) guidance channel. *J Neural Eng* 1 (2), 91-98 (2004).

[180] Schmidt, C.E., Shastri, V.R., Vacanti, J.P., & Langer, R., Stimulation of neurite outgrowth using an electrically conducting polymer. *Proc Natl Acad Sci U S A* 94 (17), 8948-8953 (1997).

[181] Zhang, Z. *et al.*, Electrically conductive biodegradable polymer composite for nerve regeneration: electricity-stimulated neurite outgrowth and axon regeneration. *Artif Organs* 31 (1), 13-22 (2007).

[182] Ateh, D.D., Navsaria, H.A., & Vadgama, P., Polypyrrole-based conducting polymers and interactions with biological tissues. *Journal of the Royal Society Interface* 3 (11), 741-752 (2006).

[183] Song, H.K., Toste, B., Ahmann, K., Hoffman-Kim, D., & Palmore, G.T., Micropatterns of positive guidance cues anchored to polypyrrole doped with polyglutamic acid: a new platform for characterizing neurite extension in complex environments. *Biomaterials* 27 (3), 473-484 (2006).

[184] Stauffer, W.R. & Cui, X.T., Polypyrrole doped with 2 peptide sequences from laminin. *Biomaterials* 27 (11), 2405-2413 (2006).

[185] Collier, J.H., Camp, J.P., Hudson, T.W., & Schmidt, C.E., Synthesis and characterization of polypyrrole-hyaluronic acid composite biomaterials for tissue engineering applications. *J Biomed Mater Res* 50 (4), 574-584 (2000).

[186] Wan, Y., Wu, H., & Wen, D., Porous-conductive chitosan scaffolds for tissue engineering, 1. Preparation and characterization. *Macromol Biosci* 4 (9), 882-890 (2004).

[187] Wadhwa, R., Lagenaur, C.F., & Cui, X.T., Electrochemically controlled release of dexamethasone from conducting polymer polypyrrole coated electrode. *J Control Release* 110 (3), 531-541 (2006).

[188] Kiefer, R. & Kreutzberg, G.W., Effects of dexamethasone on microglial activation in vivo: selective downregulation of major histocompatibility complex class II expression in regenerating facial nucleus. *J Neuroimmunol* 34 (2-3), 99-108 (1991).

[189] Crossin, K.L., Tai, M.H., Krushel, L.A., Mauro, V.P., & Edelman, G.M., Glucocorticoid receptor pathways are involved in the inhibition of astrocyte proliferation. *Proc Natl Acad Sci U S A* 94 (6), 2687-2692 (1997).

[190] Zelikin, A.N. *et al.*, Erodible conducting polymers for potential biomedical applications. *Angew Chem Int Ed Engl* 41 (1), 141-144 (2002).

[191] Rivers, T.J., Hudson, T.W., & Schmidt, C.E., Synthesis of a novel, biodegradable electrically conducting polymer for biomedical applications. *Advanced Functional Materials* 12 (1), 33-37 (2002).

[192] Lofberg, J., Ahlfors, K., & Fallstrom, C., Neural crest cell migration in relation to extracellular matrix organization in the embryonic axolotl trunk. *Dev Biol* 75 (1), 148-167 (1980).

[193] Nagata, I. & Nakatsuji, N., Rodent CNS neuroblasts exhibit both perpendicular and parallel contact guidance on the aligned parallel neurite bundle. *Development* 112 (2), 581-590 (1991).

[194] Hatten, M.E., Riding the glial monorail: a common mechanism for glial-guided neuronal migration in different regions of the developing mammalian brain. *Trends Neurosci* 13 (5), 179-184 (1990).

[195] Hynes, R.O., Patel, R., & Miller, R.H., Migration of neuroblasts along preexisting axonal tracts during prenatal cerebellar development. *J Neurosci* 6 (3), 867-876 (1986).

[196] Deumens, R. *et al.*, Alignment of glial cells stimulates directional neurite growth of CNS neurons in vitro. *Neuroscience* 125 (3), 591-604 (2004).

[197] Webb, A., Clark, P., Skepper, J., Compston, A., & Wood, A., Guidance of oligodendrocytes and their progenitors by substratum topography. *J Cell Sci* 108 (Pt 8), 2747-2760 (1995).

[198] Norris, C.R. & Kalil, K., Guidance of callosal axons by radial glia in the developing cerebral cortex. *J Neurosci* 11 (11), 3481-3492 (1991).

[199] Bozkurt, A. *et al.*, In vitro assessment of axonal growth using dorsal root ganglia explants in a novel three-dimensional collagen matrix. *Tissue Eng* 13 (12), 2971-2979 (2007).

[200] Madaghiele, M., Sannino, A., Yannas, I.V., & Spector, M., Collagen-based matrices with axially oriented pores. *J Biomed Mater Res A* 85 (3), 757-767 (2008).

[201] Moore, M.J. *et al.*, Multiple-channel scaffolds to promote spinal cord axon regeneration. *Biomaterials* 27 (3), 419-429 (2006).

[202] Hsu, S.H., Lu, P.S., Ni, H.C., & Su, C.H., Fabrication and evaluation of microgrooved polymers as peripheral nerve conduits. *Biomedical Microdevices* 9 (5), 665-674 (2007).

[203] Recknor, J.B., Sakaguchi, D.S., & Mallapragada, S.K., Directed growth and selective differentiation of neural progenitor cells on micropatterned polymer substrates. *Biomaterials* 27 (22), 4098-4108 (2006).

[204] Lietz, M., Dreesmann, L., Hoss, M., Oberhoffner, S., & Schlosshauer, B., Neuro tissue engineering of glial nerve guides and the impact of different cell types. *Biomaterials* 27 (8), 1425-1436 (2006).

[205] Bruder, J.M., Lee, A.P., & Hoffman-Kim, D., Biomimetic materials replicating Schwann cell topography enhance neuronal adhesion and neurite alignment in vitro. *Journal of Biomaterials Science-Polymer Edition* 18 (8), 967-982 (2007).

[206] Miller, C., Shanks, H., Witt, A., Rutkowski, G., & Mallapragada, S., Oriented Schwann cell growth on micropatterned biodegradable polymer substrates. *Biomaterials* 22 (11), 1263-1269 (2001).

[207] Schmalenberg, K.E. & Uhrich, K.E., Micropatterned polymer substrates control alignment of proliferating Schwann cells to direct neuronal regeneration. *Biomaterials* 26 (12), 1423-1430 (2005).

[208] Sorensen, A. *et al.*, Long-term neurite orientation on astrocyte monolayers. aligned by microtopography. *Biomaterials* 28 (36), 5498-5508 (2007).

[209] Hsu, S.H., Chen, C.Y., Lu, P.S., Lai, C.S., & Chen, C.J., Oriented Schwann cell growth on microgrooved surfaces. *Biotechnol Bioeng* 92 (5), 579-588 (2005).

[210] Heng, J.I., Moonen, G., & Nguyen, L., Neurotransmitters regulate cell migration in the telencephalon. *Eur J Neurosci* 26 (3), 537-546 (2007).

[211] Borta, A. & Hoglinger, G.U., Dopamine and adult neurogenesis. *J Neurochem* 100 (3), 587-595 (2007).

[212] Popolo, M., McCarthy, D.M., & Bhide, P.G., Influence of dopamine on precursor cell proliferation and differentiation in the embryonic mouse telencephalon. *Dev Neurosci* 26 (2-4), 229-244 (2004).

[213] Hiramoto, T., Kanda, Y., Satoh, Y., Takishima, K., & Watanabe, Y., Dopamine D2 receptor stimulation promotes the proliferation of neural progenitor cells in adult mouse hippocampus. *Neuroreport* 18 (7), 659-664 (2007).

[214] Belluardo, N., Mudo, G., Blum, M., & Fuxe, K., Central nicotinic receptors, neurotrophic factors and neuroprotection. *Behav Brain Res* 113 (1-2), 21-34 (2000).

[215] Berger, F., Gage, F.H., & Vijayaraghavan, S., Nicotinic receptor-induced apoptotic cell death of hippocampal progenitor cells. *J Neurosci* 18 (17), 6871-6881 (1998).

[216] Bernardini, N., Tomassy, G.S., Tata, A.M., Augusti-Tocco, G., & Biagioni, S., Detection of basal and potassium-evoked acetylcholine release from embryonic DRG explants. *J Neurochem* 88 (6), 1533-1539 (2004).

[217] Tata, A.M., Cursi, S., Biagioni, S., & Augusti-Tocco, G., Cholinergic modulation of neurofilament expression and neurite outgrowth in chick sensory neurons. *J Neurosci Res* 73 (2), 227-234 (2003).

[218] McCobb, D.P., Cohan, C.S., Connor, J.A., & Kater, S.B., Interactive effects of serotonin and acetylcholine on neurite elongation. *Neuron* 1 (5), 377-385 (1988).

[219] Bixby, J.L. & Harris, W.A., Molecular mechanisms of axon growth and guidance. *Annu Rev Cell Biol* 7, 117-159 (1991).

[220] Greenberg, M.E., Ziff, E.B., & Greene, L.A., Stimulation of neuronal acetylcholine receptors induces rapid gene transcription. *Science* 234 (4772), 80-83 (1986).

[221] Young, S.H. & Poo, M.M., Spontaneous release of transmitter from growth cones of embryonic neurones. *Nature* 305 (5935), 634-637 (1983).

[222] Toborek, M. *et al.*, ERK 1/2 signaling pathway is involved in nicotine-mediated neuroprotection in spinal cord neurons. *J Cell Biochem* 100 (2), 279-292 (2007).

[223] De Sarno, P. *et al.*, Muscarinic receptor activation protects cells from apoptotic effects of DNA damage, oxidative stress, and mitochondrial inhibition. *J Biol Chem* 278 (13), 11086-11093 (2003).

[224] Belachew, S. *et al.*, Glycine triggers an intracellular calcium influx in oligodendrocyte progenitor cells which is mediated by the activation of both the ionotropic glycine receptor and Na+-dependent transporters. *Eur J Neurosci* 12 (6), 1924-1930 (2000).

[225] Gudz, T.I., Komuro, H., & Macklin, W.B., Glutamate stimulates oligodendrocyte progenitor migration mediated via an alphav integrin/myelin proteolipid protein complex. *J Neurosci* 26 (9), 2458-2466 (2006).

[226] Kirchhoff, F., Mulhardt, C., Pastor, A., Becker, C.M., & Kettenmann, H., Expression of glycine receptor subunits in glial cells of the rat spinal cord. *J Neurochem* 66 (4), 1383-1390 (1996).

[227] Whitaker-Azmitia, P.M., Shemer, A.V., Caruso, J., Molino, L., & Azmitia, E.C., Role of high affinity serotonin receptors in neuronal growth. *Ann N Y Acad Sci* 600, 315-330 (1990).

[228] Saifuddin, U. *et al.*, Assembly and characterization of biofunctional neurotransmitter-immobilized surfaces for interaction with postsynaptic membrane receptors. *J Biomed Mater Res A* 66 (1), 184-191 (2003).

[229] Vu, T.Q. *et al.*, Activation of membrane receptors by a neurotransmitter conjugate designed for surface attachment. *Biomaterials* 26 (14), 1895-1903 (2005).

[230] Liu, J., Kolar, C., Lawson, T.A., & Gmeiner, W.H., Targeted drug delivery to chemoresistant cells: folic acid derivatization of FdUMP[10] enhances cytotoxicity toward 5-FU-resistant human colorectal tumor cells. *J Org Chem* 66 (17), 5655-5663 (2001).

[231] Zheng, J.Q., Wan, J.J., & Poo, M.M., Essential role of filopodia in chemotropic turning of nerve growth cone induced by a glutamate gradient. *J Neurosci* 16 (3), 1140-1149 (1996).

[232] Tata, A.M. *et al.*, Subpopulations of rat dorsal root ganglion neurons express active vesicular acetylcholine transporter. *J Neurosci Res* 75 (2), 194-202 (2004).

[233] Genzen, J.R., Van Cleve, W., & McGehee, D.S., Dorsal root ganglion neurons express multiple nicotinic acetylcholine receptor subtypes. *J Neurophysiol* 86 (4), 1773-1782 (2001).

[234] Tata, A.M., Vilaro, M.T., & Mengod, G., Muscarinic receptor subtypes expression in rat and chick dorsal root ganglia. *Brain Res Mol Brain Res* 82 (1-2), 1-10 (2000).

[235] Dillon, G.P., Yu, X., Sridharan, A., Ranieri, J.P., & Bellamkonda, R.V., The influence of physical structure and charge on neurite extension in a 3D hydrogel scaffold. *J Biomater Sci Polym Ed* 9 (10), 1049-1069 (1998).

[236] Delaney, K.A., Murph, M.M., Brown, L.M., & Radhakrishna, H., Transfer of M2 muscarinic acetylcholine receptors to clathrin-derived early endosomes following clathrin-independent endocytosis. *J Biol Chem* 277 (36), 33439-33446 (2002).

[237] Kumari, S. *et al.*, Nicotinic acetylcholine receptor is internalized via a Rac-dependent, dynamin-independent endocytic pathway. *J Cell Biol* 181 (7), 1179-1193 (2008).

[238] Corey, J.M. *et al.*, Aligned electrospun nanofibers specify the direction of dorsal root ganglia neurite growth. *J Biomed Mater Res A* 83 (3), 636-645 (2007).

[239] Sakiyama, S.E., Schense, J.C., & Hubbell, J.A., Incorporation of heparin-binding peptides into fibrin gels enhances neurite extension: an example of designer matrices in tissue engineering. *FASEB J* 13 (15), 2214-2224 (1999).

[240] Svendsen, C.N., Bhattacharyya, A., & Tai, Y.T., Neurons from stem cells: preventing an identity crisis. *Nat Rev Neurosci* 2 (11), 831-834 (2001).

[241] Hammond, C., *Cellular and Molecular Neurobiology*, 2nd ed. (Academic Press, London, 2001).

[242] Ishii, M. & Kurachi, Y., Muscarinic acetylcholine receptors. *Curr Pharm Des* 12 (28), 3573-3581 (2006).

[243] De Jaco, A., Augusti-Tocco, G., & Biagioni, S., Muscarinic acetylcholine receptors induce neurite outgrowth and activate the synapsin I gene promoter in neuroblastoma clones. *Neuroscience* 113 (2), 331-338 (2002).

[244] Loreti, S., Ricordy, R., Egle De Stefano, M., Augusti-Tocco, G., & Maria Tata, A., Acetylcholine inhibits cell cycle progression in rat Schwann cells by activation of the M2 receptor subtype. *Neuron Glia Biol* 3 (4), 269-279 (2007).

[245] Guizzetti, M., Costa, P., Peters, J., & Costa, L.G., Acetylcholine as a mitogen: muscarinic receptor-mediated proliferation of rat astrocytes and human astrocytoma cells. *Eur J Pharmacol* 297 (3), 265-273 (1996).

[246] Larocca, J.N. & Almazan, G., Acetylcholine agonists stimulate mitogen-activated protein kinase in oligodendrocyte progenitors by muscarinic receptors. *J Neurosci Res* 50 (5), 743-754 (1997).

[247] Cui, Q.L., Fogle, E., & Almazan, G., Muscarinic acetylcholine receptors mediate oligodendrocyte progenitor survival through Src-like tyrosine kinases and PI3K/Akt pathways. *Neurochem Int* 48 (5), 383-393 (2006).

[248] Loreti, S. *et al.*, Rat Schwann cells express M1-M4 muscarinic receptor subtypes. *J Neurosci Res* 84 (1), 97-105 (2006).

[249] Cohen, R.I. & Almazan, G., Rat oligodendrocytes express muscarinic receptors coupled to phosphoinositide hydrolysis and adenylyl cyclase. *Eur J Neurosci* 6 (7), 1213-1224 (1994).

[250] Oikawa, H., Nakamichi, N., Kambe, Y., Ogura, M., & Yoneda, Y., An increase in intracellular free calcium ions by nicotinic acetylcholine receptors in a single cultured rat cortical astrocyte. *J Neurosci Res* 79 (4), 535-544 (2005).

[251] Smit, A.B. *et al.*, A glia-derived acetylcholine-binding protein that modulates synaptic transmission. *Nature* 411 (6835), 261-268 (2001).

[252] Emirandetti, A., Graciele Zanon, R., Sabha, M., Jr., & de Oliveira, A.L., Astrocyte reactivity influences the number of presynaptic terminals apposed to spinal motoneurons after axotomy. *Brain Res* 1095 (1), 35-42 (2006).

[253] den Dunnen, W.F. *et al.*, Biological performance of a degradable poly(lactic acid-epsilon-caprolactone) nerve guide: influence of tube dimensions. *J Biomed Mater Res* 29 (6), 757-766 (1995).

[254] Aebischer, P., Guenard, V., & Valentini, R.F., The morphology of regenerating peripheral nerves is modulated by the surface microgeometry of polymeric guidance channels. *Brain Res* 531 (1-2), 211-218 (1990).

[255] Jenq, C.B. & Coggeshall, R.E., Permeable tubes increase the length of the gap that regenerating axons can span. *Brain Res* 408 (1-2), 239-242 (1987).

[256] Knoops, B., Hurtado, H., & van den Bosch de Aguilar, P., Rat sciatic nerve regeneration within an acrylic semipermeable tube and comparison with a silicone impermeable material. *J Neuropathol Exp Neurol* 49 (4), 438-448 (1990).

[257] Kim, D.H. *et al.*, Comparison of macropore, semipermeable, and nonpermeable collagen conduits in nerve repair. *J Reconstr Microsurg* 9 (6), 415-420 (1993).

[258] Rodriguez, F.J., Gomez, N., Perego, G., & Navarro, X., Highly permeable polylactide-caprolactone nerve guides enhance peripheral nerve regeneration through long gaps. *Biomaterials* 20 (16), 1489-1500 (1999).

[259] Kim, Y.T., Haftel, V.K., Kumar, S., & Bellamkonda, R.V., The role of aligned polymer fiber-based constructs in the bridging of long peripheral nerve gaps. *Biomaterials* 29 (21), 3117-3127 (2008).

[260] Cai, J., Peng, X., Nelson, K.D., Eberhart, R., & Smith, G.M., Permeable guidance channels containing microfilament scaffolds enhance axon growth and maturation. *J Biomed Mater Res A* 75 (2), 374-386 (2005).

[261] Brayfield, C.A., Marra, K.G., Leonard, J.P., Tracy Cui, X., & Gerlach, J.C., Excimer laser channel creation in polyethersulfone hollow fibers for compartmentalized in vitro neuronal cell culture scaffolds. *Acta Biomater* 4 (2), 244-255 (2008).

[262] Stokols, S. & Tuszynski, M.H., The fabrication and characterization of linearly oriented nerve guidance scaffolds for spinal cord injury. *Biomaterials* 25 (27), 5839-5846 (2004).

[263] de Ruiter, G.C. *et al.*, Methods for in vitro characterization of multichannel nerve tubes. *J Biomed Mater Res A* 84 (3), 643-651 (2008).

[264] Huang, Y.-C., Huang, Y.-Y., Huang, C.-C., & Liu, H.-C., Manufacture of porous polymer nerve conduits through a lyophilizing and wire-heating process. *Journal of Biomedical Materials Research Part B-Applied Biomaterials* 74B (1), 659 - 664 (2005).

[265] Flynn, L. & Schoichet, M.S., Fiber ternplating of poly(2-hydroxyethyl methacrylate) for neural tissue engineering. *Biomaterials* 24 (23), 4265-4272 (2003).

[266] Wong, D.Y. *et al.*, Macro-architectures in spinal cord scaffold implants influence regeneration. *J Neurotrauma* 25 (8), 1027-1037 (2008).

[267] Sundback, C.A. *et al.*, Biocompatibility analysis of poly(glycerol sebacate) as a nerve guide material. *Biomaterials* 26 (27), 5454-5464 (2005).

[268] Wang, Y., Kim, Y.M., & Langer, R., In vivo degradation characteristics of poly(glycerol sebacate). *J Biomed Mater Res A* 66 (1), 192-197 (2003).

[269] Lim, J.Y. & Donahue, H.J., Cell sensing and response to micro- and nanostructured surfaces produced by chemical and topographic patterning. *Tissue Eng* 13 (8), 1879-1891 (2007).

[270] Dalby, M.J., Topographically induced direct cell mechanotransduction. *Med Eng Phys* 27 (9), 730-742 (2005).

[271] Chou, L., Firth, J.D., Uitto, V.J., & Brunette, D.M., Substratum surface topography alters cell shape and regulates fibronectin mRNA level, mRNA stability, secretion and assembly in human fibroblasts. *J Cell Sci* 108 (Pt 4), 1563-1573 (1995).

[272] Nederberg, F., Watanabe, J., Ishihara, K., Hilborn, J., & Bowden, T., Biocompatible and biodegradable phosphorylcholine ionomers with reduced protein adsorption and cell adhesion. *J Biomater Sci Polym Ed* 17 (6), 605-614 (2006).

[273] Harder, P.M., Shedd, T.A., & Colburn, M., Static and Dynamic Wetting Characteristics of Nano-patterned Surfaces. *JOURNAL OF ADHESION SCIENCE AND TECHNOLOGY* 22 (15), 1931-1948 (2008).

[274] Carpenter, J., Khang, D., & Webster, T.J., Nanometer polymer surface features: the influence on surface energy, protein adsorption and endothelial cell adhesion. *Nanotechnology* 19 (50) (2008).

[275] dos Santos, E.A., Farina, M., Soares, G.A., & Anselme, K., Surface energy of hydroxyapatite and beta-tricalcium phosphate ceramics driving serum protein adsorption and osteoblast adhesion. *J Mater Sci Mater Med* 19 (6), 2307-2316 (2008).

[276] Deligianni, D.D. *et al.*, Effect of surface roughness of the titanium alloy Ti-6Al-4V on human bone marrow cell response and on protein adsorption. *Biomaterials* 22 (11), 1241-1251 (2001).

[277] Fujii, T., Watanabe, Y., Inoue, T., & Kawashima, K., Upregulation of mRNA encoding the M5 muscarinic acetylcholine receptor in human T- and B-lymphocytes during immunological responses. *Neurochem Res* 28 (3-4), 423-429 (2003).

[278] Wang, H. *et al.*, Nicotinic acetylcholine receptor alpha7 subunit is an essential regulator of inflammation. *Nature* 421 (6921), 384-388 (2003).

[279] de la Torre, E. *et al.*, Proliferative actions of muscarinic receptors expressed in macrophages derived from normal and tumor bearing mice. *Biochim Biophys Acta* 1782 (2), 82-89 (2008).

[280] Henley, J.R., Huang, K.H., Wang, D., & Poo, M.M., Calcium mediates bidirectional growth cone turning induced by myelin-associated glycoprotein. *Neuron* 44 (6), 909-916 (2004).

[281] Cohen, R.I., Molina-Holgado, E., & Almazan, G., Carbachol stimulates c-fos expression and proliferation in oligodendrocyte progenitors. *Brain Res Mol Brain Res* 43 (1-2), 193-201 (1996).

[282] Guizzetti, M., Moore, N.H., Giordano, G., & Costa, L.G., Modulation of neuritogenesis by astrocyte muscarinic receptors. *J Biol Chem* 283 (46), 31884-31897 (2008).

[283] Soeda, S. *et al.*, Plasminogen activator inhibitor-1 aids nerve growth factor-induced differentiation and survival of pheochromocytoma cells by activating both the extracellular signal-regulated kinase and c-Jun pathways. *Neuroscience* 141 (1), 101-108 (2006).

[284] Karasewski, L. & Ferreira, A., MAPK signal transduction pathway mediates agrin effects on neurite elongation in cultured hippocampal neurons. *J Neurobiol* 55 (1), 14-24 (2003).

[285] Berridge, M.J., Lipp, P., & Bootman, M.D., The versatility and universality of calcium signalling. *Nat Rev Mol Cell Biol* 1 (1), 11-21 (2000).

[286] Neumann, S., Bradke, F., Tessier-Lavigne, M., & Basbaum, A.I., Regeneration of sensory axons within the injured spinal cord induced by intraganglionic cAMP elevation. *Neuron* 34 (6), 885-893 (2002).

[287] Hanson, M.G., Jr., Shen, S., Wiemelt, A.P., McMorris, F.A., & Barres, B.A., Cyclic AMP elevation is sufficient to promote the survival of spinal motor neurons in vitro. *J Neurosci* 18 (18), 7361-7371 (1998).

[288] Lu, P., Yang, H., Jones, L.L., Filbin, M.T., & Tuszynski, M.H., Combinatorial therapy with neurotrophins and cAMP promotes axonal regeneration beyond sites of spinal cord injury. *J Neurosci* 24 (28), 6402-6409 (2004).

[289] Meyer-Franke, A. *et al.*, Depolarization and cAMP elevation rapidly recruit TrkB to the plasma membrane of CNS neurons. *Neuron* 21 (4), 681-693 (1998).

[290] Conti, A. *et al.*, Nitric oxide in the injured spinal cord: synthases cross-talk, oxidative stress and inflammation. *Brain Res Rev* 54 (1), 205-218 (2007).

[291] Zochodne, D.W., Misra, M., Cheng, C., & Sun, H., Inhibition of nitric oxide synthase enhances peripheral nerve regeneration in mice. *Neurosci Lett* 228 (2), 71-74 (1997).

[292] Hirschberg, D.L., Yoles, E., Belkin, M., & Schwartz, M., Inflammation after axonal injury has conflicting consequences for recovery of function: rescue of spared axons is impaired but regeneration is supported. *J Neuroimmunol* 50 (1), 9-16 (1994).

[293] Stoll, G., Jander, S., & Schroeter, M., Detrimental and beneficial effects of injury-induced inflammation and cytokine expression in the nervous system. *Adv Exp Med Biol* 513, 87-113 (2002).

[294] Streit, W.J. *et al.*, Cytokine mRNA profiles in contused spinal cord and axotomized facial nucleus suggest a beneficial role for inflammation and gliosis. *Exp Neurol* 152 (1), 74-87 (1998).

[295] Yoshikawa, H. *et al.*, Nicotine inhibits the production of proinflammatory mediators in human monocytes by suppression of I-kappaB phosphorylation and nuclear factor-kappaB transcriptional activity through nicotinic acetylcholine receptor alpha7. *Clin Exp Immunol* 146 (1), 116-123 (2006).

[296] Kaplan, D.R. & Miller, F.D., Signal transduction by the neurotrophin receptors. *Curr Opin Cell Biol* 9 (2), 213-221 (1997).

[297] Airaksinen, M.S., Titievsky, A., & Saarma, M., GDNF family neurotrophic factor signaling: four masters, one servant? *Mol Cell Neurosci* 13 (5), 313-325 (1999).

[298] Wiklund, P., Ekstrom, P.A., & Edstrom, A., Mitogen-activated protein kinase inhibition reveals differences in signalling pathways activated by neurotrophin-3 and other growth-stimulating conditions of adult mouse dorsal root ganglia neurons. *J Neurosci Res* 67 (1), 62-68 (2002).

[299] Lanzafame, A.A., Christopoulos, A., & Mitchelson, F., Cellular signaling mechanisms for muscarinic acetylcholine receptors. *Receptors Channels* 9 (4), 241-260 (2003).

[300] Anderson, J.M., Rodriguez, A., & Chang, D.T., Foreign body reaction to biomaterials. *Semin Immunol* 20 (2), 86-100 (2008).

[301] Sato, K.Z. *et al.*, Diversity of mRNA expression for muscarinic acetylcholine receptor subtypes and neuronal nicotinic acetylcholine receptor subunits in human

mononuclear leukocytes and leukemic cell lines. *Neurosci Lett* 266 (1), 17-20 (1999).

[302] Fujii, T. & Kawashima, K., Calcium signaling and c-Fos gene expression via M3 muscarinic acetylcholine receptors in human T- and B-cells. *Jpn J Pharmacol* 84 (2), 124-132 (2000).

[303] Peng, H. *et al.*, Characterization of the human nicotinic acetylcholine receptor subunit alpha (alpha) 9 (CHRNA9) and alpha (alpha) 10 (CHRNA10) in lymphocytes. *Life Sci* 76 (3), 263-280 (2004).

[304] Basso, D.M., Beattie, M.S., & Bresnahan, J.C., A sensitive and reliable locomotor rating scale for open field testing in rats. *J Neurotrauma* 12 (1), 1-21 (1995).